The Thesis Committee for Stuart Hedrick Coleman
Certifies that this is the approved version of the following thesis:

The Reservoir Performance and Impact from Using Large-Volume, Intermittent, Anthropogenic CO_2 for Enhanced Oil Recovery

APPROVED BY
SUPERVISING COMMITTEE:

Supervisor:

Steven L. Bryant, Co-Supervisor

Susan D. Hovorka, Co-Supervisor

The Reservoir Performance and Impact from Using Large-Volume, Intermittent, Anthropogenic CO_2 for Enhanced Oil Recovery

by

Stuart Hedrick Coleman, B.S.Geo.E.; M.A.

Thesis

Presented to the Faculty of the Graduate School of

The University of Texas at Austin

in Partial Fulfillment

of the Requirements

for the Degree of

Master of Science in Engineering

The University of Texas at Austin

May 2012

Dedication

This thesis is dedicated to the sacrifices of my mother to give me the best possible education and chance to succeed from boarding school to grad school. Also, the influential life of my grandfather as an engineer and inventor encouraged me to return to engineering.

Acknowledgements

As with any big project, this work could not have been done without the help of many people. First I would like to thank Dr. Sue Hovorka for her advising and funding of this research. Dr. Steve Bryant provided more helpful advising and keen engineering perspective for this work. Within the Gulf Coast Carbon Center, there are a number of people who directly and indirectly helped with this study. I'd like to thank Hamid Reza Lashgari, Seyyed A. Hosseini, and Silvia Solano for their help and direct contributions towards modifying the existing Cranfield model to fit the needs of this study. I'd also like to acknowledge the work of Jong-Won Choi, J.P. Nicot, Tip Meckel, Jiemin Lu, Masoumeh Kordi, Sue Hovorka, and Ramon Trevino for their work towards developing the Cranfield reservoir model or the data analysis integrated into it. This entire study was built from the previous work of these fellow researchers.

Abstract

The Reservoir Performance and Impact from Using Large-Volume, Intermittent, Anthropogenic CO_2 for Enhanced Oil Recovery

Stuart Hedrick Coleman, M.S.E.

The University of Texas at Austin, 2012

Supervisors: Steven L. Bryant, Susan D. Hovorka

Anthropogenic CO_2 captured from a coal-fired power plant can be used for an enhanced oil recovery (EOR) operation while mitigating the atmospheric impact of CO_2 emissions. Concern about climate change caused by CO_2 emissions has increased the motivation to develop carbon capture and sequestration (CCS) projects to reduce the atmospheric impact of coal and other fossil fuel combustion. Enhanced oil recovery operations are typically constrained by the supply of CO_2, so there is interest from oil producers to use large-volume anthropogenic (LVA) CO_2 for tertiary oil production.

The intermittency of LVA CO_2 emissions creates an area of concern for both oil producers and electric utilities that may enter into a CO_2 supply contract for EOR. An oil producer wants to know if intermittency from a non-standard source of CO_2 will impact oil production from the large volume being captured. Since the electric utility must supply electricity on an as-needed basis, the CO_2 emissions are inherently intermittent on

a daily and seasonal basis. The electric utility needs to know if the intermittent supply of CO_2 would reduce its value compared to CO_2 delivered to the oil field at a constant rate.

This research creates an experimental test scenario where one coal-fired power plant captures 90% of its CO_2 emissions which is then delivered through a pipeline to an EOR operation. Using real emissions data from a coal-fired power plant and simplified data from an actual EOR reservoir, a series of reservoir simulations were done to address and analyze potential operational interference for an EOR operator injecting large-volume, intermittent CO_2 characteristic of emissions from a coal-fired power plant. The test case simulations in this study show no significant impact to oil production from CO_2 intermittency. Oil recovery, in terms of CO_2 injection, is observed to be a function of the total pore volumes injected. The more CO_2 that is injected, the more oil that is produced and the frequency or rate at which a given volume is injected does not impact net oil production. Anthropogenic CO_2 sources can eliminate CO_2 supply issues that constrain an EOR operation. By implementing this nearly unlimited supply of CO_2, oil production should increase compared to smaller-volume or water-alternating-gas (WAG) injection strategies used today.

Mobility ratio and reservoir heterogeneity have a considerable impact on oil recovery. Prediction of CO_2 breakthrough at the production wells seems to be more accurate when derived from the mobility ratio between CO_2 and reservoir oil. The degree of heterogeneity within the reservoir has a more direct impact on oil recovery and sweep efficiency over time. The volume of CO_2 being injected can eventually invade lower

permeability regions, reducing the impact of reservoir heterogeneity on oil recovery. This concept should mobilize a larger volume of oil than a conventional volume-limited or WAG injection strategy that may bypass or block these lower permeability regions.

Besides oil recovery, a reservoir's performance in this study is defined by its CO_2 injectivity over time. Elevated injection pressures associated with the large-volume CO_2 source can substantially impact the ability for an oil reservoir to store LVA CO_2. As CO_2, a less viscous fluid, replaces produced oil and water, the average reservoir pressure slowly declines which improves injectivity. This gradual improvement in injectivity is mostly occupied by the increasing volume of recycled CO_2. Sweep efficiency is critical towards minimizing the impact of CO_2 recycling on reservoir storage potential. Deep, large, and permeable oil reservoirs are more capable of accepting LVA CO_2, with less risk of fracturing the reservoir or overlying confining unit. The depth of the reservoir will directly dictate the injection pressure threshold in the oil reservoir as the fracture pressure increases with depth. If EOR operations are designed to sequester all the CO_2 delivered to the field, additional injection capacity and design strategies are needed.

Table of Contents

List of Tables

List of Figures

Chapter 1: Principals for Implementing a CO_2-EOR Operation

1.1 Reasons for Using Anthropogenic CO_2 For EOR

As primary and secondary production of crude oil continues to decline in the United States, many U.S. oil companies are implementing tertiary production strategies to maintain domestic oil production. The use of carbon dioxide (CO_2) has become an effective enhanced oil recovery strategy, but extensive development of such projects has been limited by the availability of economically viable CO_2 sources. Most CO_2-EOR projects are supplied with natural CO_2. Operators typically inject water after a slug of CO_2 to maintain efficient oil displacement and manage CO_2 supply issues. The demand for CO_2 as a reservoir solvent is growing and more companies are looking towards anthropogenic CO_2 sources. As oil companies are looking to supply their aging oil fields with CO_2, the electric utilities, operating large CO_2 emitters, are concerned with potential regulation on CO_2 emissions. This could create a mutual operating interest between oil companies and electric utilities.

The idea of using large-volume, intermittent, anthropogenic CO_2 for enhanced oil recovery could have many benefits. By using these neoteric CO_2 sources to supply EOR projects, U.S. oil production could significantly increase given the number of domestic oil fields with declining production and volume of CO_2 emissions. Each barrel of domestic oil has value to the U.S. in terms of reducing foreign imports, creating domestic labor opportunities, and reducing the influence of political uncertainties associated with foreign oil. As climate change becomes an increasing concern for the U.S., EOR can help cover the development costs of carbon capture and sequestration (CCS) projects.

Current domestic oil production from CO_2-EOR is about 250,000 bbl/d and it has been estimated that 87 billion barrels of oil could be recovered from CO_2 injection in the U.S. (ARI 2010). Anthropogenic CO_2 sources supply about 15% of the CO_2 currently used for EOR in the U.S. (Moritis 2009). These sources are typically gas processing facilities, which have a significantly lower volume of CO_2 emissions compared to a coal-fired power plant. To increase CO_2 supply for EOR projects, operators have to look towards larger, inherently intermittent sources like coal and gas-fired power plants. The intermittency of these anthropogenic sources is a consequence of meeting electricity demand fluctuations on a daily and seasonal basis.

The U.S. Department of Energy projects that coal will continue to provide at least 43% of the U.S. electric supply until 2035,even while gas-fired power generation is expected to grow (EIA 2011). Given their domestic abundance, it is clear that coal and natural gas will continue to fuel the majority of U.S electricity demand over the next century. With any potential climate legislation in the U.S., electric utilities will quickly look towards oil companies and their EOR projects to help implement a combined CCS/EOR operation. CCS projects are a primary mitigation option for electric utilities to minimize their large volume of CO_2 emissions while continuing to produce power from fossil fuels.

1.1.1 Research Objectives

The objectives of this report are to establish the operational changes a CO_2-EOR operator could expect from using a large-volume, intermittent CO_2 source, like a coal-fired power plant, to provide the injection volume. Current anthropogenic sources supply a small, consistent volume of CO_2 to the EOR operator. Since a coal-fired power plant is

built to supply electricity, its CO_2 emissions are dictated by electricity demand fluctuations and periodic maintenance. This research aims to quantify the impact to CO_2 storage capacity, oil production, and reservoir pressure from using a large-volume, intermittent CO_2 source for an EOR/CCS operation. Throughout this study the performance of an injection well or entire well pattern is defined by its CO_2 injectivity and efficient oil recovery.

A significant amount of research has been done on using CO_2-EOR as a CCS strategy. Many of the reports associated with this type of research make general assumptions about oil production volumes, CO_2 breakthrough time, and recycling volumes. These assumptions are usually based on previous EOR projects and standard performance prediction methods for miscible flooding. Most of these past and current EOR operations use a water-alternating-gas (WAG) injection strategy, which limits the pore volume available for CO_2 storage. The industry standards for miscible flooding are not based on a LVA supply of CO_2. No CO_2-EOR operation has used the full volume of CO_2 emissions from a coal plant in a "one source-to-one reservoir" setup.

This study has the unique opportunity to implement three years of hourly CO_2 emissions data from a large Texas coal plant and directly use that CO_2 as the injection rate for an existing EOR project that has a robust reservoir model. Using compositional modeling software, various operational scenarios and assumptions are tested and analyzed to better reflect the reservoir response to a large-volume, intermittent CO_2 injection scheme. From these tests, oil producers can better prepare for operational changes, effectively negotiate a CO_2 supply contract with an electric utility, and engineer efficient injection strategies to handle this new source of CO_2.

To clearly focus on the stated objectives, the limits of this study had to be defined. The infrastructure design and costs associated with using LVA CO_2 for EOR are not

analyzed. The EOR economics of using LVA CO_2 including recycling costs are also not evaluated. Additional research can build from and go beyond the limits of this study.

1.2 CARBON CAPTURE TECHNOLOGIES

In 2009, the consumption of coal accounted for 80.6% of the U.S. CO_2 emissions from electricity generation (EIA 2011). This makes coal-fired power plants the primary focus of any legislation built around CO_2 emissions, creating a significant need for efficient carbon capture technologies. Capturing large volumes of CO_2 from a coal-fired power plant is a relatively new process that requires additional energy and capital. The energy requirement or energy penalty for a carbon capture operation can range from 25-40% of the power output from a coal-fired power plant (Rao 2007). Implementing a carbon capture system onto an existing 500 MW coal plant, would require 125 – 200 MW of power, decreasing that coal plant's net output to as low as 300 MW. With a greater energy penalty, the increase to electricity costs from carbon capture systems is significant. Improving CO_2 capture efficiency is imperative to reduce the energy penalty and minimize the increase in electricity costs, capital investment, and operating expenses.

1.2.1 Post-Combustion Capture

Through this report, the anthropogenic CO_2 source is a pulverized coal-fired power plant, fueled by a blend of mostly lignite and some bituminous coal. In a scenario where this coal plant would be capturing its CO_2, it is assumed to be equipped with post-combustion capture technology. Post-combustion capture is a downstream process within a coal-fired power plant operation. It involves the removal of CO_2 from the flue gas produced after the combustion of coal for electricity generation (Kothandaraman, Nord et

al. 2009). The economic burden of separating CO_2 from the flue gas is attributed to the low partial pressure of CO_2 and the large volume of gas emitted from a coal-fired power plant. This large volume of gas contains about 10-13% CO_2 and significant energy is needed for CO_2 recompression (Merkel, Lin et al. 2009). Large volumes of amine solutions are used to capture the CO_2 from the flue gas, but reusing the amine solutions requires additional energy to supply heat for solvent regeneration (Kanniche, Gros-Bonnivard et al. 2010). In Figure 1.1, an average 600 MW_e coal power plant emits 500 m^3/s (1540 MMscf/d) of flue gas containing 13% CO_2, which equates to about 11,000 tCO_2/day (Merkel, Lin et al. 2009). Current CO_2 capture operations, with conventional absorption technology, are seen in the chemical and natural gas industries, but compared to a coal-fired power plant, these CO_2 removal systems have a 5-10 times lower CO_2 flow rate (Merkel, Lin et al. 2009).

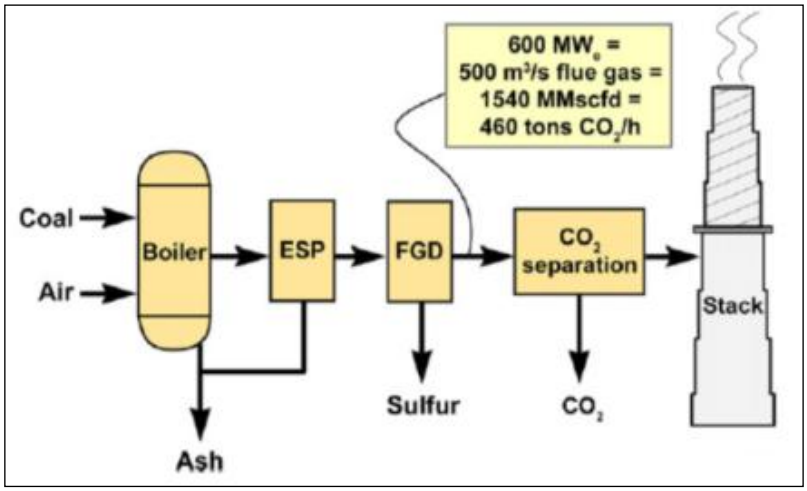

Figure 1.1 - Schematic diagram of a standard post-combustion CO_2 capture process. [ESP = electrostatic precipitator, FGD = flue gas desulfurization unit] (Merkel, Lin et al. 2009)

An amine system used to capture 90% of the CO_2 from the flue gas will require about 30% of the power produced by the coal-fired power plant, resulting in a CO_2 capture cost of \$40-100/tCO_2 and increasing electricity costs by 50 – 90% (Figueroa,

Fout et al. 2008). This demonstrates the importance of improving capture efficiency and costs so that these large anthropogenic sources can economically supply CO_2 for an EOR operation and lower the overall costs of a CCS project. Any price on carbon will significantly be dictated by capture costs and efficiency.

1.3 CO_2 INTENSITY OF THE U.S. GULF COAST

Development of large-scale CO_2-EOR/CCS operations could be focused in the Gulf Coast, an area characterized by its anthropogenic CO_2 intensity. In 2009, CO_2 emissions in the US was 5.40 Gt, where 0.95 Gt or 17.7% came from the Gulf Coast region of Texas, Louisiana, Mississippi, and Alabama (EIA 2011). Texas alone emitted 605.5 Mt of CO_2, which accounts for 11.2% of U.S. CO_2 emissions (EIA 2011).

About 36% of anthropogenic CO_2 emissions in Texas are attributed to electric power generation, and about two-thirds of that is from coal-fired power plants (EIA 2008). The carbon intensity of coal-fired power plants in Texas is partially linked to the fact that Texas coal is mostly lignite, the lowest rank of coal. The heat content or energy density of lignite ranges from 9 to 17 million BTU per ton, compared to higher grade bituminous coal which has a heat content of 21 to 30 million BTU per ton (EIA 2008). Due to its high sulfur content, most Texas coal plants blend lignite with bituminous coal from Wyoming to meet environmental regulations. Transporting bituminous coal from Wyoming increases the operating costs for Texas coal-fired power plants. This coal blend still has a lower energy density than pure bituminous coal, meaning Texas coal plants must burn more coal per BTU output compared to a coal plant that burns only bituminous coal.

The CO_2 intensity of the Gulf Coast is not only attributed to power plants but also the abundance of industrial CO_2 emitters like petroleum refineries, cement plants, ethylene plants, and ammonia plants. Texas and Louisiana were the top two states in U.S. industrial CO_2 emissions in 2007, with 184 and 92 million tons of carbon emissions respectively (EIA 2008). Together the two states accounted for 28.2% of U.S. industrial CO_2 emissions. The CO_2 intensity in Texas is high because of large population, a heavy industry of refined products, and combustion of lignite in coal-fired power plants. These three characteristics create a huge source of CO_2 for both EOR and CCS in a carbon-restrained environment.

1.4 DEVELOPMENT OF CO_2 PIPELINE INFRASTRUCTURE

Once carbon dioxide is captured from large-scale power plants it must be transported to a designated geologic storage site. The most efficient method of transporting CO_2 is through pipelines. CO_2 pipeline networks have been operated for three decades to supply EOR projects in the United States, but the natural gas pipeline infrastructure is considerably larger (Fig 1.2). Unless retrofitted, these natural gas pipelines cannot transport CO_2, but the right-of-way may provide adequate space for expanding CO_2 pipelines between Gulf Coast sources and local ageing oil fields.

Developing a large-scale CO_2 pipeline network from existing infrastructure will be a significant undertaking. There are about 1,500 miles of large CO_2 pipelines in the United States, with a capacity of 20 million tons per year or about the equivalent CO_2 emissions of four coal plants (Gale and Davison 2004). To put in comparison, in 2000, the U.S. had about 320,000 miles of natural gas pipelines and about 154,000 miles of hazardous liquid pipelines (Gale and Davison 2004).

Carbon dioxide is most effectively transported by pipeline as a supercritical fluid. To maintain CO_2 as a supercritical fluid (Fig. 1.3), temperature must remain above 87.8°F (31°C) and above a critical pressure of 1070 psi (7.38 MPa). By maintaining single-phase supercritical flow, pipeline operators avoid two-phase flow that can create pressure surges and flow transients (Barrie, Brown et al. 2008).

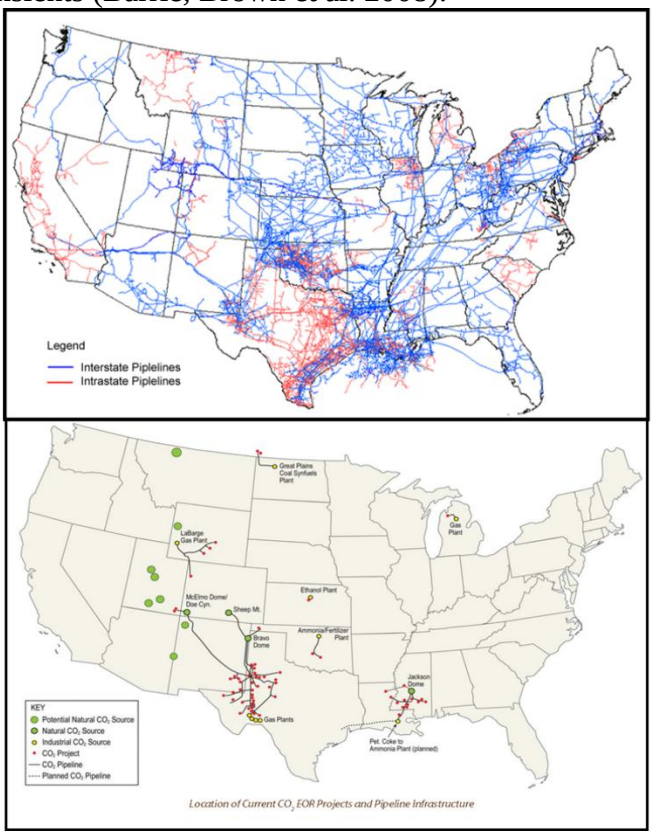

Figure 1.2 - A comparison between existing natural gas pipelines (top) and current CO_2 pipelines (bottom). Modified from (EIA 2008) and (Dolence, Kirschner et al. 2009) respectively.

The purity of CO_2 is a significant issue for pipeline design and efficiency. When transporting CO_2, there is a need to dehydrate the gas to reduce pipeline corrosion from carbonic acid, which forms when CO_2 is mixed with water. The ability to maintain supercritical CO_2 in the pipeline requires higher pressures as other flue gases, like hydrogen sulfide (H_2S) or methane (CH_4), are mixed into the flow stream (Barrie, Brown

et al. 2008). A balance is needed as achieving higher concentrations of CO_2 (95-100%) captured from a coal plant requires more energy and capital, while lower concentrations of CO_2 increase pipeline costs and inefficiencies (Gale and Davison 2004).

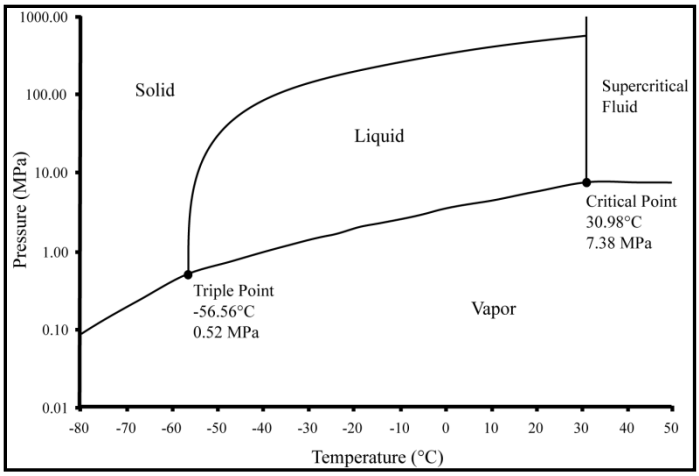

Figure 1.3 - A phase diagram for carbon dioxide (CO_2) illustrating the temperature and pressure needed to sustain CO_2 as a supercritical fluid for transporting and injection. Modified from (McCoy 2008)

1.5 ENGINEERING PRINCIPLES FOR CO_2 - EOR

Throughout this report, enhanced oil recovery (EOR), refers to the use of CO_2 as a miscible and oil-displacing fluid. This technique is one of many different strategies for improving oil recovery beyond waterflooding or secondary recovery. Carbon dioxide is intended to mobilize and displace the residual oil left from a waterflood. The effectiveness of this displacement is significantly linked to the miscibility between the remaining reservoir oil and the CO_2. Additional oil is recovered from miscible CO_2 injection by (Taber, Martin et al. 1997):

- Swelling the oil
- Lowering oil viscosity
- Lowering interfacial tension between oil and the CO_2/oil phase

The viscosity of CO_2 is significantly less than any reservoir oil or water, creating unfavorable displacement conditions. To reduce the mobility of CO_2 and address CO_2 supply issues, a water-alternating-gas (WAG) injection scheme is typically used for current CO_2-EOR projects (Fig. 1.4). It is important to note that the CO_2-EOR referred to in this report assumes 100% continuous CO_2 injection, where no water is injected between slugs of CO_2. Immiscible displacement is another form of CO_2-EOR, but it is less effective than miscible injection and not relevant to the test case.

As with any EOR project, implementing a CO_2-EOR operation requires thorough analysis of the reservoir and fluid characteristics. This section aims to review and highlight the main criteria and physics associated with injecting CO_2 into an oil reservoir. Despite being mostly review for a petroleum engineer, these principles will be critical to understand for all engineers involved with designing an anthropogenic CO_2 - EOR system.

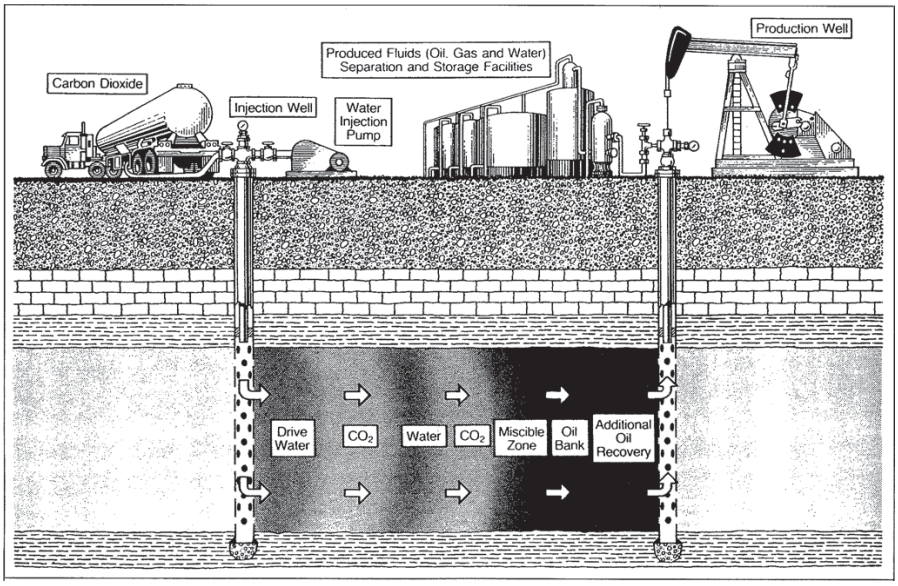

Figure 1.4 - A simple schematic of CO_2-EOR using WAG injection. This report assumes 100% continuous injection of anthropogenic CO_2, with no water injected between slugs of CO_2. Modified from (Green and Whillhite 1998).

1.5.1 Reservoir Parameters and Criteria

The majority of CO_2-EOR projects are in the United States, focused around the CO_2 pipeline infrastructure illustrated in Figure 1.2. This creates a significant geographical restriction on the oil fields that can currently implement CO_2-EOR operations. A major assumption of this report is that a large-volume anthropogenic source is within an economically viable distance from the EOR field, eliminating any geographical and supply issues typically associated with such operations.

Excluding the geographic and supply limitations associated with CO_2-EOR, not all oil reservoirs are suitable for CO_2 flooding. The miscibility of CO_2 within a reservoir becomes critical for an efficient displacement of oil. Controlled by the critical pressure and temperature of CO_2, miscibility is dictated by reservoir depth and oil composition. Displacement from CO_2 injection is called multiple-contact miscible (MCM), where the minimum miscibility pressure (MMP) is a critical factor. The MMP must be exceeded to maintain miscible displacement through the reservoir. It is determined by experimental measurements, empirical correlations, and equation-of-state (EOS) calculations (Green and Willhite 1998). A depth of 2,500 feet is typically accepted as the minimum depth for maintaining miscible displacement, but this standard depth can increase with heavier reservoir oils. With greater depth, the reservoir pressure and temperature increase enough to create CO_2 miscibility with denser oils.

Oil gravity is typically measured in units of °API, where oils with higher API gravity are considered lighter crude, while heavier oils have a lower API number. Water has an API number of 10, so oil greater than 10 °API is buoyant relative to water. For miscible displacement of oil using CO_2 it's widely accepted that the oil gravity must be greater than 22 °API (Klins 1984). Table 1.1 shows the relationship between oil gravity and depth to achieve miscible displacement. In line with oil gravity, an oil viscosity less

than 10 cp is preferred, where most field projects have an oil viscosity near 1.5 cp (Taber, Martin et al. 1997). In terms of oil composition, a high percentage of C_5 to C_{12} components is important for implementing an effective CO_2-EOR project (Taber, Martin et al. 1997).

Gravity (°API)	Min. Depth (ft)
>40	2,500
32-39.9	2,800
28-31.9	3,300
22-27.9	4,000

Table 1.1 - A table showing the relationship between oil gravity and minimum depth to achieve the MMP. Modified from (Taber, Martin et al. 1997).

Along with depth, another critical reservoir characteristic for CO_2-EOR is oil saturation. A minimum of 20% oil saturation is needed to maintain an economic EOR operation, where most CO_2-EOR projects begin with around a 50% oil saturation (Taber, Martin et al. 1997). Reservoir thickness is a secondary criterion, as displacement becomes less efficient in thicker reservoirs. With thinner, greater dipping reservoirs a stable displacement front is more likely to develop as buoyancy between fluids is less of a factor (Green, 1998 #205). Permeability is also a main criterion, where high vertical permeability in horizontal reservoirs can create preferential flow paths or thief zones for the CO_2. These thief zones cause CO_2 to bypass a significant volume of recoverable oil and allow early breakthrough of CO_2 in the production wells. In terms of lithology, both carbonate and clastic reservoirs are viable for CO_2-EOR. Table 1.2 is a summary of key screening criteria for CO_2-EOR.

Oil Properties			Reservoir Characteristics			
Gravity	Viscosity	Composition	Lithology	Net Pay	Avg. Perm.	Depth
(°API)	(cp)			(ft)	(md)	(ft)
>22	<10	High % of C_5 to C_{12}	Sandstone or Carbonate	>100 not preferred	not critical	>2,500

Table 1.2 - Summary of the main screening criteria for achieving miscible displacement in a CO2 flood (Taber, Martin et al. 1997).

1.5.2 Reservoir Fluid Characteristics

As mentioned in the previous section, exceeding the minimum miscibility pressure (MMP) is the main criteria for miscible CO_2 flooding. Calculating the MMP incorporates fluid characteristics of both CO_2 and reservoir crude oil. This section will describe two common methods used to calculate the MMP, but it is important to note these are only correlations to help as a screening tool. Laboratory tests using slim tube sand packs are the best way for determining the pressure needed for miscibility (Green and Willhite 1998)

The first common method for calculating MMP comes from (Johnson and Pollin 1981). Developed from experimental results, Johnson's miscibility correlation incorporates oil gravity, molecular weight, reservoir temperature, and injection gas composition. For reservoir temperatures between 80°F and 280°F, the correlating equation is:

$$P_{mdmp} - P_{c,inj} = \alpha_{inj}\left(T_{res} - T_{c,inj}\right) + I\left(\beta M - M_{inj}\right)^2 \quad \text{(Eq. 1-1)}$$

P_{mdmp} = predicted minimum dynamic miscibility pressure, psia
$P_{c,inj}$ = CO_2 critical pressure, psia
M = average molecular weight of the reservoir oil
β = constant, 0.285
T_{res} = reservoir temperature, °K
$T_{c,inj}$ = CO_2 critical temperature, °K
M_{inj} = molecular weight of injection gas
α_{inj} = 18.9 psia/°K (for pure CO_2)

As seen in Figure 1.3, knowing the critical pressure (1070.4 psi) and temperature (87.8°F) of CO_2 is important for both pipeline design and reservoir development. It is also important to note that the previous equation assumes pure CO_2. Similar to pipeline design, impurities like H_2S and CH_4, can alter the critical pressure ($P_{c,inj}$), critical temperature ($T_{c,inj}$), molecular weight (M_{inj}) and the α_{inj} term used in Equation 1-1. The second correlation commonly used is from (Cronquist 1978):

$$P_{mdmp} = 15.988(T_{res})^{0.744206+0.0011038\left(MWC_5^+\right)+0.0015279(Y_{C1})} \quad \text{(Eq. 1-2)}$$

P_{mdmp} = predicted minimum dynamic miscibility pressure, psia
T_{res} = reservoir temperature, °F
MWC_5^+ = molecular weight of pentanes and heavier fraction
Y_{C1} = mole percentage of methane and nitrogen

This empirical equation was derived from an experiment with 58 data points. The crude oils tested ranged from 23.7 to 44°API with reservoir temperatures ranging from 71 to 248 °F, creating a range of miscibility pressures of 1,075 to 5,000 psi (Klins 1984). It should be noted that this empirical correlation only accounts for methane and nitrogen as possible impurities within the CO_2 injection stream. Laboratory tests of oil composition are needed to establish the molecular weights of all hydrocarbon components within the crude oil, in particular pentanes (C_5) and heavier.

The performance of a miscible displacement process depends on physical fluid properties, like density, that affect flow behavior in a reservoir (Green and Willhite 1998). Density differences between the displacing and displaced fluid can result in displacement mechanisms like gravity override, underride, or fingering. Since the density of CO_2 is significantly less than the displaced crude oils, it is important to understand the relative densities of all fluids within the reservoir.

At standard conditions, CO_2 has a density of 0.124 lb/ft^3 (1.98 kg/m^3), which is about 1.5 times denser than air. Despite not being a toxic gas, a surface leakage of CO_2 can create a suffocation risk in low lying areas since it is denser than air. At reservoir conditions, the density of CO_2 significantly increases (Fig. 1.5).

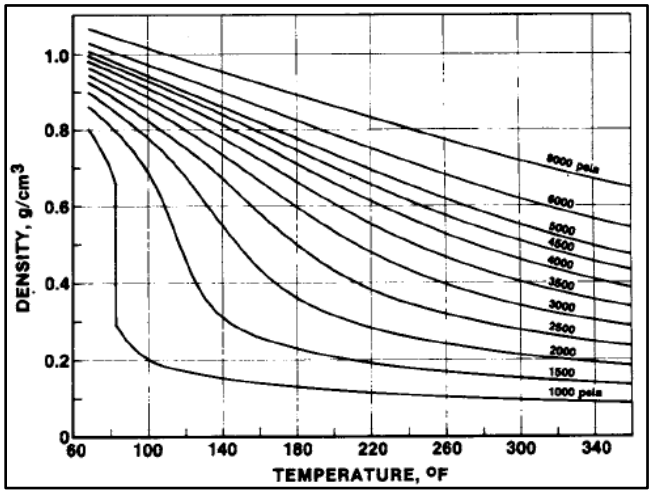

Figure 1.5 - Density of CO_2 as a function of temperature and pressure. Modified from (Holm and Josendal 1982).

Figure 1.6 illustrates the graphical method for finding the compressibility factor (Z) of CO_2 relative to temperature and pressure. By using a compressibility factor, which quantifies the deviation from the ideal gas law, CO_2 density can be calculated with the EOS (Green and Willhite 1998).

$$pv = ZRT \quad \text{(Eq. 1-3)}$$

p = pressure, psia
v = specific volume, ft^3/lb$_m$
T = temperature, °R
R = ideal gas constant, 10.73 (psi-ft^3)/(°R-lb$_m$-mol)
Z = compressibility factor, dimensionless.

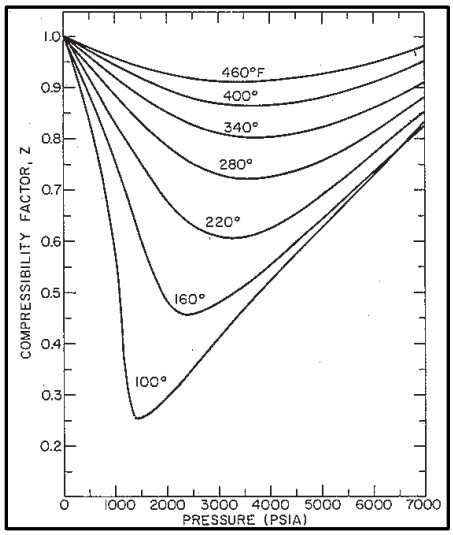

Figure 1.6 - Compressibility factor of CO_2 relative to pressure and temperature. Modified from (Reamer, Olds et al. 1944).

The compressibility factor can also be used to calculate the CO_2 formation volume factor, which is the ratio of reservoir volume to standard surface volume. The following equation illustrates this calculation:

$$B_g = \frac{P_{sc}ZT}{T_{sc}P} \quad \text{(Eq. 1-4)}$$

B_g = gas (CO_2) formation volume factor
P_{sc} = standard surface pressure, 14.7 psi
Z = compressibility factor
T = reservoir temperature, ºR
T_{sc} = standard surface temperature, 520 ºR
P = reservoir pressure, psi

To calculate a CO_2 formation volume factor in units of ft^3/scf and incorporating the standard temperature and pressure, the following equation can be used

$$B_g = 0.02828\frac{ZT}{P} \quad \text{(Eq. 1-5)}$$

Reservoir oil density can vary significantly given the hydrocarbon composition and volume of dissolved gas. The density of crude oil can range from 45 lb/ft^3 (~720 kg/m^3) to 65 lb/ft^3 (~1040 kg/m^3). As mentioned before, the API gravity is the preferred density scale in the petroleum industry. The following two equations can be used to convert crude oil density from lb/ft^3 to °API:

$$\gamma_o = \frac{\rho_o}{\rho_w} \quad \text{(Eq. 1-6a)}$$

$$°API = \frac{141.5}{\gamma_o} - 131.5 \quad \text{(Eq. 1-6b)}$$

γ_o = specific gravity of the crude oil
ρ_o = crude oil density, lb/ft^3
ρ_w = water density, lb/ft^3

In reservoir conditions there is some volume of natural gas dissolved into the crude oil. As the crude oil is produced, the natural gas comes out of solution from the oil. This point where the solution gas begins to come out of solution is called the bubble point (Fig. 1.7). The following equation is accepted across the petroleum industry as the best gas solubility correlation (Standing 1947):

$$R_s = \gamma_g \left[\left(\frac{p}{18.2} + 1.4\right) 10^x\right]^{1.2048}, x = 0.0125(API) - 0.00091(T - 460) \quad \text{(Eq. 1-7)}$$

R_s = gas solubility or dissolved GOR, scf/STB
γ_g = solution gas gravity, fraction (air = 1)
p = system pressure, psi
API = oil gravity, °API
T = temperature, °R

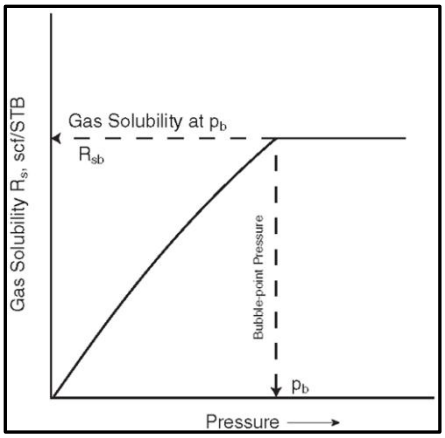

Figure 1.7 - Schematic of gas solubility and bubble-point pressure (Ahmed 2006)

The volume of residual oil decreases as gas is liberated during production. This shrinkage in oil volume is called the oil-formation volume factor (B_o), and it is also a relative volume ratio between reservoir and surface conditions. B_o is defined as the volume in barrels at reservoir pressure and temperature occupied by one barrel of stock tank oil, including the gas in solution at that reservoir temperature and pressure (Klins 1984). As the pressure is reduced, the undersaturated crude oil increases in volume until the bubble-point pressure (P_b) is reached. At the bubble-point the oil reaches maximum volume and as the pressure decreases from the bubble-point the oil volume decreases (Fig. 1.8). Standing (1947) also developed a graphical correlation for calculating the oil formation volume factor (B_o):

$$B_o = 0.9759 + 0.00012\left[R_s\left(\frac{\gamma_g}{\gamma_o}\right)^{0.5} + 1.25(T - 460)\right]^{1.2} \quad \text{(Eq. 1-8)}$$

R_s = gas solubility or dissolved GOR, scf/STB
γ_g = solution gas gravity, fraction (air = 1)
γ_o = stock-tank oil gravity
T = temperature, ^{o}R

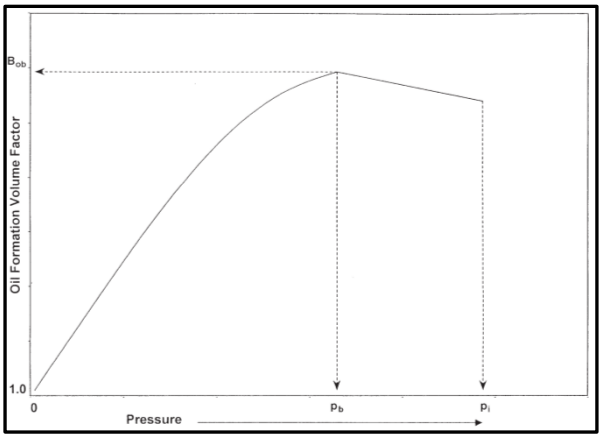

Figure 1.8 - Relationship of the oil formation volume factor before and after reaching the bubble point (P_b) as pressure decreases. (Ahmed 2006)

1.5.2 Miscible Displacement & Phase Behavior

Once the MMP of the injected fluid is exceeded, there are several reservoir principles that dictate the performance of miscible displacement. Primarily considered a MCM displacement process, miscibility from CO_2 injection is generated through in-situ composition changes resulting from multiple-contacts and mass transfer between reservoir oil and the CO_2 (Green and Willhite 1998). It is widely believed through many published reports that multiple-contact miscibility (MCM) occurs in a very brief time period and over a very short reservoir distance but true first-contact miscibility (FCM) is rarely achieved. Assuming pure CO_2 injection and ideal oil composition, very high injection pressures (> 5,000 psi) are needed to achieve first-contact miscibility(Klins 1984).

Gas composition is critical for characterizing a MCM or FCM displacement process, as some impurities like CH_4 can reduce CO_2 miscibility, while others like H_2S can improve miscibility. The extent or distance of a MCM displacement beyond the wellbore is dictated by injection pressure, oil composition, and injectate composition.

This process involves multiple contacts between the reservoir oil and CO_2 that develops a hydrocarbon-rich gas phase which is then miscible with uncontacted crude oil. At the same temperature and pressure, this hydrocarbon-rich vapor phase will have a larger volume away from the wellbore when injecting methane compared to CO_2. Carbon dioxide achieves dynamic miscibility at lower pressures than methane by extracting higher molecular weight hydrocarbons ($C_2 - C_{30}$) than the C_2 through C_5 components that methane vaporizes (Stalkup Jr. 1983). It is important to fully characterize the injection fluid composition when anthropogenic CO_2 is being used for miscible displacement. Methane, flue gas, and nitrogen are potential impurities in the CO_2 stream that can be detrimental to miscible displacement by increasing the characteristically low MMP associated with pure CO_2.

Vaporization of the reservoir oil's components is the primary mechanism for recovery during a MCM process (Klins 1984). The C_2 through C_{30} hydrocarbon components are extracted into this hydrocarbon-rich vapor. This hydrocarbon enrichment of the two-phase vapor (liquid and vapor) continues until a critical composition is reached. The critical composition must be continually re-established to counter dispersion effects within the reservoir (Klins 1984). For CO_2, the MCM process occurs at reservoir temperatures greater than 120°F and as the reservoir pressure increases the two-phase (L+V) region decreases (Fig. 1.9).

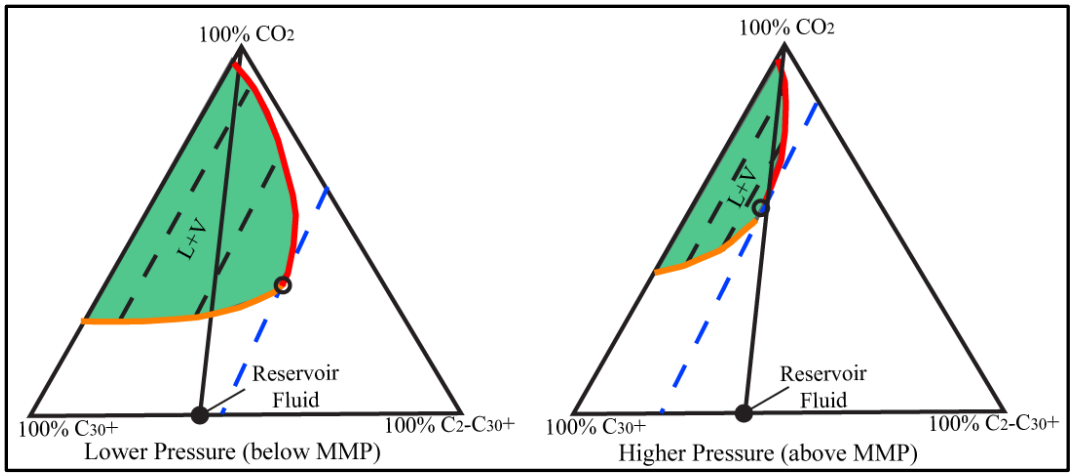

Figure 1.9 - Ternary Diagrams illustrating pressures above and below dynamic miscibility. The reservoir fluid must be to the left of the blue tie line for dynamic miscibility. Modified from (Stalkup Jr. 1983).

The two ternary diagrams represent pressure conditions below dynamic miscibility requirements (lower pressure) and above dynamic miscibility requirements (higher pressure). Colored green in Figure 1.9, the two-phase hydrocarbon vapor/liquid region decreases in size with higher reservoir pressure. Hypothetically, with high enough pressure, the green region would become so small that the reservoir fluid would not pass through the green two-phase region, creating first contact miscibility conditions. The orange line along the bottom of the green two-phase region, in Figure 1.9, represents a saturation curve of bubble points, while the red line represents a saturation curve of dew points. Both lines meet at a critical or plait point for CO_2. In the higher pressure case, the two-phase region is entered by crossing the dewpoint curve as CO_2 is added to the reservoir. This does not have to be the case, dynamic miscibility can also occur by crossing the bubble point curve. To achieve dynamic miscibility the initial reservoir fluid must be to the left of the blue tie line that intersects the CO_2 critical point. It is clear that a higher percentage of extractable oils ($C_2 - C_{30}$) will increase the ability to achieve dynamic miscibility.

1.5.3 Sweep Efficiency

As CO_2 sweeps through the reservoir, displacing oil, there are three mechanisms that dictate oil recovery potential (Stalkup Jr. 1983):

- molecular diffusion
- microscopic convective dispersion
- macroscopic convective dispersion

Molecular diffusion is dictated by thermal motion between the CO_2 and oil molecules. Microscopic convective dispersion is dictated by pore-scale phenomena like capillary pressure, viscous forces, interfacial tension, and rock wettability. Macroscopic convective displacement is controlled by larger-scale permeability heterogeneities and preferential flow paths characterized by depositional and diagenetic processes.

Since oil and CO_2 are miscible above the MMP, the two fluids are considered one phase eliminating relative permeability, interfacial tension (IFT), and capillary forces seen between the fluids during immiscible displacement. With no IFT between oil and CO_2, under miscible conditions, there is no tendency for CO_2 to trap oil and create a residual oil saturation. Miscible displacement is implemented to reduce the residual oil saturation to its lowest possible value. For actual reservoir conditions, MCM displacements actually leave a small residual oil saturation between 2 and 10% (Klins 1984).

Molecular diffusion has a significant impact on miscible displacement efficiency. In the presence of porous media, with varying grain sizes and pore throats, molecular diffusion has different mixing characteristics compared to standard molecular diffusion with no porous media. The mixing between fluids is increased in a porous media due to uneven fluid flow and concentration gradients in both the longitudinal and transverse direction. It has been generally accepted that diffusion in a porous medium is related to

the formation electrical resistivity factor, as shown in the following equation (Perkins and Johnston 1963):

$$\frac{D}{D_o} = \frac{1}{F\phi} \quad \text{(Eq. 1-9)}$$

D = effective reservoir diffusion coefficient, L^2/t
D_o = molecular diffusion coefficient, L^2/t
F = formation factor
ϕ = porosity, fraction

The extent that longitudinal dispersion (normal to flow) differs from transverse dispersion (perpendicular to flow) is dictated by vertical heterogeneities and gravity forces. At higher injection rates, the mixing zone can become more asymmetrical as the trailing edge is stretched out. Through several laboratory tests it has been observed that significant mass transfer by dispersion can reduce displacement efficiencies.

Following a waterflood, the reservoir oil is blocked from the injected CO_2 by previously injected water. To displace and contact the oil, the CO_2 must first displace the water. Since CO_2 is soluble in water, the impact to oil recovery from high water saturations is relatively small (Stalkup 1970). If the reservoir rock is strongly water-wet, the impact of high initial water saturations can be more significant, but as large volumes of water are produced during CO_2 injection the oil displacement becomes easier.

On a macroscopic level, oil recovery depends on the volume of reservoir pore space contacted by injected CO_2. This can be a significant benefit of using large-volume anthropogenic (LVA) CO_2 sources where supply no longer becomes an issue and nearly all the connected pore space can be eventually contacted by CO_2. Macroscopic displacement is dictated by fluid properties, depositional characteristics, reservoir rock properties, and well pattern orientation. It is important to note that these macroscopic reservoir properties and characteristics are not adequately captured in core samples as

variations are seen over several feet compared to microscopic variations that occur at the pore level.

1.5.4.1 Viscous Forces

For miscible displacement, the relative permeability between the displacing (CO_2) and displaced (oil) fluids is considered equal. For immiscible displacement, the mobility ratio accounts for differences in relative permeability and viscosity. In the case of equal relative permeabilities, the mobility ratio of a miscible CO_2 flood is determined by the ratio of displaced and displacing fluid viscosities, as seen in the following equation:

$$M = \frac{\mu_o}{\mu_{CO2}} \quad \text{(Eq. 1-10)}$$

M = mobility ratio
μ_o = oil viscosity, cp
μ_{CO2} = carbon dioxide viscosity, cp

Figure 1.10 shows the range of viscosity values for CO_2 and hydrocarbon components at different pressures and temperatures. It can be observed that oil composition directly influences viscosity and therefore mobility ratio. For a mobility ratio of one or less, where the viscosity of CO_2 is equal to or greater than oil, the displacement front is considered stable. It is more common to have a mobility ratio greater than one, because CO_2 is usually much less viscous than oil. For mobility ratios greater than one, the displacement front can become very unstable as viscous fingers of CO_2 can develop and propagate through the reservoir (Fig. 1.11).

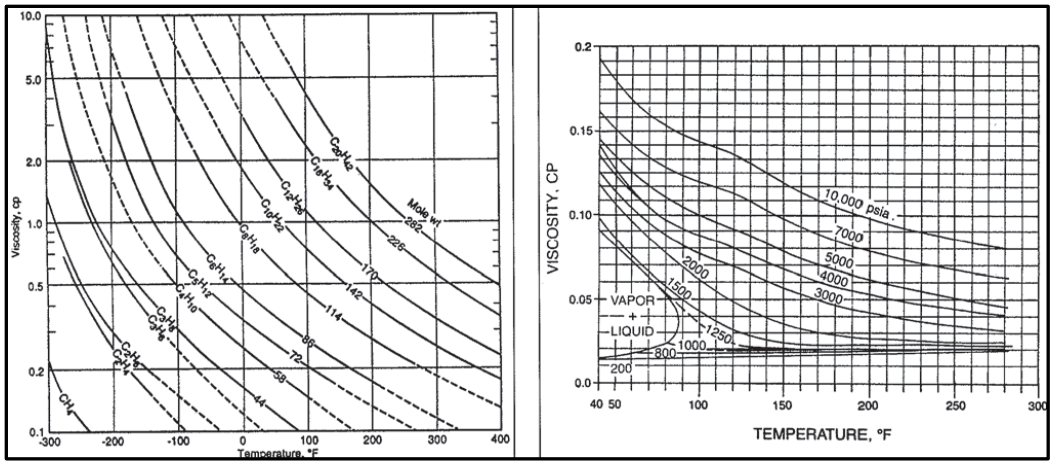

Figure 1.10 - Two graphs showing hydrocarbon (right) and CO_2 (left) viscosities. The hydrocarbon viscosities are measured at 14.7 psi. Modified from (Green and Willhite 1998).

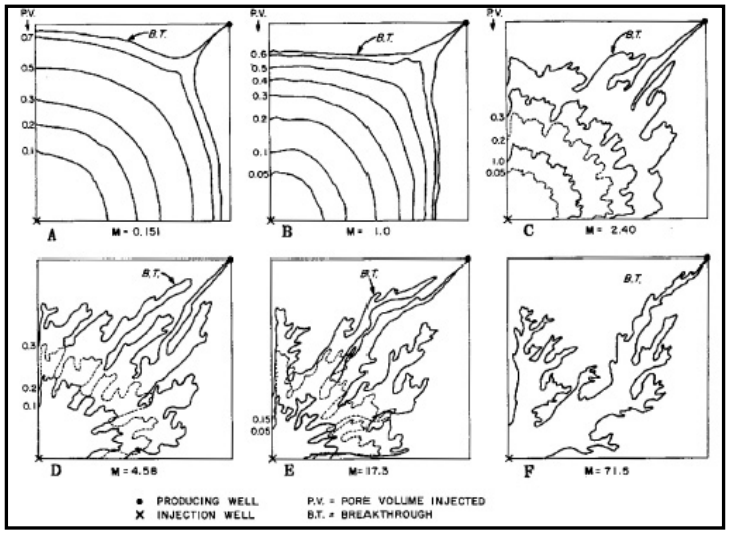

Figure 1.11 - An illustration showing the effect of viscous fingering under different mobility ratios (M). Higher mobility ratios create more unstable fingering and quicker CO_2 breakthrough times (Habermann 1961).

As the viscous fingers penetrate through the reservoir, as shown in Figure 1.11, the CO_2 breakthrough time is significantly reduced. These unfavorable mobility ratios that develop between oil and CO_2 also decrease the areal sweep efficiency, defined as the fraction of the total reservoir area that is invaded by the injected fluid (Klins 1984). Figure 1.12 shows the relationship between mobility ratios and the areal percentage of

reservoir swept by CO_2 in a standard five-spot pattern (4 injectors and 1 producer). It is also important to note from Figure 1.12 that as the volume of injected CO_2 increases the areal sweep efficiency increases, creating a situation where large volumes of anthropogenic CO_2 can reduce the areal sweep inefficiencies associated with higher mobility ratios. This is particularly true for mobility ratios between two and twenty.

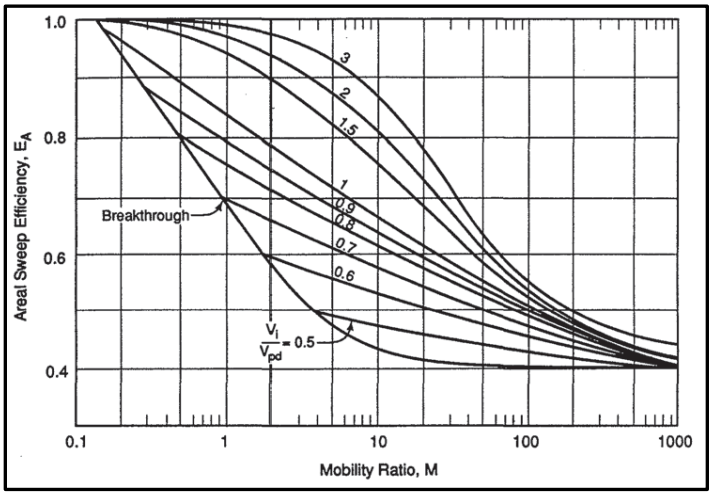

Figure 1.12 - Graphical representation showing the relationship between, mobility ratio, volumes injected, and areal sweep efficiency in a standard five-spot pattern. Modified from (Caudle and Witte 1959)

Viscous forces influence both microscopic and macroscopic convective dispersion. The microscopic and macroscopic variations seen in a geologic reservoir are the mechanisms for initiating a viscous finger. On the microscopic level, varying pore throat sizes can create fingering which can manifest to larger scale fingers. As low-viscosity CO_2 preferentially flows through wider pore throats, oil trapped by small pore throats is bypassed. With a viscosity closer to oil, CO_2 is less likely to bypass the smaller pore throats and contact more of the trapped oil. On a macro level, preferential flow paths develop from permeability variations or simply referred to as heterogeneity.

The K-factor method, developed by E.J. Koval for linear miscible displacement, is a modification of the Buckley-Leverett method used for predicting oil recovery from

an immiscible displacement. This K-factor technique is used to estimate areal sweep efficiency and oil recovery for miscible floods based on viscous fingering and reservoir heterogeneity. Matching laboratory results from various studies, Koval derived the following equation for an effective viscosity ratio (Koval 1963):

$$E = \left[0.78 + 0.22\left(\frac{\mu_o}{\mu_{CO2}}\right)^{1/4}\right]^4 \quad \text{(Eq. 1-11)}$$

E = effective viscosity ratio between the solvent (CO_2) and oil fingers
μ_o = oil viscosity, cp
μ_{CO2} = carbon dioxide viscosity, cp

From this, Koval developed the K-factor, where:

$$K = EH \quad \text{(Eq. 1-12)}$$

K = K-factor
E = effective viscosity ratio (Eq. 1-11)
H = heterogeneity factor derived from Figure 1.13

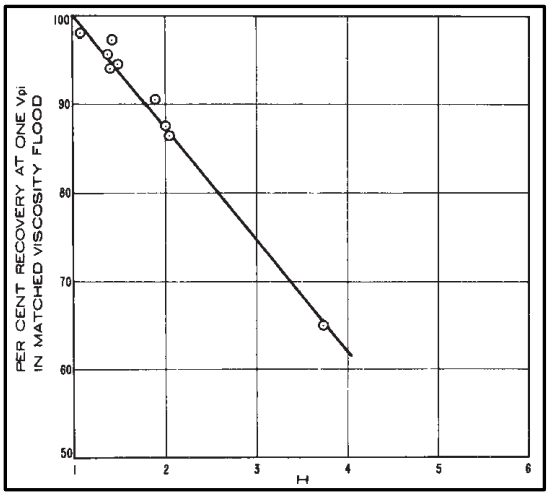

Figure 1.13 - Heterogeneity Factor (H) developed by Koval, where heterogeneity is characterized by the percent of oil recovered at 1 PV injected (V_{pi}). (Koval 1963).

With the K-factor (K), the pore volumes of solvent (CO_2) injected at breakthrough is found with the following equation (assuming 5-spot well pattern):

$$V_{pCO2,BT} = \frac{1}{K} \quad \text{(Eq. 1-13)}$$

$V_{pCO2,\,BT}$ = pore volumes of CO_2 injected at breakthrough
K = K-factor (Eq. 1-12)

After breakthrough, Koval developed the following equations to calculate oil recovery and fraction of solvent (CO_2) in the effluent, respectively (Koval 1963):

$$N_{pv} = \frac{2[(K)(V_{pi})]^{0.5} - 1 - V_{pi}}{K-1} \quad \text{(Eq. 1-14)}$$

$$f_{se} = \frac{K - \left(\frac{K}{V_{pi}}\right)^{0.5}}{K-1} \quad \text{(Eq. 1-15)}$$

N_{pv} = oil recovery, fractional PV
V_{pi} = pore volumes injected, PV
f_{se} = fractional flow of CO_2 in the effluent

The fractional oil recovery (N_{pv}) from Eq. 1-15 is equivalent to the sweep efficiency (E_A) from Figure 1.12, where N_{pv} is the volume of oil produced as a fraction relative to the total displaceable oil volume. If all the displaceable oil is produced then the sweep efficiency (E_A) equals 1.0 or 100%. The volume of displaceable oil can be found using the following equation (Green and Willhite 1998):

$$V_{pd} = 0.1781Ah\phi(S_{oi} - S_{or}) \quad \text{(Eq. 1-16)}$$

V_{pd} = displaceable PV of oil, bbl
A = reservoir area, ft^2
h = reservoir height, ft
ϕ = porosity, frac.
S_{oi} = initial oil saturation, frac.
S_{or} = residual oil saturation, frac.

Claridge developed a second areal sweep correlation, using Koval's effective viscosity ratio (E) from Eq. 1-11 and model data from (Caudle and Witte 1959). The following equations show Claridge's correlation (Claridge 1972):

$$F_{ibt} = \left[\frac{0.9}{M+1.1}\right]^{0.5} \quad \text{(Eq. 1-17)}$$

$$\frac{E_A - F_{ibt}}{1.0 - E_A} = \left(\frac{1.6}{E^{0.61}}\right)\left(\frac{F_i - F_{ibt}}{1.0 - F_{ibt}}\right)^{\frac{1.28}{E^{0.26}}} \quad \text{(Eq. 1-18)}$$

$$E_A = \frac{N_p}{V_{pd}} \quad \text{(Eq. 1-19)}$$

F_{ibt} = PV of CO_2 injected at breakthrough
M = mobility ratio (Eq. 1-10)
E_A = areal sweep efficiency, %
E = effective viscosity ratio (Eq. 1-11)
F_i = PV of CO_2 injected
N_p = oil produced
V_{pd} = displaceable PV of oil (Eq. 1-16)

Both the Koval and Claridge correlations provide established methods for estimating oil recovery and sweep efficiency for a CO_2 miscible displacement. The correlations should be used as predictive tools for EOR performance. Knowing the typical emission rates from any anthropogenic CO_2 source will be critical for EOR operators to predict and quantify the impact to oil recovery under different operational conditions. Historic emission rates can be used directly as pore volumes injected (P_{vi}, F_i) through the two correlations. With the large volumes of CO_2 emitted from coal-fired power stations, CO_2 breakthrough will be critical to manage and optimize through well placement and well pattern development.

1.5.4.2 Heterogeneity

Quantifying heterogeneity and permeability variations is a difficult task all reservoir engineers must deal with. Koval's method for quantifying heterogeneity, seen in Figure 1.13, is widely accepted because it includes the effects of dispersion and channeling within the reservoir. Koval characterized rock heterogeneity by the percentage of oil recovered after 1 PV of solvent (CO_2) has been injected (Koval 1963). From this criteria, a homogeneous system will recovery 99% of the displaceable oil after 1 PV of solvent is injected, equaling to a heterogeneity factor (H) of one. The extent of heterogeneity is then quantified from this homogeneous point (H = 1), where a heterogeneity factor greater than one represents a higher degree of heterogeneity based on a lower oil recovery after 1 PV of solvent is injected. Figure 1.13 was correlated from displacement experiments on a variety of heterogeneous sandstone cores, where Koval found that heterogeneity was constant for each core sample regardless of the mobility ratio (Koval 1963). To a geologist this is a somewhat obvious finding as heterogeneity is a property of the core sample and mobility ratio is a property of the fluids within the sample.

Koval's laboratory test of heterogeneity only represents core-scale permeability variations, not macroscopic heterogeneities that can be more influential towards the development of viscous fingering. These macroscopic heterogeneities are dictated by depositional characteristics, where reservoirs deposited in a fluvial system will have a different orientation of macroscopic heterogeneities and viscous fingering than reservoirs deposited in a shallow tidal environment, for example. It is up to the geologist to interpret inter-well and reservoir scale heterogeneities based on well log correlations and core samples from different wells across the oil field.

It is widely accepted through the petroleum industry that the Dykstra-Parsons coefficient can numerically represent reservoir-scale heterogeneity (Green and Willhite 1998). The coefficient is determined based on the assumption that permeability data across the reservoir can be represented by a log-normal distribution. The calculation requires plotting the frequency distribution of the reservoir permeability data on a log-normal probability graph. The coefficient can be found by arranging the permeability values in descending order and calculating, for each permeability measurement, the percent of samples with permeabilities greater than or equal to that value. Once this distribution is established the Dykstra-Parsons coefficient of permeability can be calculated (Dykstra and Parsons 1950):

$$V = \frac{k_{50} - k_{84.1}}{k_{50}} \quad \text{(Eq. 1-20)}$$

V = Dykstra-Parsons coefficient
k_{50} = permeability value at k ≥ 50% (the log-mean perm.)
$k_{84.1}$ = permeability value at k ≥ 84.1%, (one std. dev. from the mean)

A homogeneous reservoir has a Dykstra-Parsons coefficient that approaches zero, while a very heterogeneous reservoir approaches one. Petroleum reservoirs typically have a Dykstra-Parsons coefficient of permeability variation between 0.5 and 0.9 (Dykstra and Parsons 1950). To check his displacement experiments for quantifying heterogeneity, Koval plotted his results versus the Dykstra-Parsons coefficient, as seen in Figure 1.14.

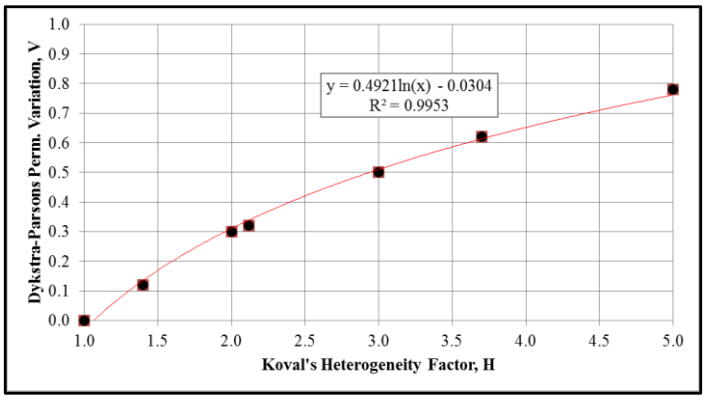

Figure 1.14 - Relationship between Koval's Heterogeneity Factor (*H*) and Dykstra-Parsons Permeability Variation (*V*). Modified from (Koval 1963).

The effect of depositional stratification or vertical heterogeneity can also be characterized using the Dykstra-Parsons coefficient. Vertical heterogeneity is a critical aspect towards estimating vertical sweep efficiency of CO_2 displacing oil.

1.5.4.3 Gravity Segregation & Vertical Sweep

To determine overall volumetric displacement efficiency, the areal sweep efficiency must be combined with the vertical sweep efficiency, which is controlled by three main factors (Green and Willhite 1998):

- gravity segregation from density differences
- vertical heterogeneity
- mobility ratio

As mentioned in Section 1.5.2, the density of CO_2 and crude oil is directly related to the reservoir temperature and pressure, while the crude oil density is also determined by hydrocarbon composition. With a large enough density difference between CO_2 and oil, vertical flow can be a significant component of fluid flow even when the principal direction of flow is horizontal (Green and Willhite 1998). At greater depths with higher temperature and pressure, the density difference between CO_2 and oil becomes smaller to the point where CO_2 can be denser than oil, reducing the impact of gravity segregation.

It has been observed that higher injection rates can increase the vertical sweep efficiency as the lighter solvent or CO_2 has less time to migrate upwards (Craig, Sanderlin et al. 1957). This observation is directly applicable to the injection environment proposed in this study, where large volumes of anthropogenic CO_2 are used for EOR. With proper well completions, higher injection rates from a LVA CO_2 source could improve the stability of CO_2 vertically sweeping through the reservoir.

Stalkup (1983) modified work from Craig et al. (1957) to create of rough method for estimating vertical sweep efficiency for tertiary recovery. The underlying assumption for this method is that no viscous fingers develop, where vertical sweep is dominated by a single gravity tongue. Given the high injection rates expected in this study and the typical viscosity difference between CO_2 and oil, this rough estimation of vertical sweep is considered irrelevant for this work. Numerical simulations are the best approach for analyzing vertical sweep given the dynamic reservoir characteristics involved with quantifying vertical sweep.

1.5.5 Well Design and Production Facilities

As seen in Section 1.4, the expansion of CO_2 pipelines for emissions mitigation and EOR supply will require considerable infrastructure development. Once the CO_2 reaches an EOR and/or storage site, additional facilities are needed to safely and effectively handle the CO_2 and any produced hydrocarbons. As a potentially corrosive gas, CO_2 can present several problems for EOR operators. On-site pipelines, packers, tubing, casing, wellbore cement, and separation facilities all need to be protected from the corrosive forces of CO_2. From over 40 years of CO_2 flooding, there is significant experience and technology for handling CO_2, a major benefit for large volume injection

and storage of CO_2. The American Petroleum Institute (API) has established specifications and recommended practices for well and field piping, cements, tubing, and wellhead design (Meyer 2007). In addition, the National Association of Corrosion Engineers (NACE) and the American Society of Mechanical Engineers (ASME) have supplemental materials that address recommended practices for safely handling CO_2.

CO_2-EOR injection wells can either be drilled as new wells or re-completed from existing production or water injection wells. In current EOR operations, using natural CO_2 sources, the injected fluid contains 92 - 97% CO_2 (Meyer 2007). With CO_2 being a corrosive fluid, both the new and re-completed wells will certainly need corrosion resistant alloys (CRA) typically made with chromium, nickel, or manganese (Benge and Dew 2005).

When re-completing a well, running cement bond logs (CBL) are important to assess the cement integrity and sealing potential between the casing and formation. If the cement bond appears inadequate, a squeeze cement procedure must be implemented and checked to ensure an effective bond between the casing and formation. A casing mechanical integrity test should also be run to check that the wellbore is competent under higher pressures. If the casing appears to leak, it must also be re-sealed by squeeze cementing (Meyer 2007).

Once a CO_2 flood is implemented for EOR, additional surface facilities are needed. A distribution system of pipelines must transport oil, brine, and CO_2 to and from various injection wells and production wells. As volumes of CO_2 are produced from the reservoir, gas processing systems are needed to separate the CO_2 and any natural gas from the produced oil. From this point, the CO_2 is recycled and re-injected into the reservoir and hydrocarbons are processed for market. Sizing the CO_2 separation facilities for recycling is a major capital expense, especially for EOR operations that would inject

large volumes of anthropogenic CO_2. The CO_2 separation process at the oil field is not considered in the LVA CO_2 supply test cases explored in this study.

1.5.6 Engineering Differences between EOR and CCS

The fundamental differences between the objectives of EOR and CO_2 storage create additional reservoir engineering challenges. For EOR, the cost associated with oil production is directly related to the purchase cost of CO_2. This causes the focus of engineering to be on minimizing the amount of CO_2 injected per barrel of oil produced (Jessen, Kovscek et al. 2005). For pure carbon sequestration, the objective changes to maximizing the amount of CO_2 ultimately stored in a reservoir. For example, when an EOR operation is decommissioned, a process of blowdown is usually implemented to vent CO_2 from the reservoir for reuse in another nearby well pattern (Bock, Rhudy et al. 2003). To maximize permanent CO_2 storage, a blowdown phase cannot be implemented in a combination EOR-CCS operation, as seen at the Weyburn Field in Canada.

A water-alternating-gas (WAG) injection, where alternating slugs of water and CO_2 are injected, can be implemented to maximize sweep efficiency of oil. A WAG injection is also implemented in areas with limited CO_2 supply. The benefit of a WAG injection is that, due to buoyant forces, water sweeps a lower portion of the reservoir while gas tends to sweep the upper portions (Jessen, Kovscek et al. 2005). With a WAG injection, water also reduces the mobility of CO_2, minimizing the effects of viscous fingering. By injecting water with CO_2, the ultimate CO_2 storage capacity of an EOR

operation is reduced by the volume of water injected. It is assumed, in this study, that a WAG injection cannot be implemented in a combined EOR-CCS operation where CO_2 supply is not an issue and void space available for permanent storage must be maximized.

Chapter 2: Analytic and Numerical Methods for Modeling Anthropogenic CO_2-EOR

2.1 CO_2 Supply Characteristics

The underlying issue with using a large coal-fired power plant to source an enhanced oil recovery (EOR) operation is the dynamic and relatively uncertain nature of its CO_2 emissions. A coal-fired power plant is built to supply electricity and the electric grid is monitored and adjusted to meet electricity demand on an as-needed basis. In order to deliver the right amount of electricity, as demand fluctuates, power-generating stations must be ramped up, ramped down, or even turned off to not exceed or fall behind current demand. Typically, coal-fired power plants and nuclear power plants operate at a relatively constant power output, supplying the baseload of electricity. Gas-fired power plants are characteristically easier to ramp up and down, so they supply base-load and peak-load electricity. Even through coal-fired power plants provide the baseload, their electricity output and therefore CO_2 emissions still have significant fluctuations on a daily and seasonal basis (Fig. 2.1). In addition to these demand fluctuations, a coal-fired power plant must shut down some or all the electricity-generating units for periodic maintenance. During this time no or little CO_2 would be delivered to any EOR operation setup to receive the coal-fired power plant's emissions.

The daily and seasonal fluctuations in electricity demand are dictated by several factors. On a daily basis, the peak periods of demand are seen in the late afternoon, early evening which is typically the hottest part of the day as most people are returning home from work. In the middle of the night when most people are asleep, the demand for

electricity is low. On a seasonal basis, the regional weather dictates the electricity demand. In more southern states, the hot summer months are periods of greatest power demand as air conditioning is running most of the day. The northern states experience their greatest electricity use during the colder winters when a lot of electricity is used to heat homes and offices. Abnormal seasonal conditions, like an extremely cold winter or hot summer will increase CO_2 emissions, with the potential to exceed pipeline and injection capacity of any EOR operation using anthropogenic CO_2.

It is clear that careful characterization is needed to understand the anthropogenic CO_2 source and its power generating patterns. If the CO_2 is being captured from a gas-fired power plant providing only peakload power, the daily and seasonal fluctuations in output will be more severe than a baseload coal-fired power plant. A CO_2 supply contract between an EOR operator and electric utility must be built from previous CO_2 emission rates and patterns. When engineering the CO_2 capacity of an EOR/CCS system, there must be flexibility to adjust to significant changes in electricity demand due to abnormal weather or local population growth.

Along with the intermittency associated with power generating CO_2 sources, the volume of emissions exceeds any volume of natural CO_2 being used in current EOR projects. The capacity to inject this large volume of CO_2 is a significant issue if the EOR operator is expected to eventually store all CO_2 received from a coal-fired power plant. Figure 2.1 illustrates both the magnitude of intermittency and increase in volume from a coal-fired power plant compared to an actual 100% CO_2-EOR operation used as an analog throughout this study. This chapter will setup the assumptions and methods for analyzing the impacts to design associated with using a coal-fired power plant as a direct CO_2 source for an EOR operation.

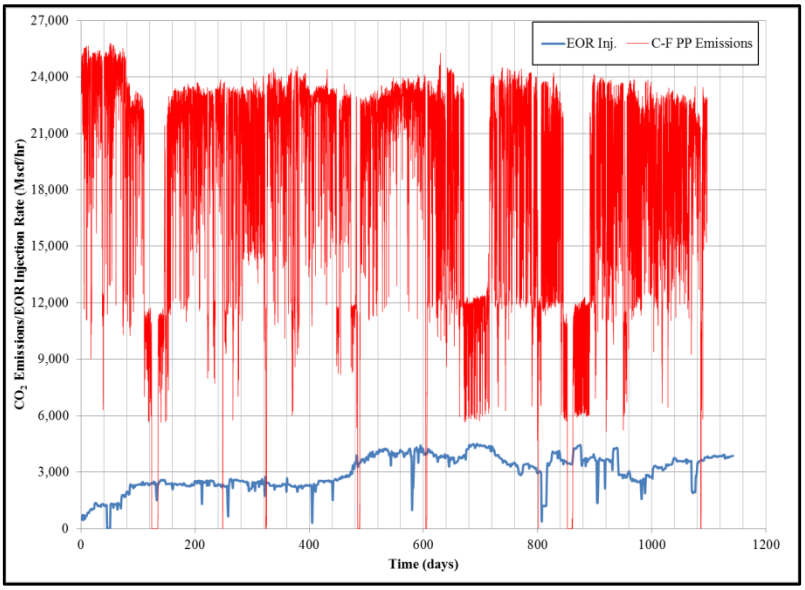

Figure 2.1 - Comparison between 3 years of CO_2 emissions from a coal-fired power plant (C-F PP) and injection rate for a 100% CO_2-EOR operation using naturally produced CO_2.

2.2 Operational Assumptions for CO2 Capture and Transport

This report has the unique opportunity to use hourly CO_2 emission rates over three years from an actual coal-fired power plant in Texas and create a scenario where the emissions are directly injected for an EOR operation. To setup this scenario some key operational assumptions must be established. The first assumption is that 90% of the actual emissions, seen in Figure 2.1, are captured using post-combustion techniques mentioned in Section 1.2.1. The capture rate of 90% is the typically accepted value for flue gas. A higher capture rate would begin to significantly increase costs with only minimal gains in capture volume as the thermodynamic limitations of the process are reached. Having a capture rate lower than 90% would not be as effective in a carbon-restrained environment, where an electric utility under some policy scenarios will pay a greater tax on every ton of CO_2 emitted to the atmosphere.

With the energy penalty associated with post-combustion capture, coal-fired power plants would have to burn more coal, or operate additional natural gas-fired power plants, to keep the net power output the same, and therefore actually increase the CO_2 emissions captured. Even though the increase in burning coal or natural gas is certain to happen to maintain power output when capturing CO_2, it is assumed to not apply to this study. The Texas coal plant used in this study is assumed to have post-combustion capture, but no adjustments to fuel burning and net power output are made. This study simply takes the current emissions from the coal plant, applies a 90% capture rate to those emissions and sends that into the pipeline.

The CO_2 that is captured and enters the pipeline is assumed to be 100% pure CO_2. The reason for using pure CO_2 is to simplify the supercritical delivery and injection of captured CO_2. Potential impurities from flue gas will change the supercritical properties of the piped CO_2. The hypothetical pipeline in this study will deliver the CO_2 to the EOR field as a pure supercritical fluid, at the exact rate it was captured. This creates a one-to-one system, where only CO_2 from one source is utilized at one injection site. The pipeline is assumed to have no storage capacity (no compressibility), so it does not act as a buffer to dampen intermittency associated with captured CO_2 emissions. It is likely that even a one-to-one pipeline system will dampen some of the CO_2 intermittency due to the volume capacity of the pipeline. In a larger pipeline system the dampening and CO_2 control will be greater between many sources and injection sites.

2.3 CO_2 INJECTION SCHEME

Once CO_2 reaches the injection site, it is equally divided and allocated to each injection well. After capturing 90% of the CO_2 from the flue gas, the average emissions rate from the coal-fired power plant is about 16,640 Mscf/hr. The EOR operation used in this study has 26 active injectors at the time of this report. When equally dividing the emissions among the 26 active injection wells the average injection rate is 640 Mscf/hr per well. The field itself has 50 potential injection wells, for scenarios that equally allocate CO_2 to all 50 injectors the average injection rate is 335 Mscf/hr per well. Figure 2.2 is a map showing the well locations of both the active injectors and producers, along with potential injection wells. The whole area of Figure 2.2 is not modeled, only the study area outlined in orange. The injection rates for each injector within the study area are dictated by the number of total injection wells assumed to be used across the field, either 26 or 50 injectors, and the equivalent CO_2 allocation per well for each scenario.

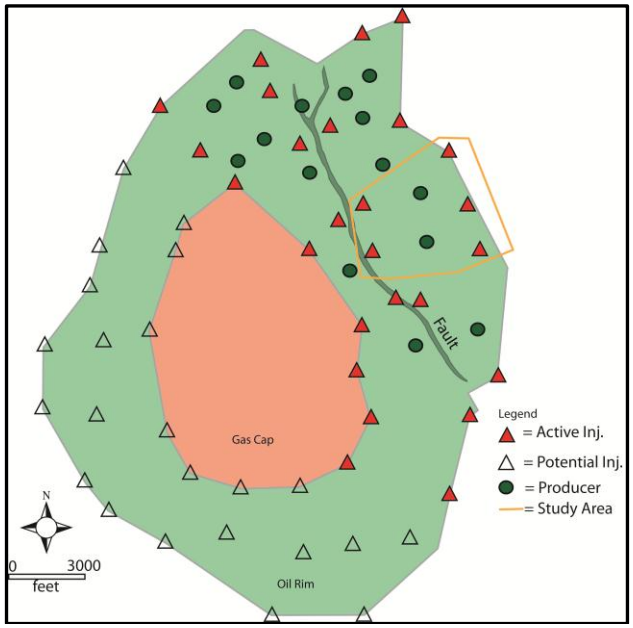

Figure 2.2 - A field map of the actual EOR operation used as an analog for this study. Simulations are run with 26 and 50 injection wells to analyze reservoir performance at different injection rates.

This study analyzes injection schemes where both the 26 active injection wells are implemented and all 50 potential injection wells are implemented, maintaining an equivalent ratio between injection and production wells. The actual number of wells within the reservoir model does not change between the 26 and 50 injection well scenarios. Within the model, injection rates per well are adjusted creating higher and lower injection rate scenarios when 26 and 50 injection wells, respectively, are used across the entire field.

The 26 injection well scenarios have an average target injection rate of 640 Mscf/hr/well for the five injectors within the reservoir model. The 50 injection well scenarios have an average target injection rate of 335 Mscf/hr/well for the five injectors in the reservoir model. Target injection rate refers to the rate of CO_2 emissions per well expected to be injected. Over time the actual injection rate per well can be reduced from the target injection rate depending on local reservoir characteristics, injection pressure limitations, and volume of CO_2 recycled and re-injected per well. If an entire field is able to inject all CO_2 as it arrives to the field then each injection well would not deviate from the target injection rate over time. As an injection well's rate declines from the target rate, it begins to lose the capacity to maintain an injection rate equal to its portion of CO_2 emissions being delivered to the field.

To improve injection capacity and production performance, optimization techniques are likely to make a significant impact. By having equal injection rates for all injectors, the results will illustrate the impact of reservoir characteristics and well placement on injection capacity and oil production. Injection capacity in this report refers to the injectivity of each injector and the entire field over time, so a well with a greater injection capacity can inject a higher rate and volume of CO_2. By definition, injection capacity for an injector declines once it is operating at the 7000 psi limit.

When CO_2 arrives at the production wells (breakthrough), all produced CO_2 is recycled and re-injected into the reservoir. The recycled CO_2 has priority and is injected before new CO_2 arriving from the coal-fired power plant. The CO_2 produced and recycled is also evenly divided among injection wells. As the volume of recycled CO_2 increases, the ability for injectors to handle their portion of the emissions arriving to the field can be affected. Once the BHP reaches its 7000 psi limit, the recycled CO_2 must be injected first, and the remaining injection capacity or injectivity of the well is used for CO_2 emissions. Eventually an injection well operating at 7000 psi can no longer handle its share of the emissions arriving to the field and its emissions injection capacity decreases. To ensure that all recycled CO_2 is re-injected, if a well cannot even handle its portion of recycled CO_2, then that remaining volume is injected by a well with higher injectivity. This is the only optimization technique used in this study, but it is important that all recycled CO_2 is injected before emissions arriving to the field. The simulations are setup where the CO_2 emissions that cannot be injected, due to extended operation at the 7000 psi limitation, are not accounted for in the numerical calculations. The volume of CO_2 emissions not injected at each well is determined by subtracting the actual CO_2 emissions injected in the simulations from the target injection rate for each injection well.

2.4 IMPLEMENTING THE EOR RESERVOIR MODEL

The reservoir model used for this study was built from an actual EOR operation in Mississippi. Denbury, the actual EOR operator, provided a generous portion of reservoir data to the Gulf Coast Carbon Center (GCCC). On-site carbon sequestration research funded by the DOE (SECARB,NETL) and conducted by the GCCC (BEG) was an additional source of reservoir data used to build the model (Choi, Nicot et al. 2008;

Hovorka, Choi et al. 2009; Meckel and Hovorka 2009; Choi, Nicot et al. 2011; Hovorka, Meckel et al. 2011). These tests and results were implemented into the calibrated and realistic GEM model used and built from in this study. The Mississippi Oil and Gas Board was a third source of data implemented into the reservoir model and used in this study. The operational scenarios developed in this study do not reflect Denbury's actual EOR operation. It is important to note that Denbury has injected 100% CO_2 without implementing any WAG injection schemes at this field.

The orange outline from Figure 2.2 shows the wells and pattern area of the reservoir model used in this study. Under different reservoir simulation scenarios, it is assumed that the performance of this well pattern is analogous to the entire field's performance. This is a simplifying assumption since each well pattern will behave differently, but excessive computing power would be required to accurately simulate the entire EOR field with all injection and production wells. It is most efficient to simulate a portion of the field, treating it as a pilot project, and assume similar reservoir response and oil recovery across the field.

2.4.1 Geologic Descriptions

The field was initially discovered in 1943 by The California Oil Company, now Chevron Oil Company, and although significant in-depth work has been done during the current revitalization, the key characteristics of the reservoir were defined during initial production (Chevron Oil Co. 1966). The geologic formation in this study is a lower Tuscaloosa reservoir deposited during the upper Cretaceous. Deep-seated salt movement shaped the dome-like structure of this field. The shape of this structure created a large gas cap overlying the oil rim seen aerially in Figure 2.2 (Chevron Oil Co. 1966). Figure

2.3 illustrates a cross-section of the dome-like structure of this oil field. From Figure 2.2 and Figure 2.3, one can see a fault oriented in a NW-SE direction. This fault is confining, acting as a barrier to fluid flow across the fault (Meckel and Hovorka 2009). An unconformity separates the lower Tuscaloosa formation from the older lower Cretaceous, Washita-Fredericksburg group (Chevron Oil Co. 1966).

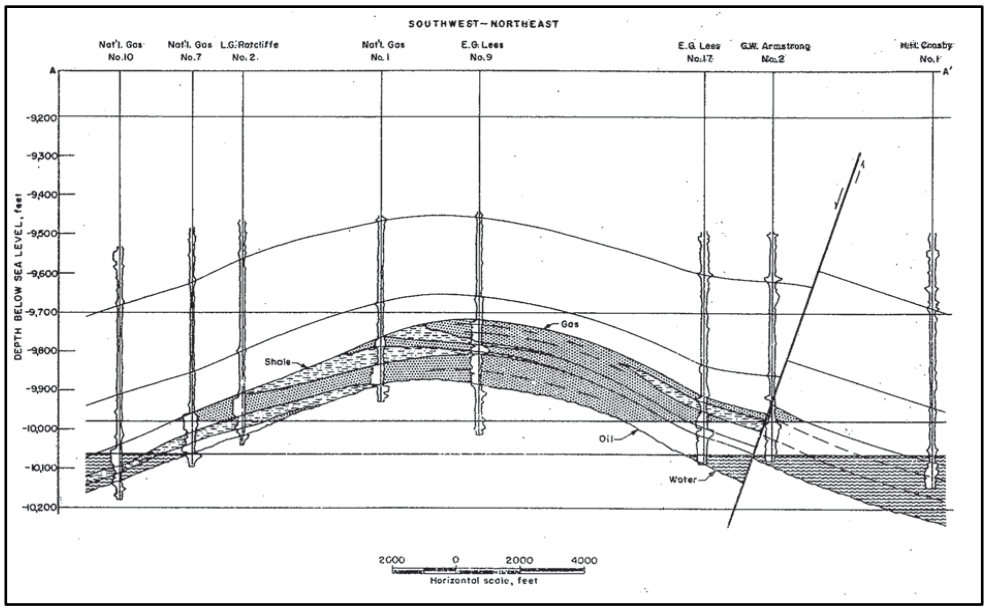

Figure 2.3 – A basic cross-section illustrating the dome-like structure and sealing fault of the actual reservoir used in this study (Chevron Oil Co. 1966).

The depositional environment of this reservoir has been interpreted as a semi-braided meandering fluvial-deltaic system (Hovorka, Choi et al. 2009), with a combination of reservoir geometries seen in the (a) and (b) illustrations of Figure 2.4. The macroscopic, inter-well fluid flow in this reservoir is dictated by the depositional geometries associated with these fluvial systems. The variation in rock types, depositional characteristics, and diagenesis created a significant degree of heterogeneity through the reservoir (Hovorka, Meckel et al. 2011). These geologic trends were

probabilistically incorporated into the reservoir model architecture. Representing depositional and diagenetic heterogeneity into this study will help test the degree to which reservoir geology impacts well placement and performance when trying to maximize oil recovery and CO_2 storage under LVA injection conditions.

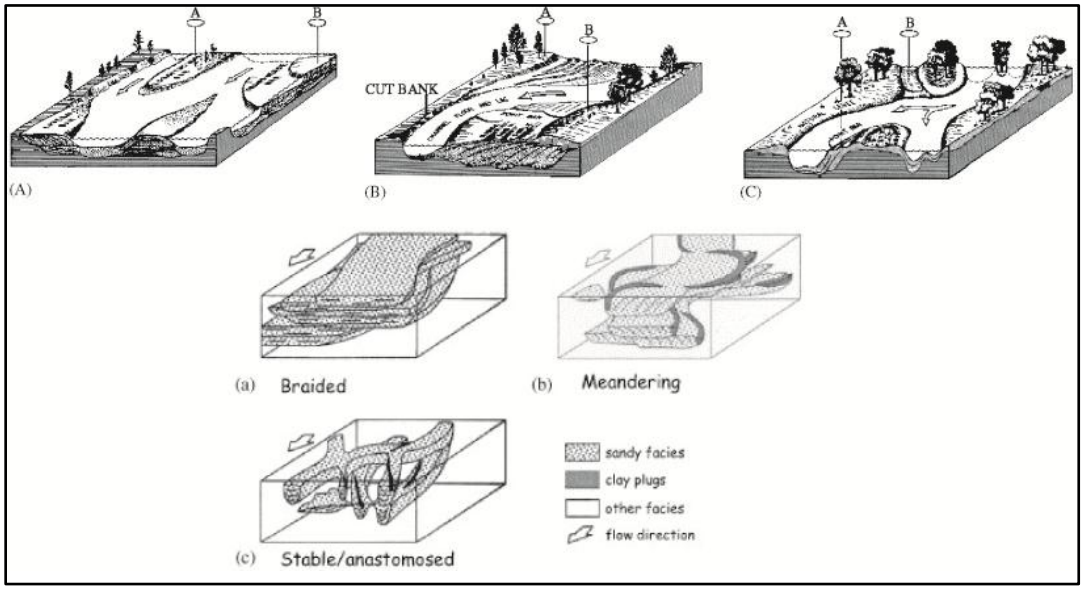

Figure 2.4 - An illustration of three primary depositional geometries associated with fluvial systems. The braided (a) and meandering (b) systems are seen in the reservoir used in this study. Modified from (Galloway and Hobday 1983).

2.4.2 Reservoir and Model Description

The reservoir model outlined in Figure 2.2 was initially constructed in Petrel (Hovorka, Meckel et al. 2011). Available data from Chevron's initial production and secondary gas recycle process (Chevron Oil Co. 1966), along with Denbury's preparation for EOR and DOE-funded research provided new logs, core, fluid samples, and 3-D seismic data (Hovorka, Meckel et al. 2011). A reservoir grid of 47x44x22 was created, with 200 feet per grid block in the x and y direction and 4 feet per grid block in the z direction. This gridding structure maintains the depositional heterogeneity of the

reservoir while reducing simulation times (Solano, Nicot et al. 2011; Hosseini 2012). With the sealing fault incorporated into the model, 253 grid blocks are empty out of the reservoir cube. The total reservoir model area is 1667 acres, with a thickness of 88 feet. Table 2.1 shows the main reservoir properties implemented into the model.

Reservoir Properties		Unit
Avg. Depth (D)	10,200	ft
Res. Thickness (h)	88	ft
Model Area (A)	1667	acre
Avg. Porosity (ϕ)	0.2042	
Avg. Horiz. Perm. (k_h)	100	mD
Avg. Vert. Perm. (k_v)	25	mD
Intitial Water Sat. (S_{wi})	0.75	
Intitial Oil Sat. (S_{oi})	0.25	
Residual Water Sat. (S_{wr})	0.40	
Residual Oil Sat. to Gas (S_{org})	0.02	
Reservoir Pressure (P_{res})	4650	psi
Reservoir Temp. (T_{res})	257	°F
Reservoir Dip	1-3°	

Table 2.1 - The main reservoir properties of this study. The red properties are initial assumptions not tied to any measured data

Having a depth greater than 10,000 feet insures that CO_2 will easily remain miscible with the reservoir oil and the hydrocarbon vapor region will only exist very close to the injection wells. The reservoir properties highlighted red, in Table 2.1, were assumptions based on typical fluid saturations after a waterflood and before CO_2 injection begins. An initial oil saturation (S_{oi}) of 25% is spread evenly through the reservoir, both horizontally and vertically. Reservoirs with a higher initial oil saturation before CO_2 injection will have a greater volume of producible oil. As mentioned in the previous chapter, one of the major benefits of CO_2 flooding as a tertiary recovery technique is the residual oil saturation relative to CO_2 (S_{org}). For analytical calculations, a value of 0.02 was assumed for S_{org} but typical values from various field studies range between 0.05 and

0.01 (Klins 1984). The residual water saturation is taken from actual relative permeability tests done on pay zone core by Core Laboratories Inc., shown in Figure 2.5 and Figure 2.6.

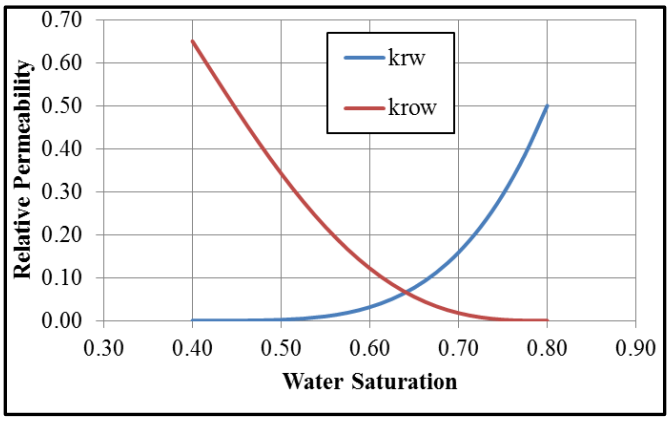

Figure 2.5 – Actual special core analysis from the reservoir pay zone showing relative permeability between oil and water (Omni Labs).

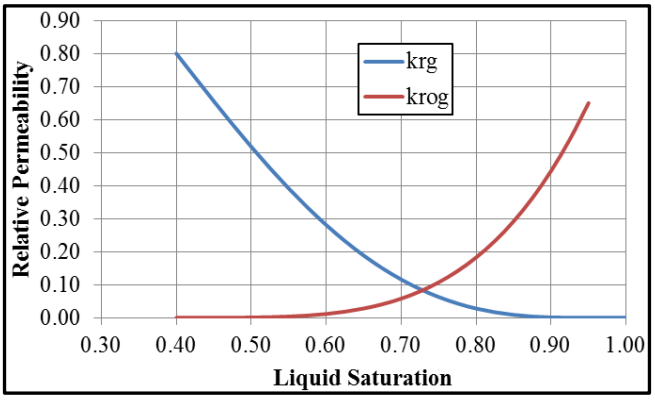

Figure 2.6 – Actual special core analysis from the reservoir pay zone, showing relative permeability between reservoir liquids and gas (Omni Labs).

Having higher residual water saturation, results of this study will reflect the lower end of reservoir performance. A field with lower residual water saturation will have a greater volume of producible oil and more pore space for CO_2 storage. From Figure 2.6 it appears that residual gas saturation is about 0.04, but as mentioned in the previous

paragraph, a S_{org} of 0.02 was used for a residual CO_2 saturation based on the fluid properties of CO_2 and the higher injection rates used in this study.

The compositional numerical simulator, GEM was used for this study because, it can assess with mass transfer between reservoir phases in a multicomponent system. The dynamic relationship between the reservoir fluids is significant in a CO_2-EOR system. In a compositional model, phase properties are calculated as strong functions of phase composition, pressure, and reservoir temperature (Klins 1984). Table 2.2 shows the primary fluid properties for this study.

Fluid Properties		Unit
Oil Density (ρ_o)	51.72	lb/ft^3
Stock Tank Oil Gravity	39.20	°API
Reservoir Oil Viscosity (μ_o)	0.317	cp
Reservoir Water Viscosity (μ_w)	0.224	cp
Formation Water Density (ρ_w)	69.20	lb/ft^3
CO_2 Viscosity (μ_{CO2})	0.067	cp
Avg. Res. CO_2 Density (ρ_{CO2})	45.11	lb/ft^3
Solution Gas Gravity (γ_g)	0.785	(air = 1)
Gas Solubility (R_s)	1,280	scf/STB
Oil FVF (B_o)	1.794	RB/STB
Oil FVF, in GEM	1.390	RB/STB

Table 2.2 - The average reservoir fluid properties used in the model (Choi, Nicot et al. 2011).

The fluid data used in this study, shown in Table 2.2, is a combination of compositional calculations done in WinProp (part of CMG) and actual fluid measurements from (Chevron Oil Co. 1966; Choi, Nicot et al. 2011). The gas solubility or dissolved gas-oil ratio (R_s) was calculated using Equation 1-7, and the oil formation volume factor (B_o) was calculated using Equation 1-8. As mentioned in the first chapter, many of the empirical equations like Equation 1-8 for oil formation volume factor (FVF) are to be used as screening tools, where the FVF calculated during numerical simulation in GEM is significantly less and probably more reasonable.

Detailed fluid composition of oil zone samples was published in (Chevron Oil Co. 1966). Unfortunately, the heptanes plus (C_6+) components were combined as one measurement. To input a correct oil phase into the numerical simulations, heavier oil components (C_7,C_{14},C_{21}) were equally added to the oil phase to match the measured oil density and gravity (Table 2.3). Appendix A contains the output file from compositional calculations done in WinProp, using the Peng-Robinson (1978) model. The output file from WinProp is inserted into the GEM input file. The viscosity calculations in WinProp were based off the Pedersen Corresponding States Model. Harvey's Method (1996) was used for Henry's Law Constant Correlation. Within the water phase, the sodium chloride (NaCl) concentration was assumed to be 0.15 weight fraction. Lastly, the simulations of this study assume no dissolution between CO_2 and reservoir water.

HC Comp.	HC mol. Frac.	Res. mol. Frac.
CO2	0.0184	0.0046
CH4	0.3999	0.1000
C2H6	0.0717	0.0179
C3H8	0.0334	0.0084
IC4	0.0104	0.0026
NC4	0.0158	0.0040
IC5	0.0123	0.0031
NC5	0.0095	0.0024
FC6	0.0248	0.0062
C7	0.1346	0.0337
C14	0.1346	0.0337
C21	0.1346	0.0337
SUM	1.0000	0.2500

Table 2.3 - Shows the hydrocarbon (HC) phase composition based off data from (Chevron Oil Co. 1966). The C7, C14, and C21 components were added to match actual oil density and gravity.

A significant amount of routine core analysis was done to develop a large distribution of porosity and permeability data over various wells. This data is critical towards creating a probabilistic reservoir model that reflects and quantifies geologic heterogeneity (Hosseini 2012). By having this data it is easier to establish both vertical

and horizontal permeability and porosity variations. Figure 2.7 shows the porosity and permeability of various sidewall and traditional core samples from three different wells in the model area.

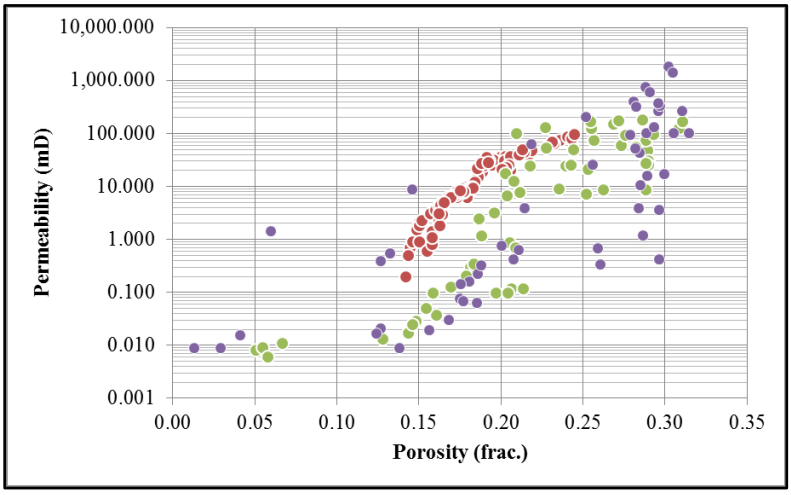

Figure 2.7 - A standard porosity-permeability plot of sidewall and normal core samples from three different wells used in this study (Omni Labs).

By extrapolating from this core data the interwell porosity and permeability were determined using geostatistics. Implementing geostatistics helps to build a three dimensional grid of porosity and permeability that accurately models the reservoir heterogeneity. Figures 2.8 and 2.9 show the porosity and permeability for each grid block of one reservoir layer, illustrating the depositional trends and degree of heterogeneity implemented into the reservoir model.

To reflect the various rock types seen in the reservoir, three main rock types were established in the model to represent some geologic variations while not creating excessive computing times from using an excessive number of different rock types. The three rock types are divided into a higher-perm sand, a silty-low-perm sand, and a low-perm shale (Hosseini 2012). Each rock type has unique relative permeability data and a distribution of potential porosity and permeability values. This orientation of rock

properties dictates the preferential flow of CO_2 through the reservoir. It was based on interpretations of heterogeneity observed in closely spaced cores and 3-D seismic data (Hovorka, Meckel et al. 2011).

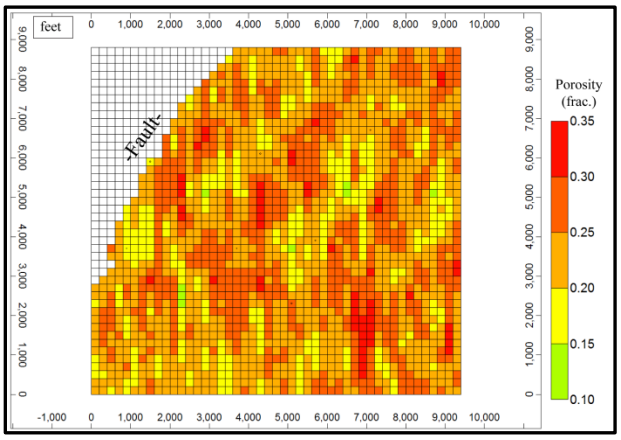

Figure 2.8 - Porosity map of the 9th layer in the reservoir model, showing the depositional trends and degree of heterogeneity associated with this reservoir.

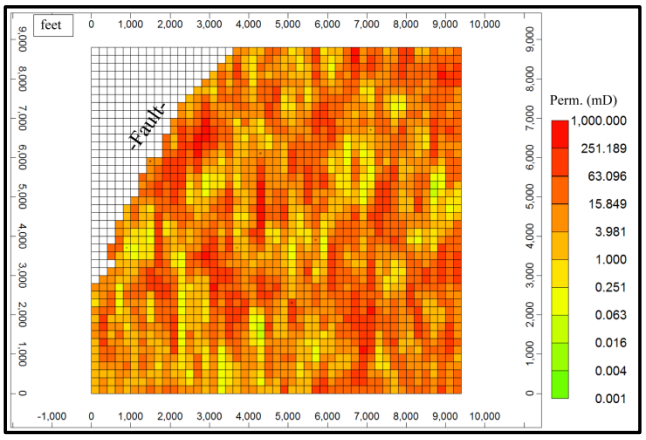

Figure 2.9 - Permeability map of the 9th layer in the reservoir model, illustrating degree of heterogeneity between high and low perm grid blocks.

From the previous two figures one can see the depositional trend of the reservoir reflecting a large meandering channel running from the bottom left to the top right. It is also easy to see the degree of heterogeneity characteristic of this reservoir, as high permeability/porosity grid blocks can neighbor a low permeability/porosity grid block.

As a fluvial system, low permeability regions can be seen parallel with the higher permeability flow paths, creating significant baffles and restrictions to fluid flow at oblique angles to the direction of depositional flow.

It is important to note that a glitch in the areal visualization occurred through the study, where the aerial view is actually from the bottom of the respective layer instead of looking from the top. This means the view of each layer is from the bottom, as if the viewer were lying under that respective layer. That is why the fault is oriented differently in Figures 2.8 and 2.9 compared to Figure 2.2. There are ways to fix this issue in the input file, but the initial attempts did not work. This glitch does not affect the physics and fluid dynamics of the reservoir simulations; it is just a flaw in the visualization output.

2.4.3 Modeling Assumptions and Boundary Conditions

This chapter focuses on establishing a reasonable and accurate injection scheme when large-volume, intermittent CO_2 sourced from a coal-fired power plant is used for enhanced oil recovery. There has been limited history matching for this model. History matching is a means of checking reservoir model assumptions to actual production and injection data, validating the accuracy of the simulations. Others have history matched the model to lower injection rates and overall recovery, but there were some imperfections in this process (Hosseini 2012). With the significantly higher injection rates and oil recovery, it is impossible to history match the model to those operating conditions. For the experiments in this study, the reservoir model is a reliable simulation environment.

The maximum injection rate is limited by pressure in the reservoir. The long term containment of CO_2 is primarily dependent on the integrity of the reservoir cap rock. Since the volume of CO_2 being injected from a coal-fired power plant is very large, the high injection pressures could fracture the cap rock. Once the cap rock, typically a thick shale, is fractured it can no longer contain the buoyant reservoir fluids as the anthropogenic CO_2 can migrate into overlying formations.

Along the U.S. Gulf coast the typical fracture gradient is between 0.7 – 0.8 psi/ft, so for a 10,200 ft deep reservoir the fracture pressure could be between 7,140 psi and 8,160 psi. For this study a safety factor of 90% was added to the fracture pressure to establish a CO_2 injection pressure limit of 7,000 psi. Since geomechanical calculations are not integrated into the reservoir simulations of this research, the actual fracture limitations from these high-pressured CO_2 injections cannot be determined directly.

Production wells, operating with no pumps and self-lifting, are assumed to produce at a constant pressure of 4,000 psi. Both injection and production wells are completed and perforated through the 88 feet of pay zone. The wells in the reservoir model were renamed to separate this study from Denbury's actual EOR operations. Figure 2.10 shows the name and placement of the wells within the reservoir model.

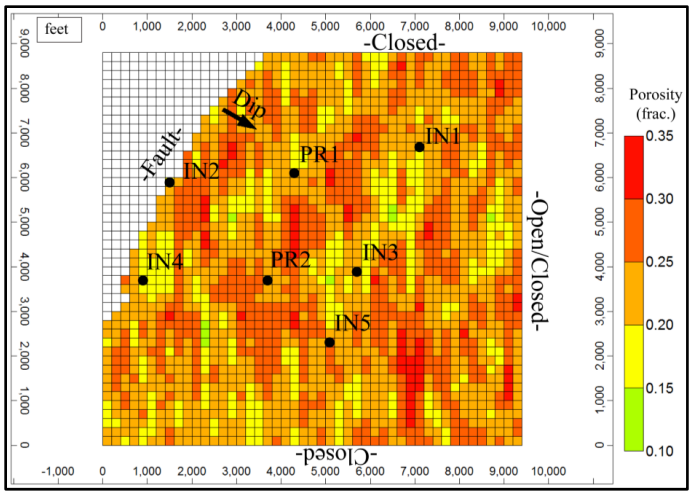

Figure 2.10 - Well name and placement map, also showing the boundary conditions. The fault is always closed. The north and south boundaries are closed for all but one simulation. The downdip boundary (east) is altered the most through the study.

Through this research, various reservoir conditions and injection schemes were changed to analyze reservoir response. The boundary conditions of this model were changed to understand how setting different boundary conditions alter simulation results. Three boundaries were unchanged and remained closed to fluid flow through the study. The overlying and underlying units of the reservoir model were assumed to be confining to fluid flow. With zero permeability, no fluids could flow vertically up or down from the reservoir into these units. The fault was assumed to also be confining to fluid flow. The other three boundaries were usually closed to fluid flow, but changed to analyze different boundary conditions. Some reservoir simulations assumed the down dip boundary was open, as if there was a moveable oil-water contact and infinite acting aquifer through the water leg. The reservoir model dips 1-3 degrees away from the fault. Figure 2.11 displays a three dimensional view of the model, showing reservoir dip away from the fault and where each well exists relative to the dip.

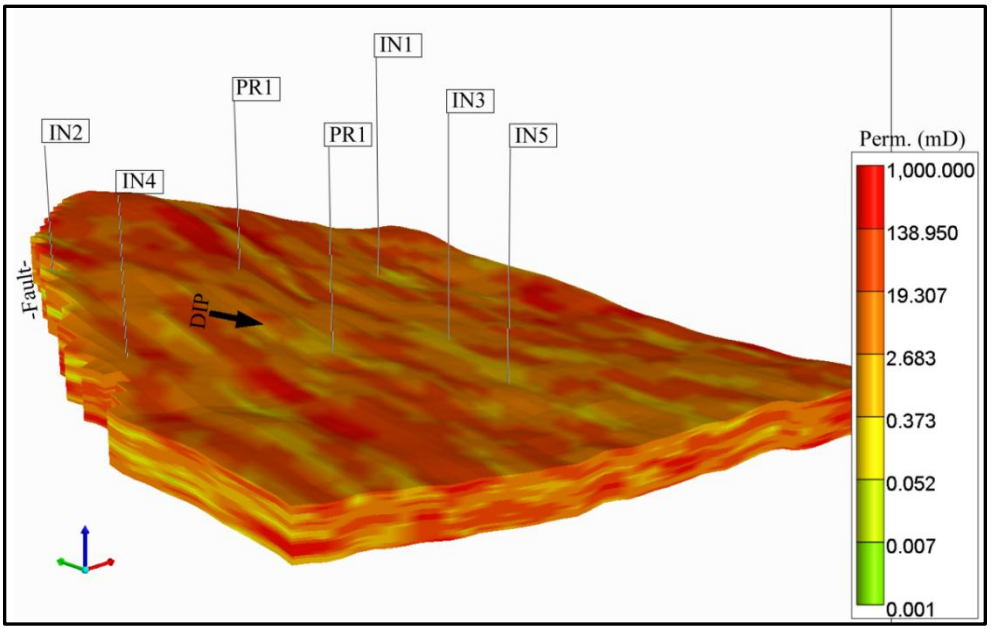

Figure 2.11 - A 3D view of the reservoir model, colored by permeability and illustrating the reservoir dipping away from the fault.

Chapter 3: Analysis of Modeling Results and Operation Implications for EOR Using a Coal-fired Power Plant to Supply CO_2

3.1 Initial Results from Reservoir Simulations

The methods and assumptions established in the previous chapter were largely modified from previous work. This chapter presents and analyzes results from various reservoir simulations using GEM, compositional modeling software within the CMG package that were run for this study to test an array of situations. Through this study, a total of 16 different simulations or experimental runs were executed. Table 3.1 displays the primary criteria of each simulation done as part of this research. This table will be referred to through the chapter. The injection pressure, rates, and degree of intermittency were the main criteria changed and analyzed through these simulations.

Run #	Duration	Pressure Limit	Recycle	Inj. Rate	Inj. Wells	Boundary
1	3 yrs	9000 psi	No	Intermittent	26	1 open
2	3 yrs	7000 psi	No	Intermittent	26	1 open
3	3 yrs	7000 psi	Yes	Intermittent	26	1 open
4	3 yrs	None	Yes	Constant	26	1 open
5	3 yrs	None	Yes	Intermittent	26	1 open
6	3 yrs	7000 psi	Yes	Intermittent	26	3 open
7	12 yrs	7000 psi	Yes	Intermittent	26	1 open
8	12 yrs	None	No	Intermittent	26	1 open
9	12 yrs	None	No	Constant	26	1 open
10	12 yrs	None	Yes	Constant	26	1 open
11	12 yrs	None	Yes	Intermittent	26	1 open
12	12 yrs	None	Yes	Fixed Intermit.	26	1 open
13	12 yrs	7000 psi	Yes	Intermittent	50	1 open
14	12 yrs	7000 psi	Yes	Intermittent	26	1 open
15	12 yrs	7000 psi	Yes	Intermittent	26	Closed
16	12 yrs	7000 psi	Yes	Intermittent	50	Closed

Table 3.1 - Details of each reservoir simulation done for this research. This table is referred to throughout the chapter.

Since the emissions data used in this study had hourly rates over three years, there were a total of 26,280 time steps used in the reservoir input file. To keep simulation times equal, the same number of time steps were used for 12 year simulations by using the emissions rate every 4th hour from the three year data and repeating that four times to create 12 years of emissions. Having over 26,000 time steps is considerably more than most reservoir simulations, so each run took over 18 hours using 2-4 processors. Macros in Microsoft Excel were vital towards properly formatting and altering the time steps between different simulations.

Initially the simulations were done over just three years, inputting the exact hourly CO_2 emissions data. This was primarily done to match directly with Denbury's EOR operation, for which there was also three years of operational data in terms of CO_2 injection rates and oil production. Given the large volume of CO_2 injection in these simulations, it was clear that matching existing production data from much smaller CO_2 injection volumes (seen in Figure 2.1) had little use to the research objectives. The injection period was extended to 12 years to better match the typical expected life of an EOR project and the longer-term operational life of a coal-fired power plant. Most engineers would consider an EOR project that can directly handle the CO_2 emissions from a coal-fired power plant for 12 years a successful project. Typically, a power plant is built to last 30-40 years, so multiple CO_2-EOR and direct CO_2 storage projects would be needed to match that time, but 12 years is a reasonable time period for constructive analysis.

As with most research, the later simulations have been more refined and focused directly on the primary research objectives. The majority of simulations analyzed in this chapter are from the more refined 12 year runs, as the input file was tweaked to more effectively evaluate the research objectives. The output data, from all simulation runs,

were systematically organized to build a standard database through the study. For most of the three year simulations, results and data are imbedded into the equivalent twelve year simulation.

It is important to note from Table 3.1, that the runs with 26 injection wells refer to a higher injection rate per well for the five injectors within the reservoir model. The runs with 50 injection wells use a lower injection rate per well for the five injectors within the reservoir model. For both situations, the simulations do not actually use 26 or 50 injection wells, it is simply used to describe and label higher and lower injection rates.

3.1.1 Injection and Reservoir Pressure Response

A reservoirs response to higher CO_2 injection rates directly impacts oil production and CO_2 storage capacity. Besides how the injected CO_2 is distributed across each well pattern, the geologic characteristics determine the reservoir pressure over time. An injection well drilled into a more permeable region will have a lower surrounding pressure allowing a greater rate of CO_2 to be injected and more oil mobilized. The opposite applies to an injection well drilled into a tighter permeability region, where the reservoir has less connected pore space, creating a higher surrounding pressure in response to the restricted flow. The response of bottom-hole pressure (BHP) for the five injection wells within the study area and reservoir model can be seen in Figure 3.1.

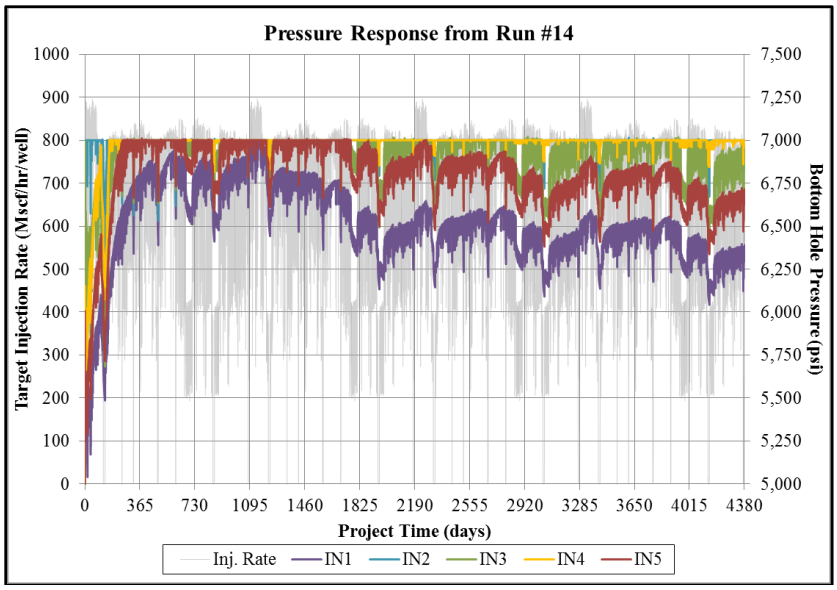

Figure 3.1 - Bottom hole pressure response relative to the target injection rate (Inj. Rate) per well. The longer an injection well operates at the 7000 psi limit, the less it is able to maintain its share of CO_2 emissions and recycled CO_2.

The target injection rate for each injector is defined as a well's equal share of the CO_2 emissions arriving to the field. From Figure 3.1 it is clear that injection pressures directly respond to changes in CO_2 injection rates. During periods of low emission rates arriving to the field, where the target injection rate per well decreases, there is an equivalent BHP response. The extent of BHP response is dictated by the surrounding geologic characteristics. The geologic characteristics also dictate the injection well performance, based on extent of operation below the 7000 psi injection limit. The best performing injector is IN1, as it operates well below the 7000 psi injection limit during the entire 12 year simulation. IN2 and IN4 operate at an almost constant BHP of 7000 psi as the permeability and surround geologic characteristics are less desirable. Once an injection well hits the 7000 psi injection limit, the injection rate begins to decline (Fig. 3.2), reducing its performance in terms of injectivity. As the injection rate declines the injector loses injectivity as it cannot meet the target injection rate. This target injection

rate is the emissions rate from the coal-fired power plant divided by the total number of injectors at the field (set at 26 or 50 wells through the study).

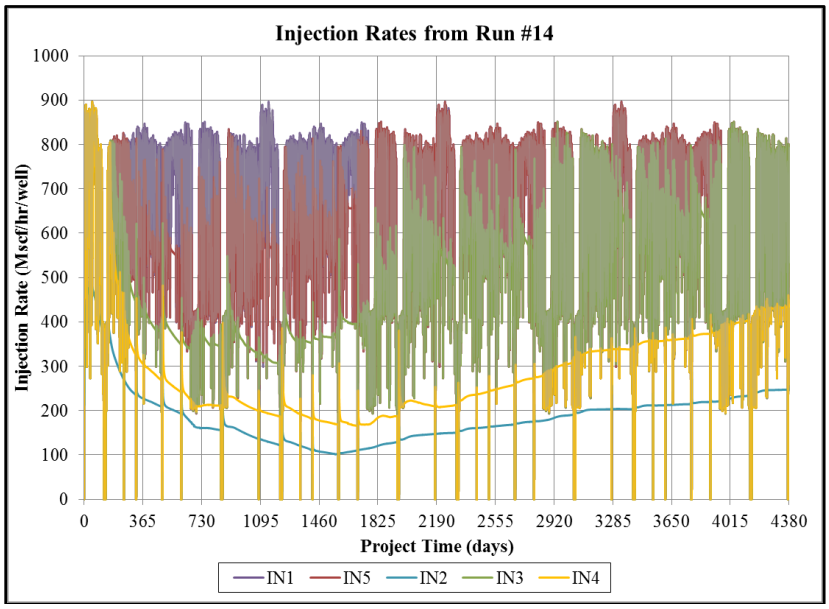

Figure 3.2 - Injection rates for each injector over time, assuming 26 injection wells for the entire field. As the BHP reaches 7000 psi, the injection rates significantly decline.

Periods of low emission rates, only temporarily relieve pressure and increase injectivity. Simulations where the entire field is assumed to have 50 active injection wells (lower inj. rate per well), the target injection rate per well is essentially cut in half. The lower injection rates improve injection well performance as three of the five injectors in the model never reach the 7000 psi injection limit (Fig. 3.3). Since these three wells never reach the pressure limit, they are able to meet the target injection rate along with their share of recycled CO_2 through the entire 12 years (Fig. 3.4). Only injection wells IN4 and IN2, which operate for significant periods at 7000 psi, are not able to meet the lower target injection rate for the 50 injection well scenarios. Both Figure 3.3 and Figure 3.4 show an increase in injectivity as injection pressures decline and injection rates increase for IN4 and IN2. Having more injection wells, which lowers the target injection

rate per well, help improve storage capacity and injectivity per well as overall injection pressures are reduced.

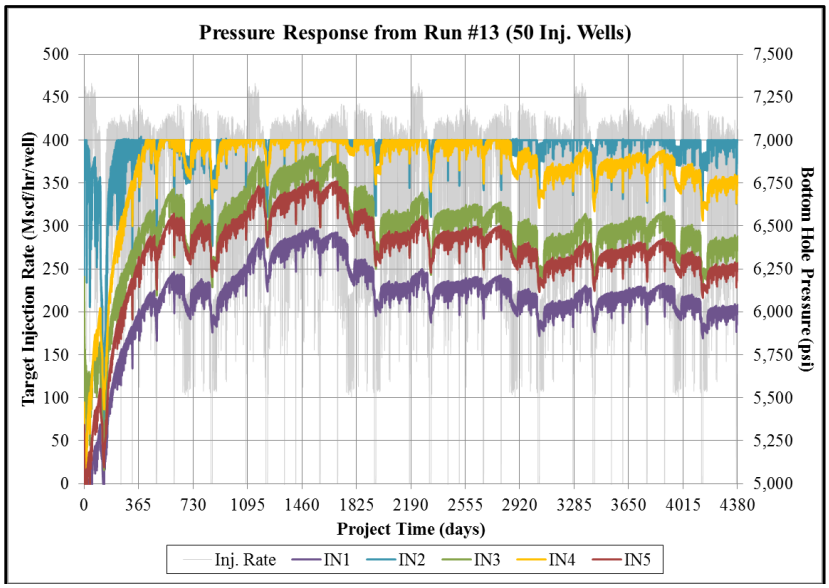

Figure 3.3 - Bottom hole pressure response for a scenario with 50 injection wells. Lower injection rates in three of the five injectors don't reach the 7000 psi injection limit.

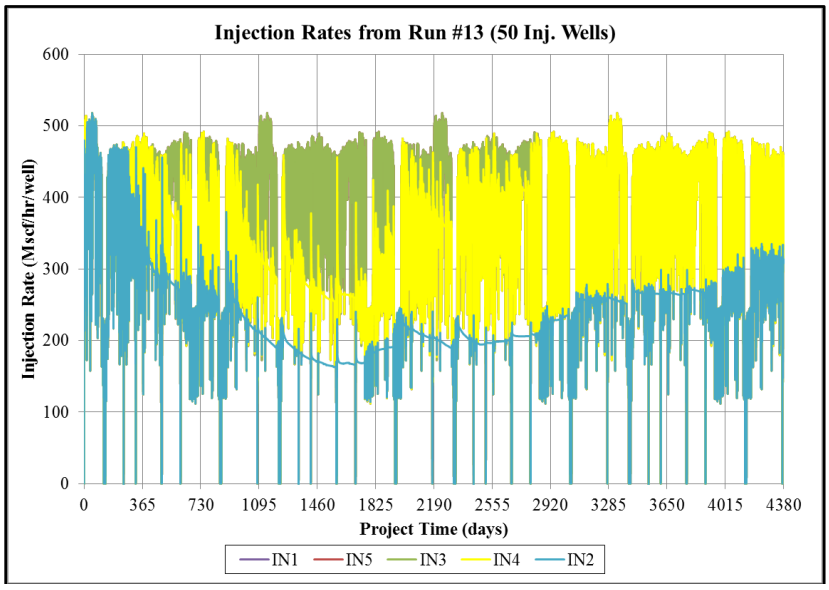

Figure 3.4 - Injection rates over time, assuming 50 injection wells for the entire field. Only injection wells IN4 and IN2 are not able to meet the lower target injection rate over twelve years. Well data is not seen from IN1 and IN5 as their rates are equal to IN3, where all three maintain their target injection rate.

The injectors that have the worst performance within the model are the two updip wells (IN2 and IN4) along the fault. Being along a closed boundary decreases the permeable flow paths for CO_2 to disperse from the injectors. For the other three injectors, which are about equivalent in terms of dip away from the fault, their performance is more dictated by their placement relative to the reservoir and depositional characteristics. The fact that each of the five injectors have their own characteristics in terms of dip and local flow potential, illustrates how much geology and reservoir properties dictate long-term injectivity and storage capacity.

The previous figures in this section assume the downdip boundary is open, as if the water contact is displaceable over time as more CO_2 is injected. As CO_2 moves across this boundary the reservoir pressure within the model remains lower compared to having that boundary closed. This boundary could be assumed closed in situations where another well pattern shares that boundary. The other two (non-fault) boundaries are assumed closed to represent the effect of an equivalent pressure increase from neighboring well patterns. Figure 3.5 shows the impact to injection pressures by closing all four boundaries to flow, which is a reasonably conservative assumption for a well pattern surrounded by other equivalent well patterns. In this case, all five injectors operate at 7000 psi for most of the 12 years simulated, limiting the CO_2 injectivity over time. There would likely be flow across these boundaries into other well patterns and downdip, but net flow between well patterns should be close to zero assuming each well pattern is relatively similar.

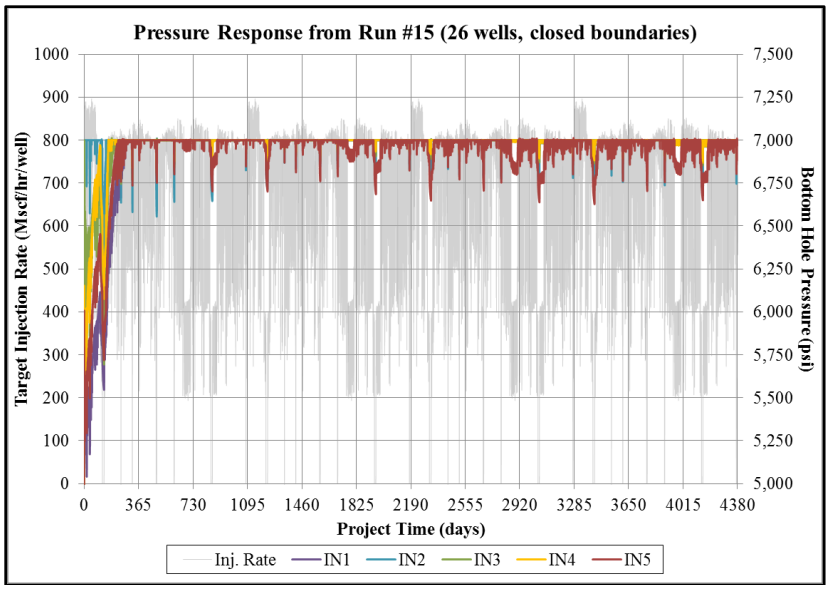

Figure 3.5 - BHP response for injectors, assuming all four boundaries are closed, where injectivity is significantly reduced because of extended operation at the 7000 psi limit.

The boundary conditions assumed for each simulation have a direct impact on the average reservoir pressure and BHP over time. Establishing reasonable boundary conditions is important to accurately model the reservoir response to different injection scenarios. It seems reasonable that each well pattern would have zero or one open boundary depending on its placement relative to the reservoir structure and characteristics of neighboring well patterns. Figure 3.6 shows how reservoir pressure within the model responds to different boundary conditions. Boundaries to neighboring well patterns are assumed closed, as net flow should be zero across the boundary. A situation where three non-fault boundaries are open (Run 6) does not seem practical as it assumes the reservoir model is the only well pattern operating within the field. From Figure 3.6 the different injection rates for the 26 and 50 injection well scenarios have a greater impact on average reservoir pressure with one open boundary. With all closed boundaries, the wells are operating at 7000 psi with nearly equal injection rates despite the number of total injectors at the field.

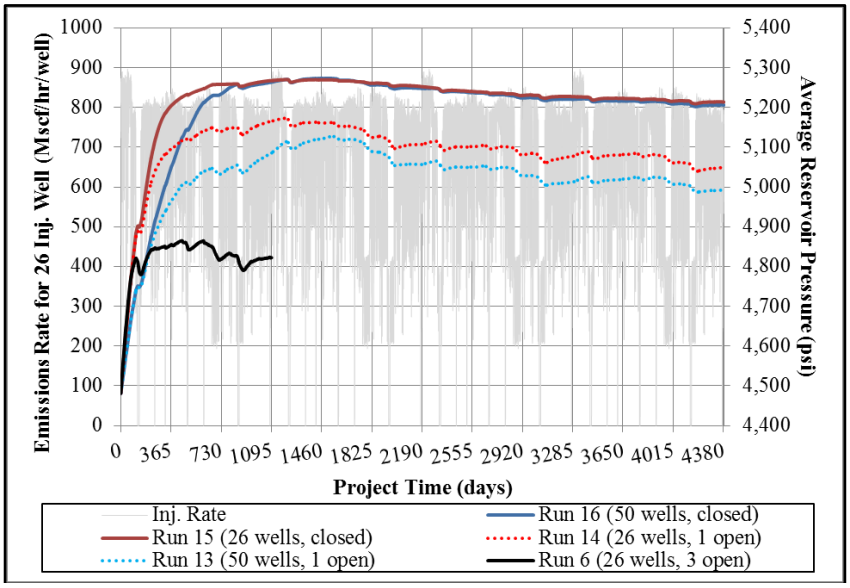

Figure 3.6 - The average reservoir pressure over time under different boundary conditions. The number of injection wells and boundary conditions are stated in the parentheses in the legend.

The fluctuations and intermittency associated with the injection stream are dampened when looking at the average reservoir pressure in Figure 3.6 compared to the grey injection rate. The BHP of the injection wells shows greater fluctuations relative to intermittent emission rates, but as the CO_2 flows from the injection wells the intermittency is dampened. For Run #6, a three year simulation with the fault acting as the only closed boundary, the average reservoir pressure has a greater response to changes in emission/injection rates and it is significantly lower than other closed-boundary simulations. The two simulations, with all closed boundaries, have only a minor response in reservoir pressure to the intermittency of the injection stream. Once an injection well is operating at the 7000 psi limit, a large decrease in the emissions rate is needed to temporarily relieve the injection pressure and decrease the overall reservoir pressure.

3.1.2 Fluid Dynamics of the Reservoir Model

The geologic characteristics and reservoir pressure determine the flow characteristics during a CO_2-EOR operation. The preferential flow paths, created by depositional trends, dominate the orientation of flow through the reservoir. Predicting how the different fluids will be distributed through the reservoir over time helps to optimize well placement and spacing. This section looks at the oil and gas saturations over time and vertically through the reservoir to understand the dynamic nature of fluid flow during a LVA CO_2 injection. The closed boundary scenarios are the main focus of this section, since no fluid is flows across any open boundaries.

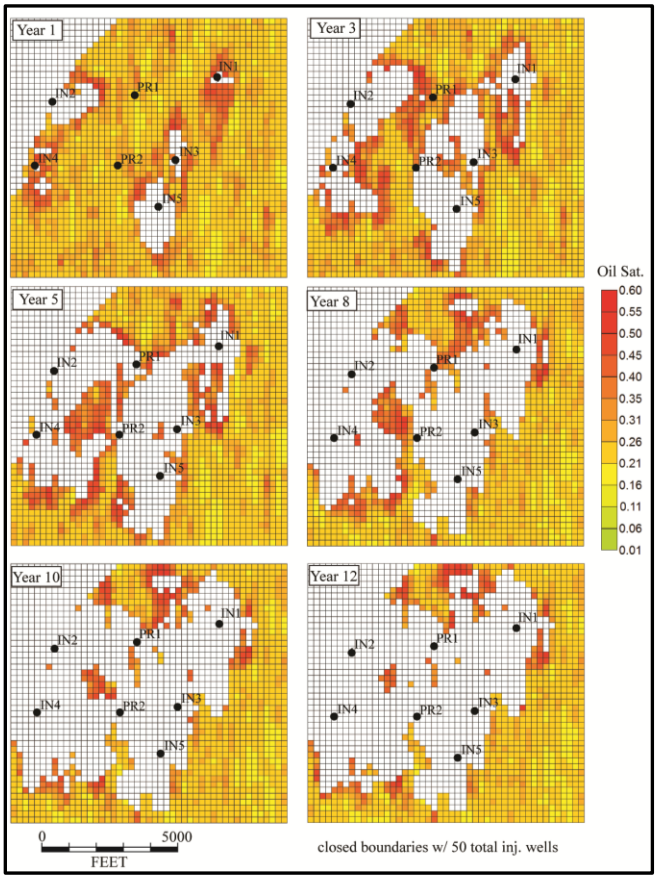

Figure 3.7a – The oil saturation in the 13th layer (middle) of the reservoir model. With all closed boundaries there is limited displacement downdip away from the fault. The fluvial depositional trends within the reservoir are also evident.

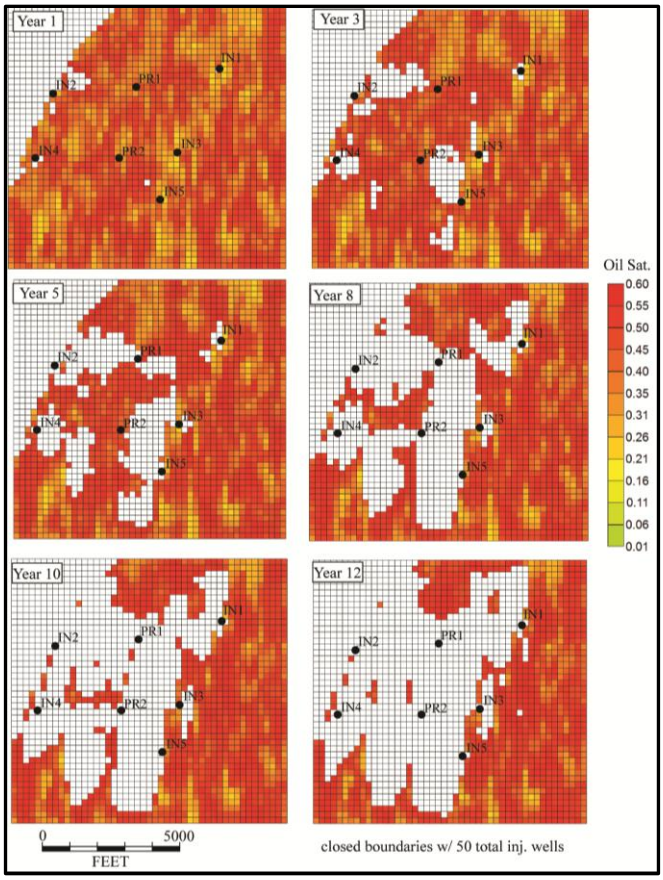

Figure 3.7b – Oil Saturation over time in the 2nd layer (top) of the reservoir model. The vertical oil distribution through the simulation can be seen by comparing this with Figure 3.7a.

At the beginning of the simulations, the oil saturation is assumed to be 25% through the reservoir. In both Figure 3.7a and 3.7b, there is a significant volume of oil remaining beyond the well pattern. Comparing Figure 3.7b to Figure 3.7a shows that a higher concentration of oil remains in the top layers along the seal. Oil production optimization could be based off the remaining oil saturation seen in Figure 3.7a and 3.7b. A larger well spacing would improve production beyond the actual well pattern used in this study. Since the placement and re-completion of these wells is based on the current, smaller-volume CO_2-EOR operation of this field, the remaining oil volume beyond the well pattern is an artifact of the reservoir model. Given the volume of CO_2 injected, most

oil is produced within the current well pattern, so a larger well spacing would seem to be effective with a LVA CO_2 injection.

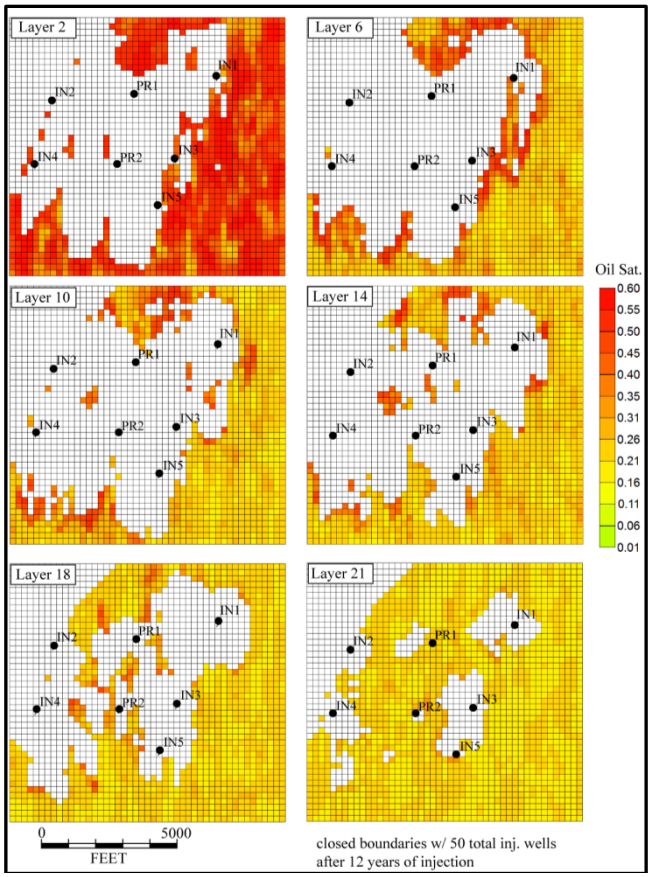

Figure 3.8 - Oil Saturation through the model after 12 years of CO_2 injection. From buoyancy effects, less oil is displaced in the lower layers, but greater saturations of oil are found in the upper layers.

The impact of CO_2 buoyancy can also be seen in Figure 3.8, where only a small portion of oil is displaced in the deeper reservoir layers compared to the more shallow layers. Since the CO_2 is more buoyant than oil, a significant volume of oil in the lower layers is bypassed and never mobilized by CO_2. From Figure 3.7b and Figure 3.8, oil is more concentrated along the top portion of the reservoir, especially in layer 2. The middle layers appear to have a similar oil distribution, while the bottom layers clearly

have minimal oil displacement from the original oil saturation of 25%. Given the vertical distribution of oil, optimized perforations or a horizontal production well completed along the top of the reservoir could help improve oil recovery. Horizontal injection wells completed along the bottom of the reservoir could further improve recovery and utilize the buoyancy of CO_2.

In Figure 3.7a and 3.7b, an oil bank forms in front of the advancing CO_2. This oil bank has a higher saturation than the static oil saturation before CO_2 began to mobilize oil. The advancement and characteristics of the oil bank are dictated by preferential flow paths through the reservoir. From these figures, depositional trends become apparent as CO_2 flows along preferential flow paths, displacing oil within those permeable fluvial trends first. Oil that remains between injectors and produces after twelve years has been bypassed in low perm zones, but that oil is being recovered slowly over time.

With an average horizontal permeability of 100 mD and an average vertical permeability of 25 mD, the average K_v/K_h ratio is 0.25 for this reservoir. The relatively high vertical permeability reduces the resistance to buoyant flow of CO_2. A lower vertical permeability would allow more oil in the deeper areas to be contacted by CO_2, increasing oil mobilization and recovery. The vertical permeability influences the extent of CO_2 buoyancy, along with oil production and CO_2 injectivity. Knowing this, Figures 3.9 and 3.10 illustrate the distribution of CO_2 over time and vertically through the reservoir under the same closed boundary conditions.

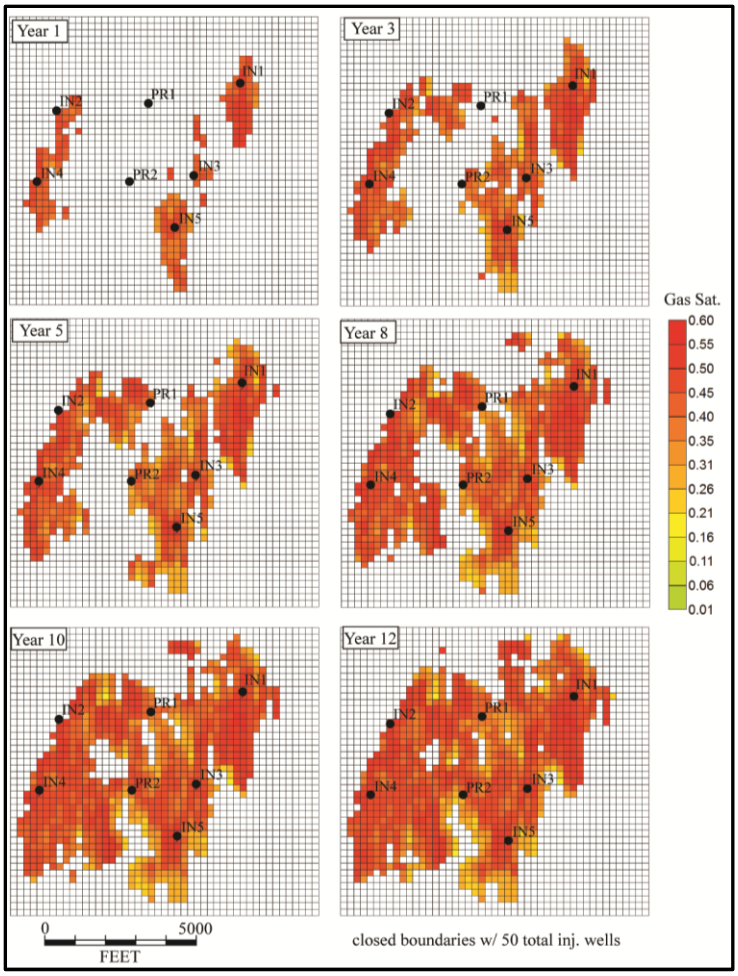

Figure 3.9 - The distribution of CO_2 over time in the 13th layer of the reservoir model. The fluvial depositional characteristics can be seen as CO_2 initially invades the higher permeability channels.

With all model boundaries closed, the expansion of the CO_2 plume becomes limited as the production of CO_2 increases and the downdip migration of CO_2 is limited. As expected, Figure 3.10 shows the buoyancy of CO_2 as higher saturations of CO_2 accumulate at the top of the reservoir.

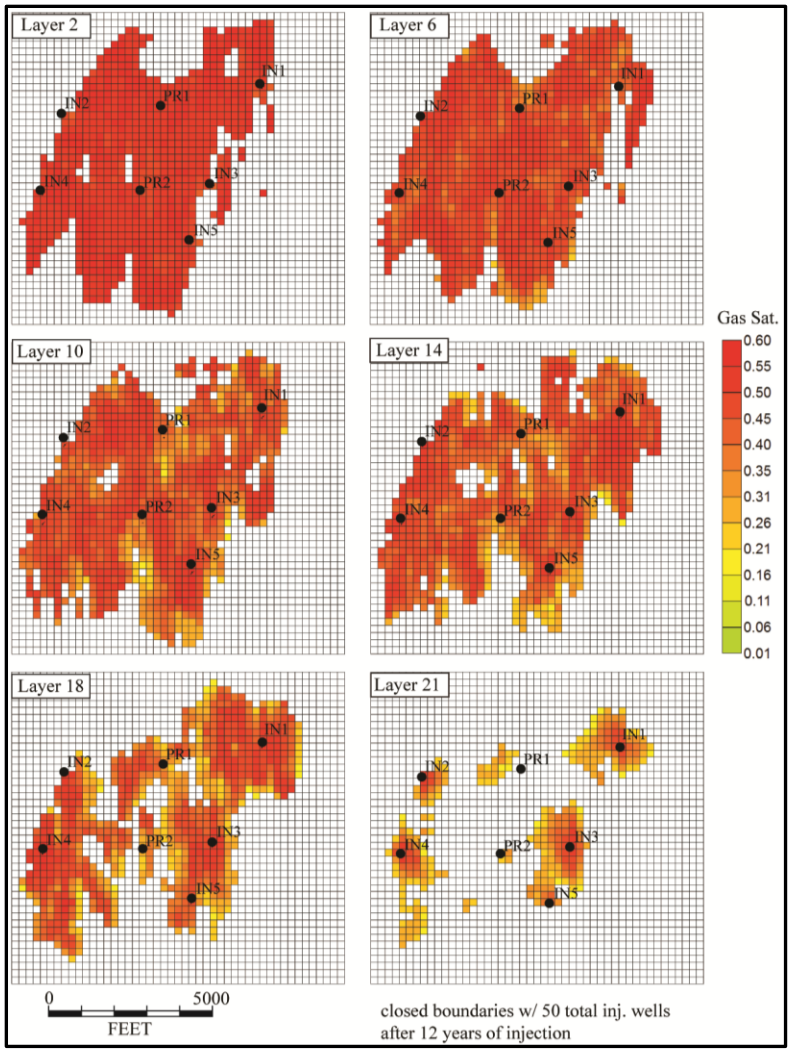

Figure 3.10 - The impact of CO_2 buoyancy is clearly illustrated in this figure as nearly maximum CO_2 saturation accumulates at the top of the reservoir after 12 years of injection.

Since the residual oil saturation to CO_2 is nearly zero, CO_2 and oil have a maximum saturation of 60% as the residual water saturation is 40%. The areas within the reservoir that the CO_2 cannot contact leaves non-contacted residual oil associated with the lower permeability units. The lack of downdip migration and vertical buoyancy of CO_2 are critical restraints for an EOR project looking to maximize oil production and long-term CO_2 storage. It seems that towards the end of the project the tendency for CO_2 to flow towards the production wells limits the downdip migration of CO_2. To mediate

this issue, additional injection wells would be needed downdip, while converting IN2, IN3, and IN5 to production wells. With greater well spacing, and more downdip production wells, the oil production and CO_2 storage volume should increase within the model.

3.2 Impact of Using a Large Volume, Intermittent CO_2 Supply

Using all of the captured CO_2 from a coal-fired power plant to supply an EOR operation creates significant operational changes in terms of CO_2 injection strategies. Both electric utilities and oil producers are interested in the impact of intermittency and large volume associated with using this type of CO_2 to supply an EOR operation. This section analyzes those unique aspects of an anthropogenic CO_2 supply in terms of oil production, CO_2 recycling and long-term CO_2 storage potential.

3.2.1 Impact of CO_2 Intermittency on Oil Production

The most unique aspect of using anthropogenic CO_2 for EOR is the inherent intermittency of CO_2 captured from a coal-fired power plant. Since the CO_2 emissions are dictated by electricity demand and periodic maintenance, the intermittency and fluctuations can be very large. The change in CO_2 emissions can go from over 20,000 tons/day to zero in the matter of hours. On a seasonal basis, the emissions volumes changes considerably but unpredictable weather and abnormal seasons can further alter normal emission rates. The capricious nature of CO_2 emission rates is a significant issue to both electric utilities and oil producers that may enter into a long-term purchasing contract for the captured CO_2. To size and design the EOR operation, oil producers need a solid understanding of what volume of CO_2 will be delivered to the field and what oil

production can be expected. If the inherent intermittency of anthropogenic CO_2 impacts oil production, then it has less value to an oil producer than more controllable, natural CO_2.

Three injection scenarios were developed to analyze the impact of CO_2 intermittency. The characteristics of each scenario are illustrated in Figure 3.11. The first scenario, Run 10, assumes a constant injection rate equal to the average CO_2 emissions rate over 12 years. The constant-rate scenario is expected to be the ideal situation for the oil producer. For an electric utility this constant scenario is almost impossible, since the CO_2 emissions are inherently variable and significant storage operations at the coal-fired power plant would be needed to absorb these fluctuations and deliver a constant CO_2 stream to the EOR operator. The second scenario, Run 12, uses the actual CO_2 emissions and its characteristic intermittency, labeled "intermit". This scenario is ideal for the electric utility as it delivers the CO_2 as it is captured, but the EOR operator must deal with the unpredictable intermittency both daily and seasonally. The third scenario, Run 13 labeled "fixed intermit.", creates an extreme situation where CO_2 emissions are delivered at a maximum rate one month and then no CO_2 is delivered over the following month. This alternation between maximum injection rates and zero CO_2 injection is repeated over the 12 year project.

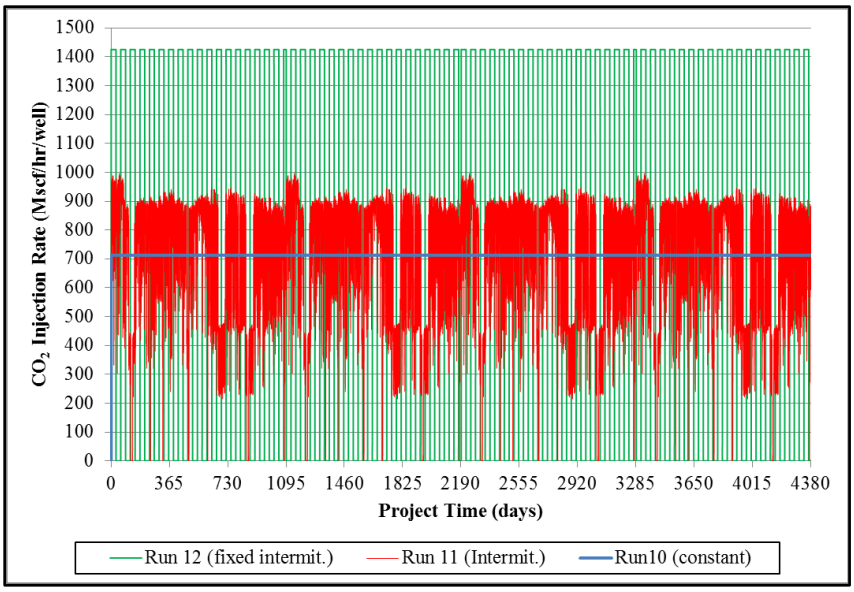

Figure 3.11 - The three different intermittency scenarios used to analyze their impact on oil production. Each scenario injects the same volume of CO_2 over 12 years.

To make each scenario comparable, after 12 years the same volume of CO_2 arrives to the oil field for all three scenarios. This insures that no scenario injects more CO_2 than another over the 12 year project life. To maintain and preserve the different intermittency characteristics, the injection pressure limit of 7000 psi is removed, allowing the injection wells to inject exactly what CO_2 is delivered to the field. In effect, this puts the reservoir at a greater depth where the fracture pressure is no longer a limiting factor for safe CO_2 injection. Instead of a depth of about 10,000 feet, one can assume the reservoir is now at a depth of 15,000 feet, allowing the injection wells to operate without any restraint.

It was originally thought that intermittency would have a negative impact on oil production. The initial 3 year simulations actually showed that intermittency increased production, but the total CO_2 injected was not equal between the scenarios and even with different volumes of CO_2 injected, the EOR efficiency in terms of BCF of CO_2 injected per MMSTB of oil produced was equal between the scenarios. Once the simulations

were carried out over 12 years and the cumulative CO_2 injected was equal across the three scenarios, it was clear that CO_2 intermittency does not impact cumulative oil production (Fig. 3.12).

Within certain time segments one scenario may produce oil at a greater rate, but over time they tend to achieve the same cumulative oil production and sweep efficiency with equal cumulative CO_2 injection. Figure 3.13 shows nearly identical sweep efficiencies over time for all three scenarios. Even at different cumulative CO_2 injection volumes, the EOR efficiency (BCF/MMSTB) for all three scenarios does not chance since this criteria is a function of reservoir characteristics and not injection rate fluctuations (Table 3.2). Figure 3.14 does show how the average reservoir pressure responds to the different intermittency scenarios, but even after 12 years the reservoir pressure is nearly the same for all three cases. As with oil production, the reservoir pressure may temporarily be greater in one of the three scenarios, but it is inevitably a function of the cumulative volume of CO_2 injected.

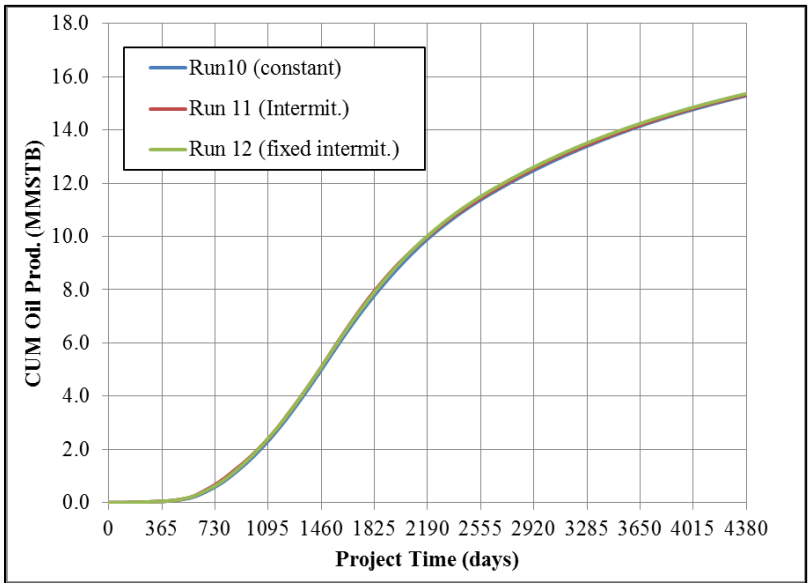

Figure 3.12 - This figure illustrates the nearly negligible impact CO_2 intermittency has on cumulative oil production.

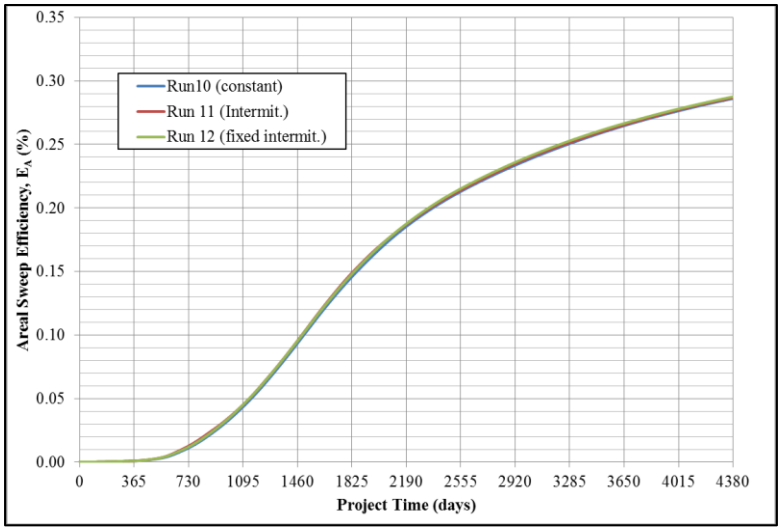

Figure 3.13 - The areal sweep efficiency for the three intermittency scenarios, using Equation 1-19. No scenario has a distinctly better areal sweep efficiency over time.

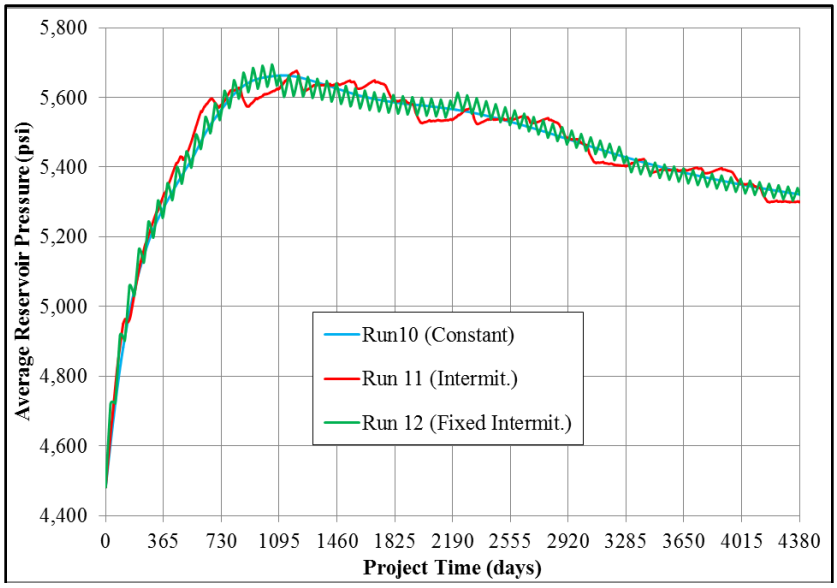

Figure 3.14 - The average reservoir pressure over time for each intermittency scenario. The two non-constant scenarios oscillate from the constant injection scenario.

Oil Efficiency (MMSTB/BCF)	
Run10	0.0215
Run11	0.0215
Run12	0.0216

Table 3.2 - EOR or oil efficiency for each intermittency scenario. This is calculated as the average volume of oil produced per billion cubic feet (BCF) of CO_2 injected.

This is a significant conclusion for oil producers, knowing that intermittency from the captured CO_2 will not impact their oil production over time. With CO_2 purchase contracts between electric utilities and oil producers, provisions about CO_2 intermittency are not necessary as long as the total volume of CO_2 delivered to the field is agreed upon and achieved over the life of the EOR operation. Since these large-volume anthropogenic sources eliminate CO_2 supply issues, oil production is completely dependent on the volume of CO_2 effectively injected into the reservoir. Knowing this, reservoir engineers can design the injection scheme in order to handle larger volumes of CO_2 and maximize the volume of oil contacted by CO_2.

3.2.2 CO_2 Storage Capacity with Injection Limitations & CO_2 Recycling

The scenarios analyzed in this study are injecting a significantly higher volume of CO_2 compared to traditional CO_2-EOR operations. A reservoir may have sufficient pore space to store the large volume of CO_2 emissions from a coal-fired power plant, but the reservoir characteristics dictate the rate that CO_2 can be injected into the reservoir. An ideal reservoir in this study would be very large, but also deep, porous, and permeable. This is difficult to find considering porosity and permeability typically decline with depth. Reservoir depth is critical for allowing higher injection pressures without fracturing the reservoir and overlying units. Given the emission rates of a coal-fired power plant, elevated injection pressures are expected. A porous and permeable reservoir will have less resistance towards higher injection pressures, allowing an EOR operation to inject CO_2 at the same rate it is captured from the power plant. Since no reservoir is ideal, a major aspect of this study is to analyze the CO_2 storage potential of a standard

EOR field given the elevated injection pressures and requirement to recycle all produced CO_2.

As stated in the previous chapter, a CO_2 injection pressure limit was set at 7000 psi, which is 90% of the fracture pressure to establish a factor of safety. Being a deep reservoir (10,200 ft), elevated injection pressures can be safely achieved without fracturing the reservoir and confining unit. Shallower reservoirs, with less overburden stress, would have lower fracture pressures and therefore lower injection pressure limits. The local reservoir characteristics, in particular porosity and permeability, dictate how receptive the reservoir rock surrounding an injection well is to higher bottom-hole pressures. Reservoir rock with low permeability will have a greater resistance to higher flow rates, increasing the BHP at the injection wells. The performance of each well, in terms of injectivity, dictates its injection capacity. A well's injection capacity is defined as its ability to maintain injection rates that match its share of CO_2 emissions while operating below the injection pressure limit (7000psi). Once an injection well reaches the pressure limit, the injection rate declines and it loses capacity to handle the rate at which CO_2 is being delivered to the field from the coal-fired power plant.

Along with the injection pressure limit set for safe operation, the requirement to recycle all produced CO_2 impacts the capacity to inject emissions after breakthrough. Described in detail in Section 2.3, the simulations are setup to give recycled CO_2 injection priority over recently-captured CO_2 emissions. As the volume of recycled CO_2 increases, the capacity of each injection well to handle CO_2 emissions declines. Each injection well's capacity is dictated by its ability to operate below the injection pressure limit while safely injecting its share of CO_2 emissions and recycled CO_2. Table 3.3 displays the injection performance for each injector under different boundary conditions and with a different number of active injection wells in the field. An injection well's

performance is determined by the duration of time it operates below the injection pressure limit of 7000 psi. The longer an injection well operates below 7000 psi the better it performs in terms of injectivity, where the well can effectively handle its share of emissions and recycled CO_2.

Closed Bd.	Run 16 (50 inj. Wells)		Run 15 (26 inj. Wells)	
Inj. Well	Days @ 7000psi	Project % @ 7000psi	Days @ 7000psi	Project % @ 7000psi
IN1	3,555	81.2%	3997	91.3%
IN2	3,855	88.0%	4223	96.4%
IN3	3,210	73.3%	4044	92.3%
IN4	3,141	71.7%	4029	92.0%
IN5	348	7.9%	2922	66.7%

1 Open Bd.	Run 13 (50 inj. Wells)		Run 14 (26 inj. Wells)	
Inj. Well	Days @ 7000psi	Project % @ 7000psi	Days @ 7000psi	Project % @ 7000psi
IN1	0	0.0%	6	0.1%
IN2	3,383	77.2%	4,210	96.1%
IN3	0	0.0%	2,687	61.3%
IN4	1,404	32.1%	3,944	90.0%
IN5	0	0.0%	974	22.2%

Table 3.3 - Injection performance data for all five injectors under four different conditions in terms of the downdip boundary being opened or closed and the injection rate per well based on the total number of active injection wells (26 or 50).

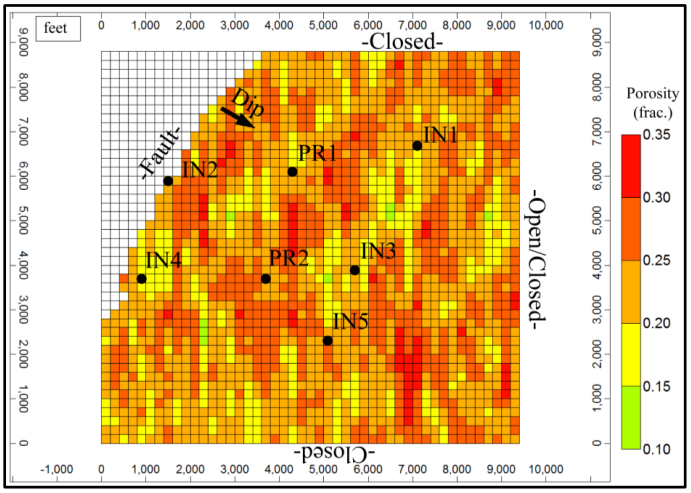

Figure 3.15 - A repeat of Figure 2.10 to help compare the data in Table 3.3

Injectors in zones with greater porosity and permeability, like IN5, perform better as the extent of heterogeneity is less and higher injection rates can be achieved without

reaching the pressure limit. Well placement is important both in terms of depositional trends and reservoir dip. From Table 3.3, well placement along dip has a greater impact on injectivity for the simulations where the downdip boundary is open. This can be seen as IN1, IN3, and IN5 are clearly the best performing injectors. Injectivity is dictated more by surrounding reservoir characteristics for the closed boundary scenarios. As expected, the scenarios with 50 active injection wells perform better in terms of operating below the pressure limit. With more injection wells there is less volume to be injected per well, allowing the wells to operate at a lower BHP. As seen in Table 3.3, this reduces the extent of operation at the pressure limit.

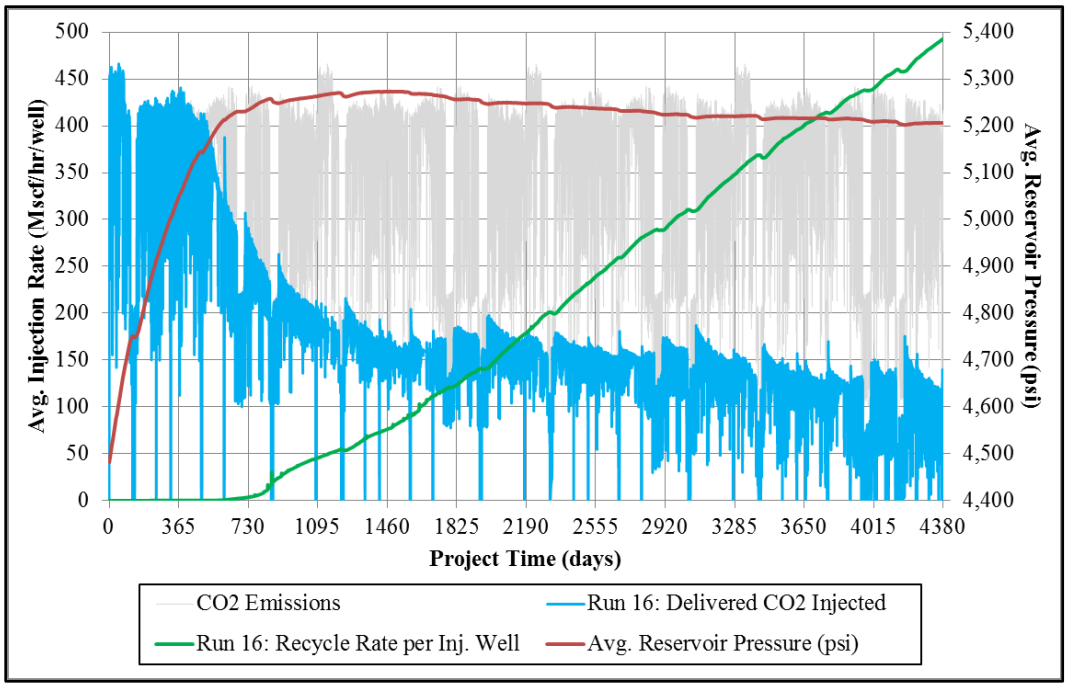

Figure 3.16 – This rapid increase in reservoir pressure decreases the rate that delivered CO_2 emissions can be injected. As reservoir pressure gradually declines, injectivity improves. The increase in recycled CO_2, after breakthrough, requires a growing portion of that injectivity.

After about 400 days of operation, the initial increase in reservoir pressure (Fig. 3.16), causes the rate that delivered CO_2 can be injected to decline below the rate at

which CO_2 emissions is captured at the coal-fired power plant. As the volume of CO_2 in the reservoir increases, the reservoir pressure begins to slowly decline. This is caused by CO_2, a less viscous fluid, replacing the produced oil and water, both more viscous than the injected CO_2. The gradual decline in reservoir pressure improves injectivity, but the majority of this injectivity improvement is occupied by the increasing rate that CO_2 is being recycled. Despite being from a different simulation run as Figure 3.16, Figure 3.4 also illustrates this increase in injectivity. In Figure 3.4, IN2 and IN4 have increasing injection rates after about 1600 days (>4 years). This supports the importance of improving sweep efficiency and delaying CO_2 breakthrough. The longer CO_2 breakthrough and recycling can be delayed, the more this injectivity improvement can be utilized for storing CO_2 delivered directly from the coal-fired power plant.

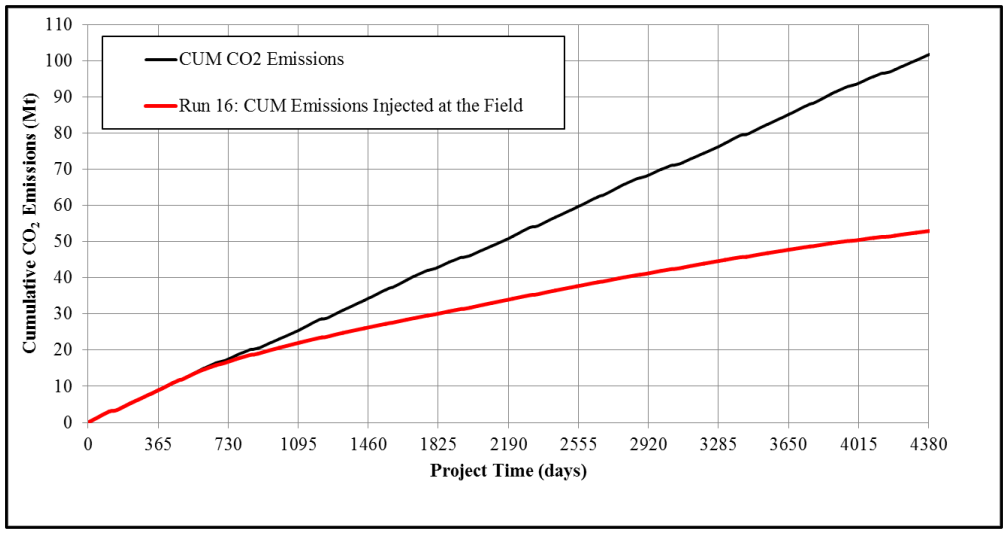

Figure 3.17 – The cumulative volume of CO_2 emissions actually injected compared to the cumulative volume emitted and piped from the coal-fired power plant. As the volume of CO_2 being recycled increases after breakthrough, the injection wells can no longer sustain an adequate injectivity to handle all the emissions being delivered to the field.

Section 2.3 states that the simulations are setup up where emissions that cannot safely be injected are not accounted for in the numerical calculations. The longer an

injection well is able to operate below the 7000 psi limit, the volume of CO_2 emissions injected at that well is more. Figure 3.17 illustrates the extent of CO_2 emissions that cannot be safely injected due to the pressure limitations and increasing volume of recycled CO_2 after breakthrough. At CO_2 breakthrough, the cumulative emissions injected at the EOR field deviate from the cumulative emissions of the coal-fired power plant. Over time this volume of CO_2 emissions that cannot be safely injected into the EOR reservoir increases to the point where after 12 years about half of the CO_2 emissions have not been injected into the reservoir.

The unaccounted volume of CO_2 emissions is significant for any potential contract between an electric utility and oil producer where all CO_2 piped to the field must be eventually stored in the subsurface. If there is no penalty for emitting CO_2 to the atmosphere, then the EOR operator could simply vent the CO_2 emissions that cannot be safely injected into the reservoir. Without a carbon tax this seems more viable then the EOR operator absorbing the additional economic burden of storing all received CO_2 into the subsurface. Research has looked at what price of CO_2 is needed to financially incentivize EOR operators to geologically store the CO_2 that cannot be safely injected into the oil-bearing formation (Coleman 2010).

Figure 3.18 further illustrates the impact of CO_2 recycling towards the decline in injection capacity for CO_2 emissions. Over time, the volume of recycled CO_2 takes up a greater portion of the injectate, reducing the volume and rate of emissions that can safely be injected. The points where recycled CO_2 occupies 100% of the injectate are associated with periods where no CO_2 emissions are delivered to the field. At any point through the project each injection well has a maximum allowable injection rate dictated by its current BHP. After CO_2 breakthrough, the volume of recycled CO_2 injected at each well increases. That remaining portion of the allowable injection rate is available to

CO_2 emissions piped to the field at that time. This makes CO_2 recycling and breakthrough a significant component towards characterizing the storage potential of an EOR reservoir. The longer that breakthrough can be delayed decreases the volume of CO_2 emissions that cannot be safely injected and stored into the oil reservoir.

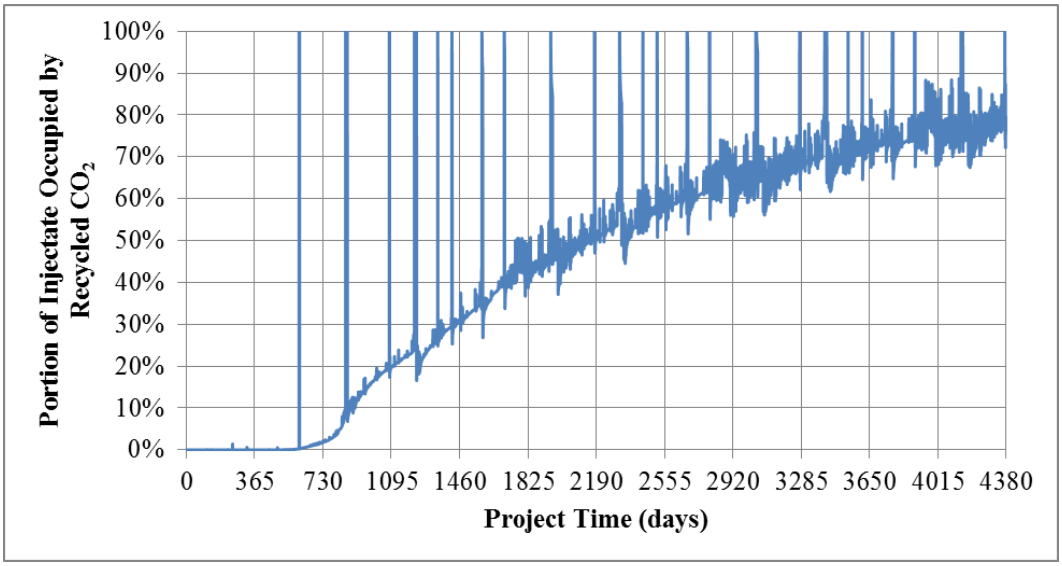

Figure 3.18 - An illustration showing the portion of injectate that is recycled CO_2. The remaining portion of injectate is left for CO_2 emissions piped to the field at that time.

To analyze the storage efficiency of these simulations, the displaceable pore volume (V_{pd}) of the reservoir model was calculated using Equation 1-16. The calculation assumes that the displaceable volume of oil represents the total pore volume available for CO_2 storage. The displaceable pore volume of the reservoir model was calculated to be 367 MMcf. By taking the volume of cumulative CO_2 emissions injected and dividing that by the displaceable pore volume, the fraction of storage volume occupied by CO_2 emissions could be determined. Figure 3.19 shows the results of this calculation.

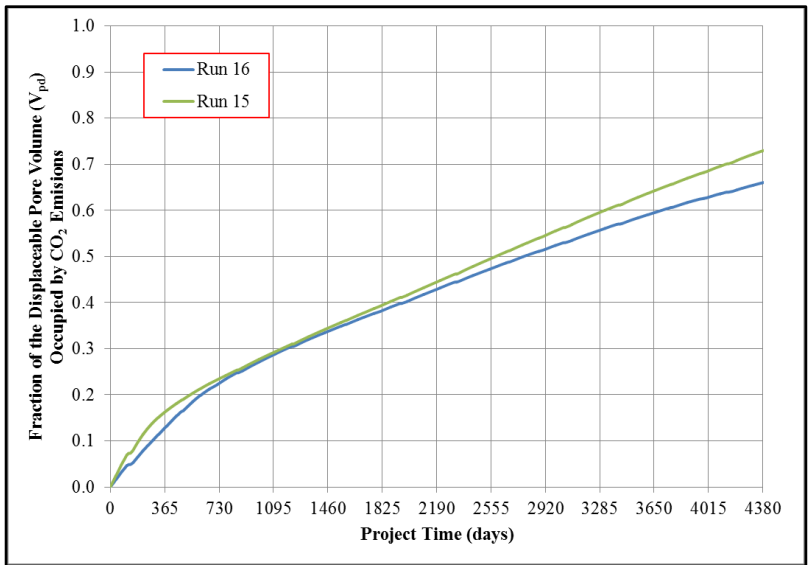

Figure 3.19 - The fraction of displaceable oil pore volume occupied by cumulative CO_2 emissions injected into the reservoir model.

From Figure 3.19, the anthropogenic CO_2 occupies between two-thirds and three-fourths of the displaceable pore volume after 12 years, depending on the simulation run. This shows that over time the tighter pore spaces can be invaded by CO_2, displacing oil and increasing the volumetric storage efficiency. Despite the higher injection rates, these simulations show an adequate storage efficiency that should continue to improve beyond 12 years. The volumetric storage efficiency is critical for both oil production and permanent CO_2 storage.

3.3 Matching Simulation Results to Koval's Methods

The principal steps for predicting oil recovery using Koval's methods were described in Section 1.5.4. This section will take those basic screening techniques and apply them to the reservoir simulation results from this research. It is important to note the scaling issues associated with Koval's methods, which are derived from core

flooding, but extrapolated to reservoir scale. Despite this scaling issue, Koval's methods are an adequate strategy for predicting oil recovery when sufficient data is available.

The first step was to calculate the mobility ratio (*M*) using Equation 1-10. With the mobility ratio, Koval's equation (Eq. 1-11) for calculating the effective viscosity (*E*) ratio between the solvent (CO_2) and oil fingers is used. The heterogeneity factor (*H*) was derived from a calculation of Dykstra-Parsons coefficient (*V*) using Figure 1.13. With a significant permeability distribution from various core samples across the field and within the reservoir model, the Dykstra-Parsons coefficient was calculated (Fig. 3.20).

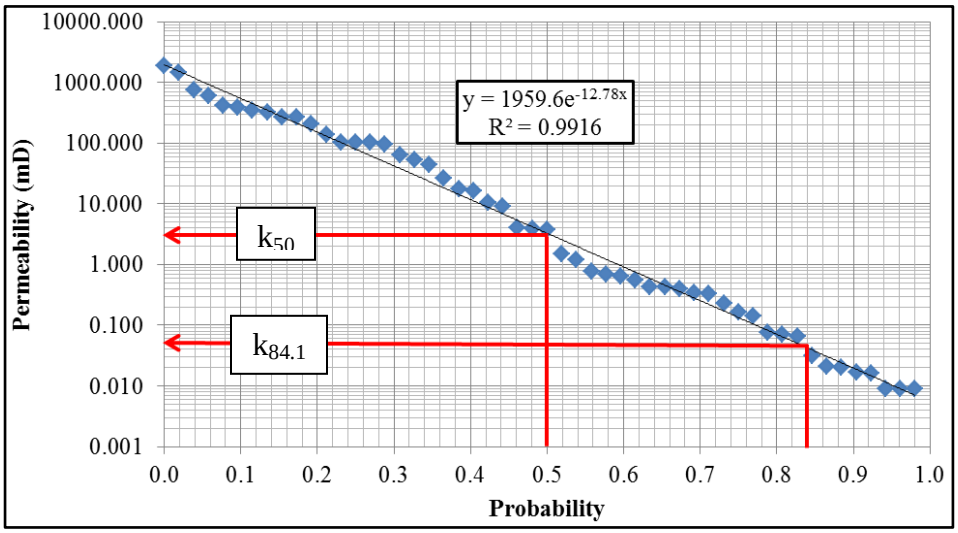

Figure 3.20 - Graphical calculation of Dykstra-Parsons coefficient using actual core data taken from wells within the reservoir model.

Using the data from Figure 3.20, Equation 1-20 was used to calculate the Dykstra-Parsons coefficient. With the heterogeneity factor derived from the Dykstra-Parsons coefficient, Koval's K-factor (*K*) was calculated using Equation 1-12. Equation 1-13 uses the K-factor to predict the pore volumes of CO_2 injected at breakthrough ($V_{pCO2,BT}$). To predict oil recovery (N_{pv}) in terms of fractional pore volume, Equation 1-14 was used. The Claridge correlation (Eq. 1-18) was incorporated to compare with the Koval's

method for predicting oil recovery. To effectively calculate oil recovery (N_p/V_{pd}) from Equation 1-18, an Excel macro was developed to incorporate solver iterations. Using the K-factor, a fractional flow analysis was done using Equation 1-15. As used in the previous section, the displaceable pore volume of oil (V_{pd}) was calculated in both barrels (bbl) and million cubic feet (MMcf). Table 3.4 shows the results of these calculations.

V_{pd}	59.48M	bbl	333.95	MMcf	Eq. 1-16
$V_{pd,wp}$	30.64M	bbl	172.03	MMcf	Eq. 1-16
HCPV	64.65M	bbl	363.00	MMcf	-
PV	258.6M	bbl	1,452.00	MMcf	-
M	4.73		Mobility Ratio		Eq. 1-10
E	1.488		Effective Viscosity		Eq. 1-11
F_{ibt}	0.3929	PV	Claridge's BT		Eq. 1-17
$V_{pCO2,BT}$	0.087	PV	Koval's BT		Eq. 1-13
V	0.9778		Dykstra-Parsons		Eq. 1-20
H	7.715		Koval's Heterogeneity		Fig. 1.13
K	11.48		K-factor		Eq. 1-12

Table 3.4 – Calculations and data used for predicting oil recovery from a miscible flood.

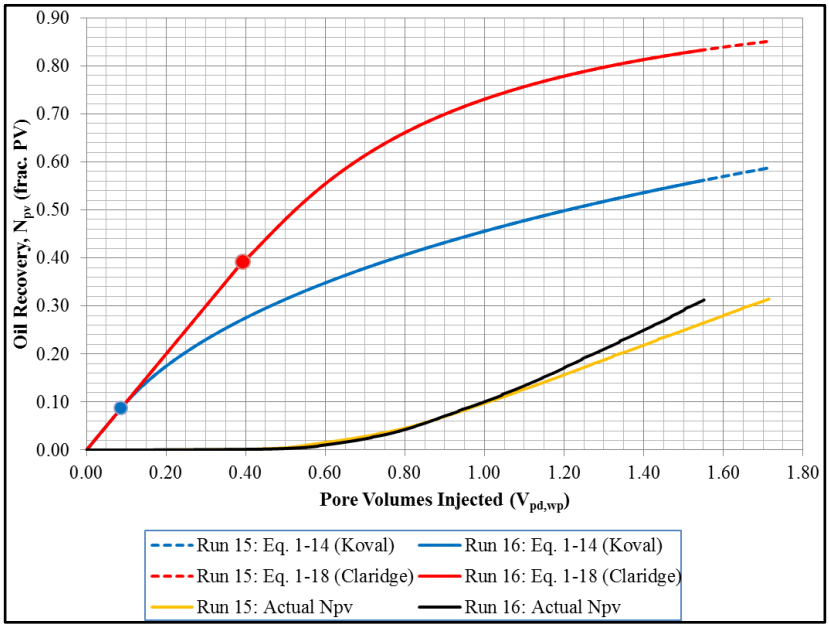

Figure 3.21 – Illustration of Koval's method and Claridge's correlation for oil recovery during miscible displacement. These two screening methods were compared to the actual simulation results. The single points represent CO_2 breakthrough predicted by their respective correlation method.

In Table 3.4, there is a new term introduced, labeled $V_{pd,wp}$. This term represents the displaceable pore volume within the well pattern of the reservoir model. The area of $V_{pd,wp}$ is outlined by the five injectors instead of the entire reservoir model. The well pattern area is about half of the entire model area. This term is used to better represent the oil recovery within the well pattern, seen in Figure 3.21.

After 12 years of injected CO_2, it is clear that the methods for predicting oil recovery, from both Koval and Claridge, overestimate the actual displaceable oil recovered through the reservoir simulations. Koval's method is derived from his heterogeneity factor, which can be correlated to the Dykstra-Parsons coefficient (Fig. 1.14). With a Dykstra-Parsons coefficient near one (V = 0.9778), the reservoir has a considerable degree of heterogeneity. Given the reservoir's heterogeneity, Koval's estimation for oil recovery is significantly lower than Claridge's correlation, which is derived from the mobility ratio. This shows that the reservoir model has a productive mobility ratio, given its depth and oil composition, but the extent of heterogeneity can limit oil recovery.

It is important to note that Koval's method was derived for a linear flow system, where the injectors are on one side and producers on the other. Claridge's correlation is based on five-spot well patterns, with four injection wells at each corner and a production well in the middle. Given the well pattern in this reservoir model, it would be reasonable to assume oil recovery would be greater with an additional injection and production well. Through Claridge's correlation, it was shown that Koval's methods fit well with the fingering observed in five-spot patterns. Despite the difference in well pattern orientation between the model and the correlations, the discrepancy in calculating oil recovery should not be significant. For these simulations, it seems that Claridge's correlation more accurately predicts CO_2 breakthrough, using the distinct term F_{ibt}, represented by the red

point in Figure 3.21. It is evident that the productive mobility ratio is extending CO_2 breakthrough, but the degree of reservoir heterogeneity is limiting overall oil recovery. Table 3.5 shows the breakthrough data for two simulations and the two correlation methods.

Run 15	BT (PV)	BT(Days)
Simulation	0.433	458.00
Koval	0.087	56.83
Claridge	0.393	384.50
Run 16	BT (PV)	BT(Days)
Actual	0.215	256.33
Koval	0.087	87.00
Claridge	0.393	495.34

Table 3.5 - Breakthrough data from the research simulations and standard miscible flooding correlations (BT=breakthrough).

The fact that oil can be displaced beyond the well pattern in this conceptualization, into the larger area of the reservoir model, contributes to the lack of recovery beyond the well pattern. While the two correlation methods show an eventual decline in oil recovery, the simulation results look to continue increasing recovery beyond 12 years. From Figure 3.21, it is evident that a significant volume of displaceable oil has not been produced within the well pattern. Despite injecting less CO_2 by pore volume, Run 16 has recovered about the same percentage of displaceable oil as Run 15. This demonstrates that with lower overall injection pressures oil recovery and displacement is more efficient per volume of CO_2 injected. For the oil recovery prediction methods of Koval and Claridge, the difference in pore volumes injected between Run 15 and Run16 is negligible, so the predictive calculations are nearly the same.

The heterogeneity associated with this reservoir limits the expansion of CO_2 as it flows along preferential flow paths. This limits CO_2 invasion into the lower permeability regions, bypassing significant volumes of producible oil. The bypassed oil is not permanently trapped, as seen in Figure 3.21, but only with the large volume of CO_2 being injected can that oil eventually be produced. Despite the inadequate sweep efficiency, it appears that more displaceable oil will be produced. This creates a situation where a LVA CO_2 supply could overcome reservoir sweep issues like heterogeneity. As more CO_2 is injected, that additional volume contacts oil in lower-permeability regions of the reservoir where flow velocities are much smaller. Given the productive mobility ratio of this reservoir, it is not clear if a large-volume CO_2 injection could overcome an undesirable mobility ratio. Compared to a smaller volume CO_2 injection, it is reasonable to conclude that less CO_2 will contact and displace oil through smaller pore throats associated with heterogeneity. It seems reasonable to assume that a higher mobility ratio will create a stronger tendency for CO_2 and oil to separate, developing very unstable viscous fingering where large-volume injection of CO_2 may not overcome this physical separation between the fluids. Additional modeling is recommended in future studies to assess this.

The use of WAG injection, besides compensating for lack of CO_2 supply, further supports these conclusions. Slugs of water separate injected CO_2 to limit its mobility through the reservoir but the water itself blocks the oil trapped in tighter pore spaces, associated with heterogeneity, from contacting and being displaced by CO_2. This means the water drive is only helpful for unproductive mobility ratios not reservoir heterogeneity. With an adequate mobility ratio and no CO_2 supply issues, the more CO_2 that can be injected reduces the impact of heterogeneity on ultimate oil recovery.

The Koval method continues with a fractional flow analysis of CO_2 in the effluent, which can be used to help predict breakthrough and the fractional flow of CO_2 through the production wells as more CO_2 is injected. Through fractional flow calculations, an ideal miscible flood has breakthrough at 1 PV injected and after 1 PV the effluent is 100% solvent or CO_2. Figure 3.22 shows the results of the fractional flow analysis using the Koval method (Eq. 1-15) on reservoir data and comparing it to the actual simulation breakthrough.

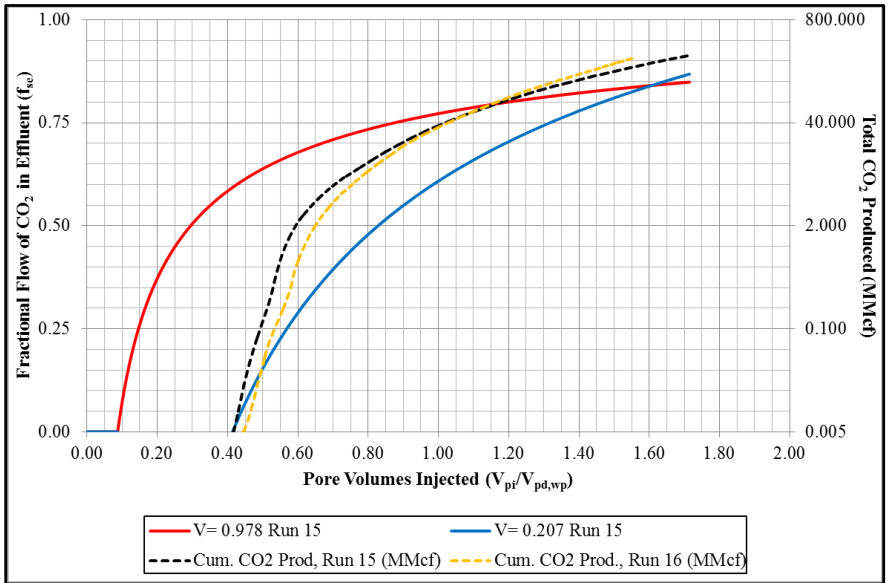

Figure 3.22 - Fractional flow analysis using the Koval method. This shows the discrepancy between predicted breakthrough (solid curves) and actual breakthrough (dashed lines).

It is clear that the Koval method has limited use towards predicting CO_2 breakthrough for this well pattern and reservoir model. The productive mobility ratio, seems to have more impact on determining breakthrough than the extent of heterogeneity characterized from the reservoir and incorporated into the model. The blue line in Figure 3.22 shows the Dykstra-Parsons coefficient needed to match the simulation results, which is abnormally low at $V = 0.207$ and a significant discrepancy from calculations of

Dykstra-Parsons coefficient using actual core data from the reservoir. There is inherently some inaccuracies incorporated into the correlation between the Dykstra-Parsons coefficient (*V*) and Koval's heterogeneity factor (*H*) in Figure 1.13. This represents the fundamental difficulty in quantifying heterogeneity. As stated before, it seems that mobility ratio has a greater influence on breakthrough, while heterogeneity has more of an impact on oil recovery and sweep efficiency.

3.3.1 Oil Production Results

The ultimate economic potential of a LVA CO_2-EOR project, with or without any carbon legislation, is dictated by the volume of oil produced. As seen in the previous section, mobility ratio and reservoir heterogeneity can have a significant impact on oil recovery, but the supply of CO_2 is no longer an issue. With a much larger supply of CO_2, over time the CO_2 should contact and displace almost all of the producible oil. The time for CO_2 to contact all of the displaceable oil is primarily governed by reservoir heterogeneity.

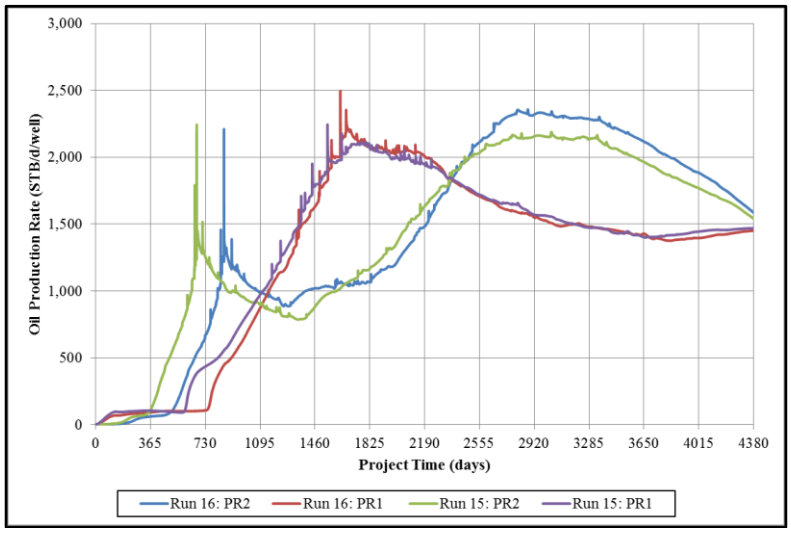

Figure 3.23 - Oil production rates for the two producers in the reservoir model. The injection intermittency can be seen at the production wells but more dampened.

Figure 3.23 demonstrates the oil production rates seen at both production wells in the model. Their placement relative to better performing injectors and local reservoir characteristics dictates the arrival and volume of oil production. Over 12 years, both wells have remained relatively productive without any significant declines in oil production. The intermittency at the injection wells can be seen at the producers through sudden spikes in the production rate. These spikes seem relatively dampened compared to the injection intermittency seen in other figures. The magnitude of these production spikes seem to decline with time, indicating the impact of injection pressure limits on intermittency through the reservoir.

From Figure 3.23, it can be inferred that the producers should still maintain adequate rates for some time beyond 12 years, as CO_2 invades more heterogeneous regions of the reservoir. The extent at which the oil producers can maintain productive rates is a significant characteristic of this reservoir and injection scheme. The considerable volume of oil that can still be produced is shown in Figure 3.24 by the cumulative production curves from Run 15 and Run 16. Graphs of cumulative production have a characteristic s-shaped curve, but the curves illustrated in Figure 3.24 have yet to reach the flat portion of the upper s-shape. The revenue generated from oil production in this injection scheme is extended for a longer period of time than low-volume, natural CO_2-EOR that has a more limited supply of CO_2. This is not an ideal economic situation from a purely oil production standpoint, but with an effective price on CO_2, this extended revenue can help cover the costs of storing CO_2 beyond the capacity of the oil reservoir.

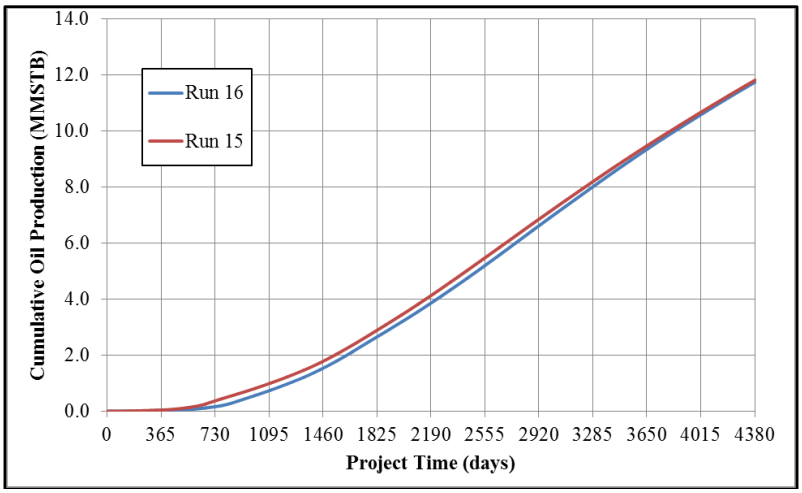

Figure 3.24 - Cumulative oil production from the two closed boundary simulations.

3.4 CONCLUSIONS

The intermittency associated with LVA CO_2 does not have a significant impact on oil production. In terms of CO_2 injection, oil recovery is only a function of the pore volumes injected, not the frequency at which the CO_2 is injected. For an EOR operator, the CO_2 supply contract with an electric utility can be based on the total emissions captured and expected to be delivered to the oil field over the EOR project's life. The frequency and fluctuations at which the CO_2 is piped to the oil field should not impact the design and economic forecasting based off predicating oil production and CO_2 injection capacity.

In a one coal-fired power plant to one oil field CO_2-EOR system, the volume of CO_2 emissions captured and piped to the field can create substantial CO_2 capacity issues if all CO_2 delivered must be sequestered into the subsurface. The rate of CO_2 emissions being delivered to the field elevates the bottom-hole pressure in the injection wells. To maintain a safe operation the injection rates must be constrained to avoid exceeding the

reservoir fracture pressure. The depth of the reservoir has a direct impact on the injection pressure limits relative to the fracture pressure. This research showed that once an injection well reaches the injection pressure limit, the CO_2 injection rate and emissions storage capacity declines substantially.

Injection wells in more permeable regions of the reservoir can sustain higher injection rates without reaching the injection pressure limit. A very large, deep, and permeable reservoir is ideal for a large-volume, anthropogenic (LVA) CO_2-EOR project. Even large, permeable reservoirs that are shallow will have issues with CO_2 injection capacity as the reservoir fracture pressure is less, lowering the safe threshold for injection pressures. Shallow reservoirs must have more ideal reservoir characteristics to compensate for the lower injection pressure threshold.

Both the injection pressure limits and CO_2 recycling directly impact the storage capacity of an EOR reservoir. After the initial rapid increase in reservoir pressure, the average reservoir pressure slowly declines. This improves reservoir injectivity as CO_2, a less viscous fluid, replaces the produced oil and water. This gradual improvement in injectivity is mostly occupied by the increasing volume of recycled CO_2. Improvement in sweep efficiency can delay CO_2 breakthrough and reduce the CO_2 recycling rate. With better sweep efficiency, more CO_2 being delivered directly from the coal-fired power plant can be effectively stored into the reservoir.

The mid-sized EOR reservoir used in this study would not be able to safely inject all the CO_2 emissions from a single coal-fired power plant into the oil-bearing formation. If an EOR operator is responsible for storing all CO_2 delivered to the field, this research supports the need for additional CO_2 storage strategies like stacked geologic storage. The idea of stacked storage has been previously researched, where an additional saline

formation is incorporated to store the CO_2 that cannot be safely injected into the oil-bearing formation of an EOR operation (Coleman 2010).

In terms of oil recovery, this research showed the impact of mobility ratio and reservoir heterogeneity on miscible flooding performance. It seems clear that CO_2 breakthrough is dictated more by the mobility ratio between CO_2 and reservoir oil. The rate and extent of oil recovery over an EOR project's life, is controlled more by reservoir heterogeneity. Given the rates and volume of CO_2 being injected during an LVA CO_2-EOR operation, more oil is contacted and displaced by CO_2 through smaller pore throats that would normally be bypassed in smaller-volume EOR operations. With extended time and volume of CO_2 supply, along with higher injection pressures, it seems that heterogeneity constraints that normally limit oil recovery can be partially overcome to increase ultimate production compared to smaller-volume EOR operations.

It is important to note that the conclusions and results from this research come from the data of one EOR reservoir. As with any oil production operation, there is no standardization for predicting oil production and CO_2 injection capacity since every geologic reservoir is different. With that being said, it is evident that a large-volume anthropogenic CO_2 source can eliminate supply issues associated with current CO_2-EOR operations. Having an essentially unlimited supply of CO_2 is certainly a desirable situation for any EOR operator, as oil production should improve compared to a limited supply of CO_2. If a significant price is put on CO_2 emissions, additional reservoir engineering will be needed to design an effective injection scheme that efficiently stores all CO_2 delivered to the oil field.

3.5 FUTURE WORK

An operation where LVA CO_2 captured from a coal-fired power plant is directly piped to an oil field for EOR is a novel problem linked to mitigation of climate change created by anthropogenic CO_2. From research results of this paper as well as other studies, it is clear that alternative injection strategies will be needed if all CO_2 arriving to the oil field must be eventually sequestered in the subsurface. Some alternative strategies include:

- Stacked geologic storage of CO_2
- Residual oil zone (ROZ) injection
- Implementation of horizontal drilling
- Injection optimization

Reconnaissance research assessed the function of a stacked CO_2 storage operation in several reservoir types, where saline injection zones are utilized to compensate for the loss of injection capacity in the oil reservoir over time. Figure 3.25 illustrates the concept of stacked CO_2 storage (Coleman 2010). The previous research on stacked storage did not utilize reservoir simulations. By incorporating reservoir simulators, a more accurate analysis could be done on injection capacity into both an oil-bearing reservoir and an underlying saline formation.

A new CO_2 EOR target below the oil-water contact, in the residual oil zone (ROZ), has been identified as a potential oil production and storage target (ARI 2010). Early assessments of ROZ in the Permian Basin show very favorable reservoir pay thickness and injectivity, so there is additional storage volume for CO_2 and marginal oil production potential. A large volume of CO_2 injected into the ROZ can help mobilize and produce the residual oil trapped by formation water. Additional research could

analyze the utility of ROZ injection of CO_2 in terms of increasing injection capacity and improving oil production.

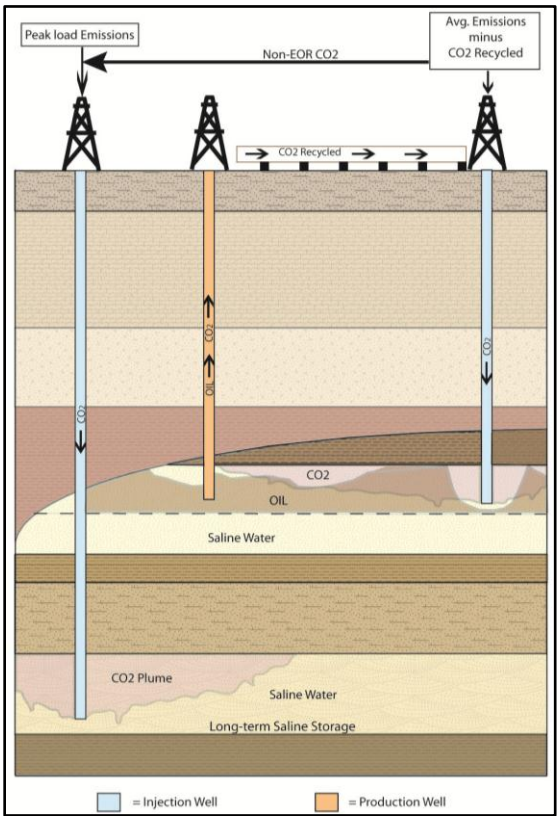

Figure 3.25 - Schematic diagram of a stacked CO_2 storage operation from (Coleman 2010).

Horizontal drilling looks to be a promising injection technique for LVA CO_2-EOR, where the buoyancy of CO_2 can be utilized to increase oil production and injection capacity. By drilling horizontal injection wells along the downdip or lower portions of the reservoir, the CO_2 can contact a greater volume of oil lower in the reservoir and invade a greater portion of the reservoir pore space. Production wells could also be drilled horizontally along the upper portion of the reservoir to produce the high concentration of oil displaced upward from the lower CO_2 injection wells. Future work

could look at implementing horizontal wells into a LVA CO_2-EOR operation and compared the performance to standard vertical wells.

It is clear that within a well pattern certain injection wells perform better than other injection wells. In a LVA situation where managing pressure is important, lower injectivity within a well pattern creates a situation where one poorly placed injection well can impact the performance of the entire well pattern. Strategies for injection optimization could be built from this research, knowing the constraints to a well's injection capacity. By optimizing how much CO_2 is injected into each well, the injection capacity of a well pattern and entire field could improve considerably. Well spacing is another reservoir engineering process that could be optimized to improve the performance of a LVA CO_2-EOR project.

Appendix A: Output of WinProp Compositional Calculations

```
**FILE NAME:     COMP.dat
*FILENAMES *OUTPUT *SRFOUT *REGLUMPSPLIT *NONE *GEMOUT
         *STARSKV *NONE *GEMZDEPTH *NONE *IMEXPVT *NONE
*WINPROP     2011.10

**=-=-=Titles/EOS/Units
**REM
*TITLE1 ''
*TITLE2 ''
*TITLE3 ''
*UNIT *FIELD
*INFEED *MOLE
*MODEL *PR *1978

**=-=-=Component Selection/Properties
**REM
*NC 12 12

*COMPNAME
'CO2'  'CH4'  'C2H6'  'C3H8'  'IC4'
'NC4'  'IC5'  'NC5'  'FC6'  'FC7'
'FC14'  'FC21'

*HCFLAG
3  1  1  1  1
1  1  1  1  1
1  1

*PCRIT
72.8  45.4  48.2  41.9  36.0
37.5  33.4  33.3  32.46  30.97000049
19.33000049  13.83000049

*TCRIT
304.2  190.6  305.4  369.8  408.1
425.2  460.4  469.6  507.5  543.2
700.7  793.3

*AC
0.225  0.008  0.098  0.152  0.176
0.193  0.227  0.251  0.27504  0.308301
0.604823  0.85772

*MW
44.01  16.043  30.07  44.097  58.124
58.124  72.151  72.151  86.0  96.0
190.0  291.0

*VSHIFT
0.0  0.0  0.0  0.0  0.0
0.0  0.0  0.0  0.0  0.0
0.0  0.0

*ZRA
0.2736  0.2876  0.2789  0.2763  0.275
0.2728  0.2716  0.2685  0.2712612671  0.2664161137
0.252526743  0.2447425343

*VCRIT
0.094  0.099  0.148  0.203  0.263
0.255  0.306  0.304  0.344  0.381
0.723  1.073
```

```
*VISVC
0.094  0.099  0.148  0.203  0.263
0.255  0.306  0.304  0.344  0.381
0.723  1.073

*OMEGA
0.4572355289  0.4572355289  0.4572355289  0.4572355289  0.4572355289
0.4572355289  0.4572355289  0.4572355289  0.4572355289  0.4572355289
0.4572355289  0.4572355289

*OMEGB
0.0777960739  0.0777960739  0.0777960739  0.0777960739  0.0777960739
0.0777960739  0.0777960739  0.0777960739  0.0777960739  0.0777960739
0.0777960739  0.0777960739

*SG
0.818  0.3  0.356  0.507  0.563
0.584  0.625  0.631  0.69  0.727
0.826  0.871

*TB
-109.21  -258.61  -127.57  -43.69  10.67
31.19  82.13  96.89  146.93  199.13
476.33  663.53

*PCHOR
78.0  77.0  108.0  150.3  181.5
189.9  225.0  231.5  250.1088  278.4048
522.88  742.2318

*ENTHALPY
4.77805  0.114433  0.000101132  -2.6494e-008  3.4706e-012  -1.314e-016
-5.58114  0.564834  -0.000282973  4.17399e-007  -1.525576e-010  1.958857e-014
-0.76005  0.273088  -4.2956e-005  3.12815e-007  -1.38989e-010  2.007023e-014
-1.22301  0.179733  6.6458e-005  2.50998e-007  -1.247461e-010  1.893509e-014
13.2866  0.036637  0.000349631  5.361e-009  -2.98111e-011  5.48662e-015
29.11502  0.00204  0.000434879  -8.181e-008  7.2349e-012  -1.456e-016
27.62342  -0.031504  0.000469884  -9.8283e-008  1.02985e-011  -2.9485e-016
-10.20523  0.2080547  -2.815438e-006  3.35665e-007  -1.763781e-010  3.018805e-014
0.0  -0.01654346295  0.0004116906899  -5.774276e-008  0.0  0.0
0.0  -0.03989923156  0.0004268529461  -6.325171e-008  0.0  0.0
0.0  -0.03783715098  0.0004178005659  -6.211165e-008  0.0  0.0
0.0  -0.0267417821  0.0004081621451  -5.928461e-008  0.0  0.0

*HEATING_VALUES
0.0  844.2900105  1478.460015  2105.160028  2711.540038
2711.540038  3353.660038  3353.660038  3975.91005  4600.280063
8970.820118  13341.36016

*IDCOMP
1  3  4  5  6
7  8  9  10  11
18  25

*VISCOR   *MODPEDERSEN

*VISCOEFF
0.0001304  2.303  0.007378  1.847  0.5173
*HREFCOR   *HARVEY

*PVC3    1.2

*BIN
4.476240252e-005
0.003424869163
```

```
0.009804018384
0.01740351238
0.01638729509
0.02280579546
0.02255753598
0.02745206848
0.03183405547
0.06580581992
0.09173130978

*SALINITY   *WTFRAC    0.15

**=-=-=Composition
**REM
**COMPONENT ARRAY
*COMPOSITION   *PRIMARY
0.0184  0.3999  0.0717  0.0334  0.0104
0.0158  0.0123  0.0095  0.0248  0.1346
0.1346  0.1346

**COMPONENT ARRAY
*COMPOSITION   *SECOND
1.0  0.0  0.0  0.0  0.0
0.0  0.0  0.0  0.0  0.0
0.0  0.0

**=-=-=CMG GEM EOS Model
**REM
**NC 12 12
*PRNGEM
*TRES  257.0
*AQUEOUS-DENSITY  *LINEAR
*SOLUBILITY
*TEMP  257.0
*PRES  4650.0

**=-=-=     END
```

Appendix B: Abbreviations

Abbreviations

- API = American Petroleum Institute
- ASME = American Society of Mechanical Engineers
- BEG = Bureau of Economic Geology
- CCS = Carbon Capture and Sequestration/Storage
- CRA = corrosion resistant alloys
- DOE = U.S. Dept. of Energy
- EIA = Energy Information Agency
- EOR = Enhanced Oil Recovery
- EOS = Equation-of-State
- ESP = Electrostatic Precipitator
- FCM = First-contact Miscible
- FGD = Flue Gas Desulfurization Unit
- FVF = formation volume factor
- GCCC = Gulf Coast Carbon Center
- GEM = Generalized EOS Model Compositional Reservoir Simulator
- GOR = gas-oil ratio
- HC = hydrocarbons
- HCPV = hydrocarbon pore volume
- LVA = large-volume anthropogenic (CO_2-EOR)
- MCM = Multiple-Contact Miscible
- MMP = Minimum Miscibility Pressure
- NACE = National Association of Corrosion Engineers
- NETL = National Energy and Technology Laboratory
- PV = pore volume (reservoir pore space)
- RB = reservoir barrel
- SECARB = Southeast Regional Carbon Sequestration Partnership
- SG = specific gravity (water = 1)
- STB = stock tank barrel
- WAG = Water-Alternating-Gas Injection

References

Ahmed, T. (2006). Reservoir engineering handbook. Burlington, MA, Elsevier.

ARI (2010). Optimization of CO_2 Storage in CO_2 Enhanced Oil Recovery Projects. Arlington, VA, Dept. of Energy & Climate Change 67.

ARI (2010). U.S. Oil Production Potential From Accelerated Deployment of Carbon Capture and Storage. Arlington, VA, Advanced Resources International, Inc.**:** 56.

Barrie, J., K. Brown, et al. (2008). "Carbon Dioxide Pipelines. A Preliminary review of design and risks." **1**.

Benge, G. and E. G. Dew (2005). Meeting the challenges in design and execution of two high rate acid gas injection wells.

Bock, B., R. Rhudy, et al. (2003). Economic Evaluation of CO_2 Storage and Sink Enhancement Options, TVA Public Power Institute.

Caudle, B. H. and M. D. Witte (1959). "Production potential changes during sweep-out in a five-spot system." Journal of Petroleum Technology **12**(12): 63-65.

Chevron Oil Co. (1966). Cranfield Prospect, Adams & Franklin Counties, Mississippi, U.S. Dept. of the Interior**:** 17.

Choi, J., J. Nicot, et al. (2008). Preliminary results of numerical investigations at SECARB Cranfield, MS field test site.

Choi, J. W., J. P. Nicot, et al. (2011). "Numerical modeling of CO2 injection into a typical US Gulf Coast anticline structure." Energy Procedia **4**: 3486-3493.

Claridge, E. L. (1972). "Prediction of recovery in unstable miscible flooding." Old SPE Journal **12**(2): 143-155.

Coleman, S. H. (2010). The Geologic and Economic Analysis of Stacked CO_2 Storage Systems, a Carbon Management Strategy for the Texas Gulf Coast. Jackson School of Geosciences. Austin, TX, The University of Texas at Austin. **Master of Arts:** 96.

Craig, F. F., J. L. Sanderlin, et al. (1957). "A laboratory study of gravity segregation in frontal drives." Trans., AIME **210**: 275.

Cronquist, C. (1978). Carbon dioxide dynamic miscibility with light reservoir oils. 4th Annual U.S. DOE Symposium, Tulsa, OK.

Dolence, R. C., C. Kirschner, et al. (2009). Storage of Captured Carbon Dioxide Beneath Federal Lands. T. Grant, National Energy Technology Laboratory, U.S. Dept. of Energy**:** 75.

Dykstra, H. and R. L. Parsons (1950). "The prediction of oil recovery by waterflood." Secondary Recovery of Oil in the United States **160**.

EIA (2008). Annual Coal Report. N. Office of Coal, Electric, and Alternate Fuels. Washington, DC, U.S. Energy Information Administration**:** 77.

EIA (2008). Energy Emissions Data & Environmental Analysis of Energy Data, Energy Information Administration, U.S. Dept. of Energy.

EIA (2011). Annual Energy Outlook 2011. U. S. D. o. Energy. Washington, D.C., U.S. Energy Information Administration.

Figueroa, J., T. Fout, et al. (2008). "Advances in CO2 capture technology--The US Department of Energy's carbon sequestration program." International Journal of Greenhouse Gas Control **2**(1): 9-20.

Gale, J. and J. Davison (2004). "Transmission of CO2--safety and economic considerations." Energy **29**(9-10): 1319-1328.

Galloway, W. E. and D. K. Hobday (1983). Terrigenous clastic depositional systems. Applications to petroleum, coal and uranium exploration.

Green, D. W. and G. P. Whillhite (1998). Enhanced Oil Recovery. Richardson, TX, SPE.

Green, D. W. and G. Willhite (1998). "Enhanced Oil Recovery, SPE textbook series, volume 6." Society of Petroleum Engineers, Richardson, Texas.

Holm, L. R. and V. Josendal (1982). "Effect of oil composition on miscible-type displacement by carbon dioxide." Old SPE Journal **22**(1): 87-98.

Hosseini, S. A. (2012). Cranfield Phase III Modeling. 6th Annual SECARB Stakeholder's Meeting, Atlanta, GA, GCCC.

Hovorka, S. D., J. W. Choi, et al. (2009). "Comparing carbon sequestration in an oil reservoir to sequestration in a brine formation—field study." Energy Procedia **1**(1): 2051-2056.

Hovorka, S. D., T. A. Meckel, et al. (2011). "Monitoring a large volume CO2 injection: Year two results from SECARB project at Denbury's Cranfield, Mississippi, USA." Energy Procedia **4**: 3478-3485.

Jessen, K., A. Kovscek, et al. (2005). "Increasing CO2 storage in oil recovery." Energy Conversion and Management **46**(2): 293-311.

Johnson, J. and J. Pollin (1981). Measurement and correlation of CO2 miscibility pressures. SPE/DOE Enhanced Oil Recovery Symposium, Tulsa, OK.

Kanniche, M., R. Gros-Bonnivard, et al. (2010). "Pre-combustion, post-combustion and oxy-combustion in thermal power plant for CO2 capture." Applied Thermal Engineering **30**(1): 53-62.

Klins, M. A. (1984). Carbon dioxide flooding; basic mechanism and project design. Boston, MA, International Human Resources Development Corp.

Kothandaraman, A., L. Nord, et al. (2009). "Comparison of solvents for post-combustion capture of CO2 by chemical absorption." Energy Procedia **1**(1): 1373-1380.

Koval, E. J. (1963). "A method for predicting the performance of unstable miscible displacement in heterogeneous media." Old SPE Journal **3**(2): 145-154.

McCoy, S. T. (2008). The Economic of CO_2 Transport by Pipeline and Storage in Saline Aquifers and Oil Reservoirs. Engineering & Public Policy. Pittsburgh, PA, Carnegie Mellon University. **Doctor of Philosophy:** 267.

Meckel, T. and S. Hovorka (2009). Results from continuous downhole monitoring (PDG) at a field-scale CO2 sequestration demonstration project, Cranfield, MS.

Merkel, T., H. Lin, et al. (2009). "Power plant post-combustion carbon dioxide capture: An opportunity for membranes." Journal of Membrane Science.

Meyer, J. P. (2007). Summary of Carbon Dioxide Enhanced Oil Recovery (CO_2EOR) Injection Well Technology, American Petroleum Institute.

Moritis, G. (2009) "More CO_2-EOR projects likely as new CO_2 supply sources become available." Oil & Gas Journal.

Perkins, T. and O. Johnston (1963). "A review of diffusion and dispersion in porous media." Old SPE Journal **3**(1): 70-84.

Rao, A. B. (2007). Technologies: Separation and Capture. Carbon Captuer and Sequestration: Integrating Technoolgy, Monitoring, and Regulation. E. J. Wilson and D. Gerard. Oxford, Blackwell Publishing Ltd.**:** 11-34.

Reamer, H. H., R. H. Olds, et al. (1944). "Phase Equilibrium in Hydrocarbon Systems. Methane Carbon Dioxide System in the Gaseous Region." Industrial & Engineering Chemistry **36**(1): 88-90.

Solano, S. V., J. P. Nicot, et al. (2011). "Sensitivity study of CO2 storage in saline aquifers in the presence of a gas cap." Energy Procedia **4**: 4508-4515.

Stalkup, F. I. (1970). "Displacement of oil by solvent at high water saturation." Old SPE Journal **10**(4): 337-348.

Stalkup Jr., F. I. (1983). Miscible Displacement. Dallas, TX, Society of Petroleum Engineers.

Standing, M. B. (1947). "A pressure-volume-temperature correlation for mixtures of California oils and gases." Drilling and production practice.

Taber, J., F. Martin, et al. (1997). "EOR Screening Criteria Revisited-Part 1: Introduction to screening criteria and enhanced recovery field projects." SPE Reservoir Engineering **12**(3): 189-198.

Taber, J., F. Martin, et al. (1997). "EOR Screening Criteria Revisited Part 2: Applications and Impact of Oil Prices." SPE Reservoir Evaluation & Engineering **12**(3): 199-206.

Vita

Stuart Hedrick Coleman was born in Washington, D.C., growing up in Middleburg, VA. For high school, he attended Woodberry Forest School, an all-boys boarding school near Orange, VA. After high school, Stuart enrolled at the University of Mississippi, majoring in geological engineering. During his undergraduate degree, Stuart had internships with the Loudoun County, Virginia, Office of Solid Waste and Jura-Search Inc., an independent oil exploration company in Jackson, MS. After graduating from the University of Mississippi, he entered the Energy & Earth Resources master's program, part of the Jackson School of Geosciences at The University of Texas at Austin. During graduate school, Stuart worked at Cook-Joyce Inc., an environmental consultant firm in Austin, TX. He then took a position as a graduate research assistant with the Gulf Coast Carbon Center (GCCC), a research group at the Bureau of Economic Geology. Continuing his position as a research assistant with the GCCC, Stuart decided to get a second masters in petroleum engineering. During his first summer in the petroleum engineering program, he had an internship with Chevron ETC, working in the Rock & Fluids Characterization Group. Upon completion of his masters in petroleum engineering, Stuart will start a full-time position with Chevron.

This thesis was typed by Stuart H. Coleman.